NASA CR-121125
MDC G4328

CONTAMINATION AVOIDANCE DEVICES FOR POPPET-TYPE SHUTOFF VALVES

by

D. L. Endicott

McDonnell Douglas Astronautics Company–West

Prepared for

NATIONAL AERONAUTICS AND SPACE ADMINISTRATION

NASA Lewis Research Center
Contract NAS3-14375
I. E. Sumner, Project Manager

NASA CR-121125
MDC G4328

FINAL REPORT

CONTAMINATION AVOIDANCE DEVICES FOR POPPET-TYPE SHUTOFF VALVES

by

D. L. Endicott

McDONNELL DOUGLAS ASTRONAUTICS COMPANY–WEST
5301 Bolsa Avenue
Huntington Beach, California 92647

prepared for

NATIONAL AERONAUTICS AND SPACE ADMINISTRATION

January 1973

CONTRACT NAS3-14375

NASA Lewis Research Center
Cleveland, Ohio
I. E. Sumner, Project Manager
Propulsion Systems Branch

NOTICE

This report was prepared as an account of Government sponsored work. Neither the United States, nor the National Aeronautics and Space Administration (NASA), nor any person acting on behalf of NASA:

A. Makes any warranty or representation, expressed or implied, with respect to the accuracy, completeness, or usefulness of the information contained in this report or that the use of any information, apparatus, method, or process disclosed in this report may not infringe privately owned rights; or

B. Assumes any liabilities with respect to use of, or for damages resulting from the use of any information, apparatus, method or process disclosed in this report.

As used above,"person acting on behalf of NASA" includes any employee or contractor of NASA, or employee of such contractor, to the extent that such employee or contractor of NASA, or employee of such contractor prepares, disseminates, or provides access to, any information pursuant to his employment or contract with NASA, or his employment with such contractor.

FOREWORD

The work described herein was performed by the McDonnell Douglas Astronautics Company—West (MDAC-West) under National Aeronautics and Space Administration contract NAS 3-14375. The work was done under the direction of the NASA Project Manager, Mr. I. E. Sumner, Propulsion Systems Branch, NASA Lewis Research Center.

ABSTRACT

This investigation covered the determination of the cycle life of the seal closure of a typical poppet-type shutoff valve in an uncontaminated GH_2 environment and then compared this component performance with simulated operation with GN_2 and LN_2 containing controlled amounts of AL_2O_3 contaminant particles. The original valve design was tested for contamination damage tolerance characteristics under full-flow and cyclic-operating conditions, redesigned to improve the damage tolerance to contaminants, and then retested. The redesigned valve was found to have acceptable tolerance characteristics under all full-flow conditions and cyclic operation with small (25-75 μ) particulate contamination. The tolerance characteristics of the valve under cyclic conditions with large (75-250 μ) particulate contamination was improved but was not found to be completely satisfactory.

A second method of approach to damage tolerance control was investigated through the evaluation of various types of particulate contamination separation devices. The design selected consisted of a venturi type of separator using multiple screens for particle retention. Preliminary testing was completed on the prototype design and it was established that the dynamic separator is capable of separating particles from a flowing fluid stream and retaining these particles in a particle entrapment zone.

Page intentionally left blank

CONTENTS

Page intentionally left blank

FIGURES

Page intentionally left blank

TABLES

Section 1
SUMMARY

A program to evaluate various methods of improving the tolerance of the seal closure of the poppet-type shutoff valves to contamination damage was completed. The program included the determination of:

- A set of baseline cycle-life characteristics of three different seal closure configurations.
- The contamination tolerance characteristics of two seal closure configurations.
- Various methods of improving the contamination avoidance characteristics and trapping of the contaminants.

1.1 CYCLE LIFE TESTS

The pneumatically actuated shutoff valves incorporated a seal closure consisting of a flat Inconel 718 poppet and a compliant, self-aligning, flat A286 seat. Three different seat surface configurations were tested:

- A286 seat
- Gold-plated A286 seat
- Teflon S plastic-coated A286 seat

The tests were conducted using GH_2 isolated in the test valves in a non-flow condition at 6.9×10^5 N/m^2 (100 psig) for a maximum of 10^5 cycles. The results indicated that:

- The A286 seat was not acceptable when loaded to seat stresses of 27.6×10^6 and 55.2×10^6 N/m^2 (4000 and 8000 psi).
- The hard gold (MIL-G-45204, Type 1, Class 5, Grade C) plated seat was acceptable for 100,000 cycles at seat stresses of 17.2×10^6 N/m^2 (2500 psi) to 33.1×10^6 N/m^2 (4800 psi)
- The Teflon S (958-203) coated seat was acceptable for 100,000 cycles at seat stresses of 12.4×10^6 and 27.6×10^6 N/m^2 (1800 and 4000 psi).

1.2 CONTAMINATION TOLERANCE TESTS

A series of contamination tolerance tests were made with the hard gold plated seat and the Teflon S coated seat configurations. These tests were conducted in a special test setup which permitted both full-flow and cyclic operation of the test valves in an open-loop mode with either GN_2 or LN_2 test media. The particulate contamination injected into the flow system consisted of $A\ell_2O_3$ particles in size ranges of 25 to 75 μ and 75 to 250 μ.

The steady full-flow tests indicated that considerable damage occurred to the raised-seat sealing surface from the injected contamination. The cyclic tests indicated that both seat configurations exhibited good contamination tolerance characteristics when contaminated with the 25 to 75 μ size particles. However, the damage-avoidance characteristics were less pronounced when testing with the 75 to 250 μ size particles.

1.3 CONTAMINATION AVOIDANCE ANALYSIS AND TESTS

One valve was redesigned with the seat sealing surface submerged into the seat assembly so that the gold plating or Teflon S coating would not be subjected to direct impingement by the particulate contaminants. The redesign valve was tested in the GN_2 flow loop. It was found that the tolerance to damage in the full-flow conditions was improved, but that tolerance to damage under cyclic conditions was not measurably improved.

A second method of improving the contamination avoidance characteristics consisted of evaluating various types of dynamic particle separators. The analysis established a simple mathematical model of particulate separation from a moving fluid stream to obtain the basic design parameters. These parameters were used in completing conceptual design studies of four different separator configurations. The venturi type separator was found to offer the greatest potential for meeting the design requirements.

The testing of a venturi type dynamic separator consisted of three test runs in the GN_2 flow system. The tests were conducted at full flow conditions with excessive quantities of injected particulate contamination. These preliminary tests indicated that the dynamic separator design was able to trap significant quantities of contaminants.

Section 2
INTRODUCTION

Component failure caused by uncontrolled particulate contamination in the various fluid systems is one of the major problems of aerospace vehicle reliability.

This problem has been encountered on the single-burn type of vehicle which has been utilized to the greatest extent in the past and which represents the least severe system. With the advent of the reusable, long life vehicle of the space shuttle/space tug type, the contamination damage problem will become more critical. The normal method of control for the one-shot mission consists of extensive preflight cleaning of the complete propellant fluid system and the filtration of the propellants during the vehicle loading process.

The contamination particles existing in the feed system originate from three different sources in a typical vehicle propulsion system. These are:

1. Residual manufacturing debris in the propellant tankage and other fluid systems.

2. Contaminate particles in the on-loaded propellants.

3. System generated particles from the wear of components in normal operation.

All three of these sources will be significant on the space shuttle vehicle. Since a new drop tank with unburned propellant will be coupled to a reusable orbitor for each mission, the concentration of contaminates in the orbiter after a number of flights may be much higher than with the single burn vehicle. Also, since the number of operating cycles which will be accomplished by the components in the orbiter system will be greater than those for a one-shot vehicle, the system generated contamination level is expected to increase proportionally.

To improve the reliability of propulsion components in reusable service, a program has been conducted at McDonnell Douglas Astronautics Corp. (MDAC) to investigate the contamination damage avoidance characteristics of typical feed system components. This program was conducted under Contract NAS 3-14375 funded by the NASA Lewis Research Center. The work conducted on this program consisted of evaluating two methods of improving the contamination damage problem, using actual flight type hardware under simulated operating conditions.

The objective of this program was to develop the technology required to provide acceptable contamination damage avoidance characteristics for poppet-type shutoff valves. This effort included evaluation of the contamination avoidance characteristics of the basic 1T32095 propellant shutoff valve (description in References 1 and 2), the cycle-life performance of three seal closures (poppet and seat configurations) in an uncontaminated environment, and the effectiveness of various seat configurations and auxiliary contamination avoidance device concepts when used in conjunction with these poppet-type valves. In addition, a secondary objective was to evaluate two methods of monitoring the performance of the test valves during actual operations using acoustical monitoring instrumentation. The approach used to achieve these objectives was implemented by the four-task program summarized below.

2.1 TASK I. VALVE CYCLE-LIFE TESTS

A. Valve Refurbishment—The 1T32095-1 and -501 valve configurations were disassembled and the valve closure elements refurbished to the basic design surface specifications of flatness and surface finish. After completion of the valve closure refurbishment, the valves were reassembled in their original configuration. The internal leakage of each valve was measured at both ambient temperature and 77.3°K (-320°F) to confirm that the measured leakages were within specifications.

B. Valve Testing—Both the -1 and -501 valves were cycle-life tested in accordance with the requirements described herein. A life-cycle test series consisted of a total of 100,000 cycles (a cycle was defined as opening and closing of the valve once) or until the internal leakage rate increased to a value which was 10 times greater than the measured pretest value. The cycle tests were conducted using gaseous hydrogen (GH_2) at 300 ± 11°K (540 ± 20°R) isolated in the test valve in a non-flow condition at 6.9×10^5 N/m^2 (100 psig). The internal leakage rate was monitored throughout each test series using acoustic monitoring equipment and was measured at least once each test day using the volume displacement method at ambient temperature. The number of valve cycles between measurements of internal leakage (volume displacement method) did not exceed 10,000 cycles for any test series. Six complete test series were made. These tests included:

1. Hard surface (Inconel 718) on hard surface (A286) poppet/seat materials (-1 valve configuration).

2. Hard surface (Inconel 718) on medium hard surface (gold-plated A286) poppet/seat materials (-501 configuration).

3. Hard surface (Inconel 718) on soft surface (plastic-coated A286) poppet/seat materials (-503 configuration).

Each of the three above listed poppet/seat material combinations was tested at two different seating stress levels, making a total of six tests. At the completion of each test series, the valves were disassembled, inspected, and refurbished before the start of a new test series.

The acoustical signature (operational vibration characteristics as measured with an accelerometer and transducer) was determined for each test valve at the start of each test series and monitored during the remainder of each test, to monitor the mechanical operation of the test valves. A transducer, by definition, is a device capable of transforming energy from one form to another. As used in this report, the term transducer refers to a device whose active element is a piezoelectric crystal which responds to ultrasonic sound waves. An accelerometer is a similar device whose active element is a piezoelectric element coupled to a spring-mass system which responds to accelerations of its internal mass.

2.2 TASK II. VALVE CONTAMINATION TOLERANCE TESTING

A series of tests were conducted to evaluate the contamination tolerance of the basic valve-sealing closure design configuration for two of the three poppet/seat material combinations that were specified in Task I, Cycle Life Testing. The selection of the two best poppet/seat material combinations was made by MDAC, based on the results of the Task I testing. The material combinations tested were Inconel 718/gold plated (-501 valve configuration) and Inconel 718/Teflon S (-503 valve configuration).

The contamination tolerance testing consisted of full-flow tests (valve held fully opened during testing) and valve cyclic tests (valve actuated fully opened and closed a minimum of 10 times) at full-flow conditions.

A. Full-Flow Tests — These tests were performed to determine the damage to the valve-closure sealing surfaces from particulate contaminants impacts (hits) at high flow velocities with the valve fully opened. This series of tests included the following:

   1. Two full-flow tests were performed on the -501 valve with ambient gaseous nitrogen containing a measured amount of solid contaminants. The contaminants selected included particles in the 25 to 75-μ range for the first test and the 75 to 250-μ range for the second test. The particle material selected for testing was aluminum oxide (Al_2O_3).

   2. The internal leakage rate of each valve was measured before and after each contamination test run. Changes in the measured internal leakage rate were used to evaluate the tolerance of the valve design to contaminated fluid flow.

B. Cycling Tests — These tests were performed to determine the damage to the sealing-closure surfaces from particulate

contaminants trapped between the poppet and seat during cyclic operation. This series of tests consisted of the following:

1. A series of seal-closure contamination-tolerance tests was performed on the -501 and -503 valves with fluid test media containing a measured amount of contaminants. The contaminants selected included particles in the 25 to 75-μ range for the first test, and 75 to 250-μ range for the second test with each fluid media. The particulate material selected for these tests was Al_2O_3.

2. The valves were tested first using GN_2 as the fluid media and then using LN_2 as the test media. Tests were made with two different contaminant particles sized for each fluid media. The GN_2 flow rate was a nominal 1.13 kg/s (2.5 lb/sec.). The LN_2 flow rate was a nominal 3.785×10^{-3} m^3/s (60 gpm).

3. During these tests, the valve was repeatedly cycled open and closed to determine whether particles were trapped on the sealing surfaces. The cycling rate was a nominal 1-cycle per second. (10-cycles per test.)

4. The internal leakage rate of each valve was measured before and after each contamination tolerance test run. The changes in measured internal leakage rate was used to evaluate the tolerance of the valve design to exposure to contaminated fluid flow.

5. The acoustical signature technique of using accelerometers and transducers for signal detection with electrical signal amplification, developed by MDAC, was used to monitor the mechanical operation of the test valves during each of the contamination tolerance tests.

2.3 TASK III. CONTAMINATION AVOIDANCE CONCEPTS

A. Analysis and Conceptual Design—Analysis and conceptual design studies of contamination avoidance concepts were conducted for the 1T32095 poppet-type shutoff valve based on the results of Tasks I and II. The purpose of these studies was to evaluate methods for shielding the sealing surfaces from impinging particulate contaminants during propellant flow and to minimize particulate contaminants entrapment between the poppet and seat at sealing closure. These studies included both basic valve design changes and the use of auxiliary particulate separation devices. One new valve seat configuration and one auxiliary avoidance device were selected for testing. The venturi type of dynamic separator was selected as the particulate separation device for testing.

B. Valve Modifications — Based on the final design selected in Part A, above, MDAC modified the -501 valve to reflect the design changes. After modification, checkout tests were performed to insure that valve operation was within design requirements.

C. Contamination Avoidance Testing — Each concept was tested in accordance with the seal closure tests performed with gaseous nitrogen media as described under Task II. The test results were compared with the results of the Task II testing to determine the improvements in tolerance of the valve to particulate contamination. Both concepts, valve seat configuration and dynamic separator, produced improved contamination damage avoidance characteristics.

2.4 TASK IV. QUALITY ASSURANCE

The quality assurance effort on this program was conducted under the direction of technical engineering personnel and included the following:

A. Critical characteristics control was applied to the valve modification of Task I and Task III.

B. The results of the physical modification were recorded in the engineering log books.

C. The instrumentation used for testing was calibrated to National Standards (when possible).

D. The records of nonconforming articles were recorded in the engineering log books.

E. The records of test failures were recorded in the engineering log books.

Page intentionally left blank

Section 3
TECHNICAL DISCUSSION

3.1 TASK I. VALVE CYCLE-LIFE TESTS

The valve cycle-life test program was conducted to provide quantitative design data necessary for establishing baseline performance levels of the seal closure (poppet and seat) for poppet-type shutoff valves operating with a noncontaminated fluid media. This is an essential step in providing the criteria needed to design long-life seal closures for service with propulsive fluids which contain particulate contamination. Since the presence of contamination has the effect of reducing the operating life of the seal closures to some value lower than the baseline value, the establishment of representative baseline values became significant in predicting the true life expectancy under various system operation conditions.

In the absence of particulate contamination, the mode of seal closures deterioration becomes a matter of surface wear of the closure element sealing surfaces. A number of different wear modes have been identified and reported (Reference 3) however, the major modes for propulsion components are:

A. Adhesive wear.

B. Abrasive wear.

C. Corrosive wear.

D. Surface Fatigue

The Task 1 Cycle-Life Tests were conducted using existing 1T32095 pneumatic actuated valves designed to prevent abrasive wear by eliminating all sliding motion between the poppet and seat during valve closure and therefore no abrasive wear was expected with these valves (Reference 2). By selecting a non-corrosive fluid for testing, the corrosive mode of wear was eliminated and the data obtained were indicative of the adhesive wear and surface fatigue modes of progressive failure. Under conditions of adhesive wear, the key factors of wear are:

A. Seat stress.

B. Wear Coefficient.

C. Energy of Adhesion ($Ergs/cm^2$).

An attempt was made to account for these three factors in a manner which would produce the greatest amount of quantitative information with the least

number of tests. However, the values for wear coefficient and the energy of adhesion are very poorly defined at present and little can be done to render these in non-dimensional terms. The stress level was better suited to non-dimensional analysis, and a relative stress factor (RSF) was generated for use on this program. This design factor is discussed in detail in Subsection 3.1.1.

To provide the most useful data for component designers, the wear rates for the valves were expressed in terms of seal leakages across the main sealing closures instead of the mechanical wear rates (i.e. change in dimension). By comparing the rate of change of the internal leakage with cycles of operation, an adhesive wear failure could be separated from a surface fatigue failure. A surface fatigue failure was expected to be entirely different from an adhesive wear failure. Surface fatigue should show little or no change in leakage for a relatively large number of cycles and then should produce a sharp increase in leakage in a short time as shown in Figure 3-1. Adhesive wear would be expected to start with the first cycle and continue at a linear rate during the total period of operation. A combination of these two wear mechanisms can occur, and under these considerations the surface wears in the adhesive mode until the surface area loss is sufficient to reduce the total surface area to a value which will no longer adequately support the applied seat loadings. Hence, surface fatigue starts, and a rapid increase in leakage occurs after a relatively small number of additional cycles.

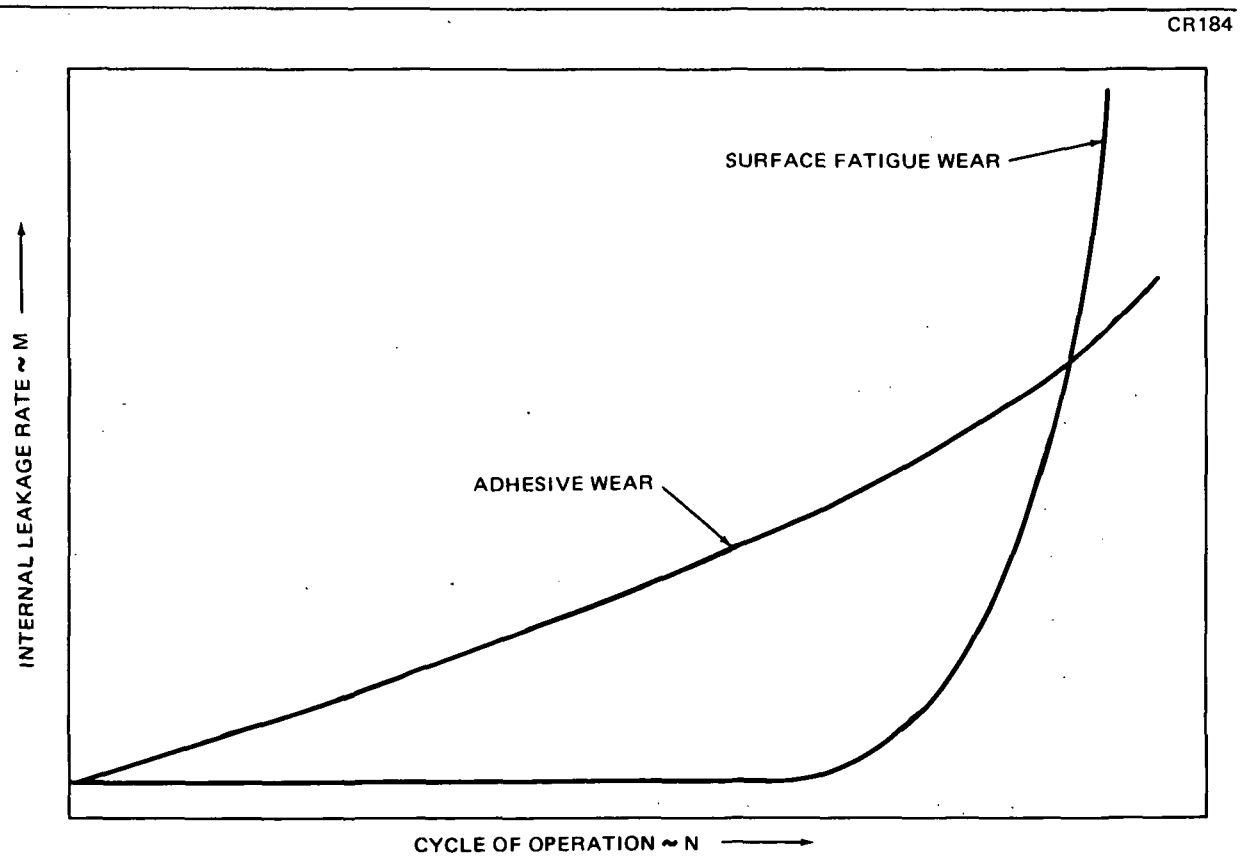

Figure 3-1. Leakage Characteristics of Valve Seal Closures

3.1.1 Valve-Seat Loading Analysis

To evaluate the cycle-life characteristics of the valve sealing surfaces under different conditions of seat loading, tests were conducted at various levels of the relative stress factor (seat loading).

The importance of the relative stress factor was unknown at the time of selection; however, it should prove to be a valuable tool for the design of long-life components. The relative stress ratio is the ratio of the apparent seat stress of the sealing member to the yield strength of the weaker of the two sealing materials. This ratio is also an index of the amount of surface area which has plastic deformation of the asperities under the prevailing conditions of load. Since it is desirable to evaluate the significance of this ratio over the broadest range possible, 4 to 90 percent, the conditions shown in Table 3-1 were selected for testing.

To investigate the RSF values in the upper load range, a plastic material was applied to one of the valve sealing surfaces so that sufficient force can be generated to provide the higher relative stress values. The material combinations selected for investigation are assumed to have the following yield strength:

A286 (Seat)	6.89×10^8 N/m^2 (100,000 psi)
Inconel 718 (Poppet)	1.2×10^9 N/m^2 (175,000 psi)
23+ Gold Plating (Seat)	2.06×10^8 N/m^2 (30,000 psi)
Teflon "S" (Seat)	3.1×10^7 N/m^2 (4,500 psi)

The material with the lowest yield strength is expected to be the critical material for each test. The Inconel 718 poppet is strong enough to be reasonably stable under the loadings selected and therefore is not included in the relative stress ratio calculation. The design stress (apparent seat stress) in the -1 valve (A286 seat/Inconel 718 poppet) is about 5.5×10^7 N/m^2 (8,000 psi). The ratio of value, $5.5 \times 10^7 / 6.9 \times 10^8$ (8,000/100,000) gives a RSF of 8 percent, which was selected as the baseline test for the entire test series. A value of 16 percent was selected as the baseline value for the gold plated -501 valve. The 16-percent figure is obtained with the -501 valve (Gold Plated Seat/Inconel 718 poppet) loaded to an apparent stress of 3.3×10^7 N/m^2 (4,800 psi). When both valves are run at one-half of the baseline values, the respective relative stress ratios are 4 and 8 percent.

The -503 valve configuration was used to provide cycle-life data in the 40-percent and 90-percent RSF range. These conditions could be met most easily if the seat sealing surface is a plastic coating having a strength in the 2.7×10^7 to 3.4×10^7 N/m^2 (4,000 to 5,000 psi) range. A number of plastic coatings were checked and the only type which was known to fall into this range was the originally selected Teflon S. This material is a single coat, nonstick, self-lubricating finish based on a special fluorocarbon resin and suitable modifier, dispersed in organic solvents. The final coating, after curing, is essentially a dispersion of Teflon FEP in a polyimide matrix.

Table 3-1

TASK I – TEST MATRIX

Test No.	Valve Designation	Seat Material	Seat Stress N/m^2 (psi)	RSF Percent	Valve Actuator Mode	Actuator Return Springs	Compliant Seat Compression mm (in.)	Shim Thickness Utilized mm (in.)	Actuator Pressure N/m^2 (psi)
1	-1	A286	2.76×10^7 (4,000)	4	Double Acting	Inner only	1.1 (0.044)	1.4 (0.056)	8.6×10^5 (125)
2	-501	23+ Gold Plate	1.72×10^7 (2,500)	8	Single Acting	Both	0.57 (0.023)	1.9 (0.077)	8.6×10^5 (125)
3	-1	A286	5.52×10^7 (8,000)	8	Double Acting	Both	2.2 (0.088)	0.3 (0.012)	1.3×10^6 (190)
4	-501	23+ Gold Plate	3.31×10^7 (4,800)	16	Double Acting	Inner only	1.1 (0.044)	1.4 (0.056)	1.3×10^6 (190)
5	-503	Teflon S	1.24×10^7 (1,810)	40	Single Acting	Both	0.5 (0.020)	2.0 (0.080)	8.6×10^5 (125)
6	-503	Teflon S	2.76×10^7 (4,000)	90	Double Acting	Inner only	1.1 (0.044)	1.4 (0.056)	8.6×10^5 (125)

Within the Teflon S series there are two basic subseries, the 953 and the 958. The coating selected for the -503 valve configuration is the 958-203. This coating requires a higher curing temperature than the coatings in the 953 series, however, its physical properties are somewhat better. Since it was desirable to provide the maximum tolerance to reactive propellants, the uncolored 958-212 clear coating was originally specified to avoid unknown effects of pigments. The clear material was not readily available however, so the -203 black coating was selected as a second choice. This coating has the least amount of coloring pigment added to the basic coating and this is considered desirable for the present usage.

The basic materials in the Teflon S coating have been used successfully in reactive propellants and at cryogenic temperature separately; however, no data were found on the coating obtained from the mixture of materials. To provide a preliminary check on the material compatibility of the coating with reactive propellants a group of 10 impact specimen disks (316 CRES) were coated with the selected coating and subjected to 10 m-kg (72 ft-lb) impact test in gaseous oxygen. No reactions were detected in the 10 tests. Several additional drops were made at the 10 m-kg (72 ft-lb) energy level in LN_2. No cracking or flaking of the coating was detected in the 77°K (-320°F) tests. These tests were performed by MDAC using MDAC funds, at no cost to the contract.

The materials and seat stresses selected allowed testing over a fairly wide range of RSF ratios (from 4 percent to 90 percent) and also permitted comparing the 8-percent data taken on two different valves with two different material combinations.

The selected stress values and valve testing configurations are shown in Table 3-1. Conditions for each of the test configurations were calculated using the following steps shown for Test Run No. 1:

A. Known Data

1.	Valve configuration	-1
2.	Seat material	A286
3.	Seat sealing width	0.25 mm (0.010 in.)
4.	Diameter of seat sealing surface	53 mm (2.078 in.)
5.	Spring force - outer spring	556 N (125 lb)
6.	Spring force - inner spring	280 N (63 lb)
7.	Spring force - poppet shaft bellows seal	222 N (-50 lb)
8.	Spring rate - compliant seat bellows	9.6×10^6 N/m (5,500 lb/in.)

9. Actuator piston area — 12.9 cm^2 (2 $in.^2$)

10. Desired apparent seat stress — 2.76 x 10^7 N/m (4,000 psi)

11. Minimum actuator pressure — 8.6 x 10^5 N/m^2 (125 psi)

B. Calculated Data

1. Area of seat surface = 0.42 cm^2 (0.065 $in.^2$)

2. Seating force required = 1.155 N (260 lb)

3. Mechanical force available

Outer spring	556 N (125)
Inner spring	280 N (63)
Shaft bellows	-222 N (-50)
Net closing force =	614 N (138 lb)

4. Required actuator closing force

1156 to 614 = 542 N (260 to 138 = 122 lb)

5. Required actuator closing pressure

$$P = \frac{F}{A} = \frac{542}{0.00129\ m^2} = 4.20 \times 10^5\ N/m^2 \quad \left(\frac{122}{2} = 61\ psi\right)$$

Since it was desired to actuate the valve in both directions with the same regulated gas pressure, the value of 4.18 x 10^5 N/m^2 (61 psi) reverse is not high enough to open the valve in the forward direction 4.18 x 10^5 < 8.6 x 10^5 (61 < 125). To eliminate the problem, the outer spring was removed. Then

6. Mechanical force available

Inner spring	280 N (63 lb)
Shaft bellows	-222 N (-50 lb)
Net closing force	58 N (13 lb)

7. Required actuator closing force

1,156 to 58 = 1,098 (260 to 13 = 247 lb)

8. Required actuator closing pressure

$$P = \frac{1095}{0.00129}$$

$$= 8.5 \times 10^5 \text{ N/m}^2 \left(\frac{247}{2} = 123.5 \text{ or approximately 125 psi}\right)$$

This value was acceptable when no frictional variations were encountered during the test period. To eliminate the possible effects of frictional variation, a second control method was employed; in that, the stroke of the poppet shaft was limited to that value which provided the proper amount of compression of the seat bellows assembly by adding shims between the actuator piston and the actuator housing.

9. Required complaint seat bellows compression

$$t = \frac{\text{load}}{\text{spring rate}} = \frac{1,156}{962} = 1.19 \text{ mm} \left(\frac{260}{5,500} = 0.047 \text{ in.}\right)$$

Assuming a piston position which allows a travel of 2.54 mm (0.100 in.) after first contact is made between the poppet and seat, the shims required were

2.54 mm - 1.19 mm = 1.35 mm (0.100 in. - 0.047 in. = 0.053 in.)

After adjusting the actuator piston shims to limit the seat compression to the desired 1.19 mm (0.047 in.), it was possible to increase the actuator driving pressure somewhat (to overcome friction) to insure that the seat stress for each stroke was always the selected amount. This increased pressure was adjusted so that positive closing was assured but was not adjusted higher than necessary. A potential problem was anticipated from the shock of the valve closing forces producing a bellows "ringing effect" such as was experienced on the NAS3-12029 program (at proof pressures) if the actuator driving pressure was adjusted higher than necessary to insure proper valve operation. It had been anticipated that a very smooth valve action would be obtained using the listed valve actuator pressures; and, this smoothness was verified with the acoustical signature monitoring equipment under actual test conditions.

3.1.2 Valve Modifications

The valve actuator was redesigned to permit operation of the test valves in a double-acting mode and a set of modified parts fabricated. After installing the modified parts in the -1 test valve, a preliminary cyclic operational checkout was made at the test site. The valve operated satisfactorily in the double-acting mode. The actuator leakages were found to be acceptable in both the normal and reverse direction.

These modifications were made to permit the actuator to operate in a double-acting mode for the Task I Cycle Tests and to provide positive piston travel

stops for adjusting the seat loading values and the maximum stress in the main shaft bellows seal. Specifically, these modifications (shown in Figure 3-2) included:

A. Actuator Piston Seal - The original piston actuator seal used on the 1T32095 valve (Parker No. 5696040) was a directionally pressurized Omniseal No. ARI 0110-223A1Q. This seal was replaced with a standard MS29561-130 O-ring and one MS28774-130 backup ring. These two parts were installed into the existing valve-seal groove through the use of the special seal retainer 1T41973 provided for this application. The seal retainer was made of aluminum, the O-ring of Buna-N rubber, and the backup ring of Teflon. While this change was accomplished without remachining the valve parts, some restrictions were placed on the selection of O-rings which would fit the assembly. The -130 size O-ring fits the assembly properly; however, this size of O-ring is not normally recommended for dynamic service. This size restriction caused a reduction in piston seal life; however, since the rings could be replaced readily, the loss of seal life was not a serious problem.

B. Poppet Shaft Seal - The portion of the actuator cavity which was subjected to the reverse pressure required a seal where the actuator shaft went through the main actuator housing as shown on Figure 3-2. This seal was needed to prevent pressure equalization between the actuator piston and the shaft seal bellows since this would have equalized the simulated shaft loading forces. These forces were necessary to obtain the desired seat stress in the valve when there was no pressure differential across the valve poppet. This requirement was applicable to the life-cycle tests only (double-acting actuator mode) and no permanent modification of the valve was warranted. Therefore, a new shaft seal was designed which would fit into the inner spring-retainer well without altering the basic valve hardware. This new seal consisted of a Teflon shaft seal (1T41974) and a CRES seal loading spacer (1T41975). The spacer permitted the main valve inner return spring to provide the seal loading forces which were needed at the seal sealing lip. This arrangement was selected over the conventional garter spring-loaded lip seal because of the size limitations of the spring retainer cavity.

While the new seal design was generated to fit an existing set of design limitations, the new design appears to be applicable to other similar configurations and therefore was reported under the "New Technology Clause" of this contract. The basic configuration of this seal arrangement is shown in Figure 3-3. Preliminary studies of this new seal configuration indicate that a greater degree of control of the seal loading forces are possible with the new seal arrangement as compared to a conventional spring-loaded lip seal and, for certain applications, improved seal performance would be expected. The limited amount of testing which was completed on this program showed acceptable seal performance with the new seal design.

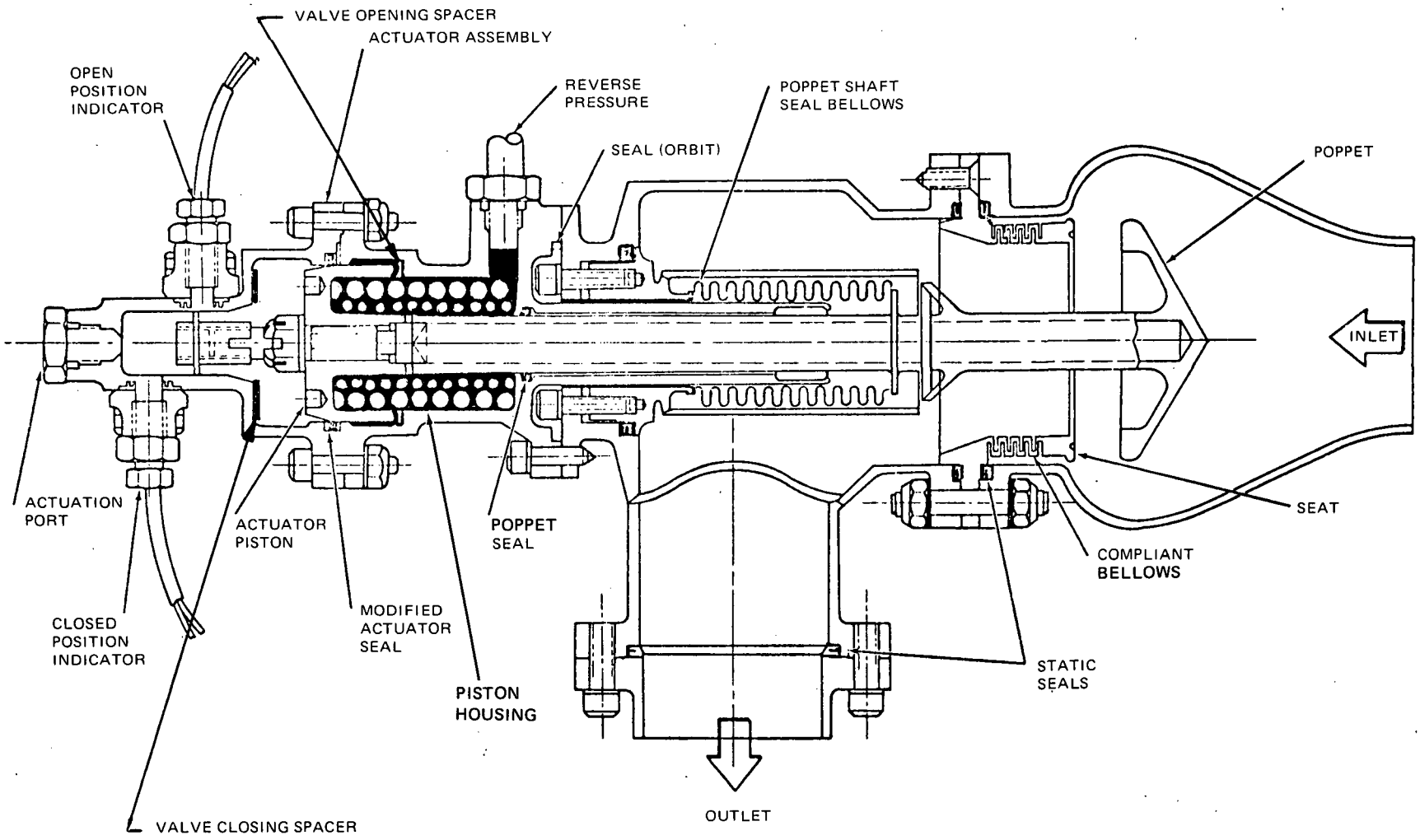

Figure 3-2. Poppet-type Shut-Off Valve Design

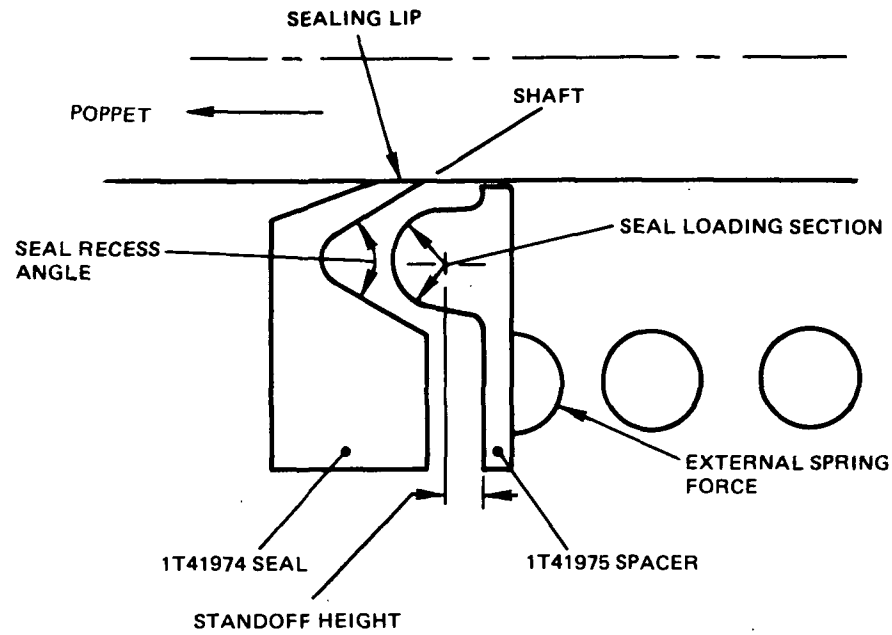

Figure 3-3. New Seal Design for Poppet Shaft

C. Valve Opening Spacer - A valve-opening spacer (1T41971) was designed to limit the valve opening stroke of the valve during the life cycle tests. The normal valve-opening stroke of 12.7 mm (0.500 in.) was reduced by this spacer to a value of 9.5 mm (0.375 in.). This shortening of the valve stroke was incorporated to reduce the peak fiber stresses in the shaft seal bellows and increase the cycle life of the bellows so that more cycles of operation could be completed on the valve selected for the -503 configuration modification.

The valve opening spacer was fabricated from soft aluminum material. Since the normal end-stop was the shoulder of the aluminum actuator housing, the addition of the aluminum spacer did not change the overall characteristics of the dynamic system.

D. Valve Closing Spacer - A valve-closing spacer (1T41972-1) was designed to limit the travel of the main poppet shaft when the valve was in the closed position. A series of these aluminum spacers were available so that a positive control of seat sealing stress could be obtained. The spacers were designed to permit the desired amount of compression in the main seat bellows (compliant seat) but to limit the travel so that no overload could be obtained. Since the actuator was pressurized in the reverse direction for valve closing (double-acting mode) and since the actuator seals were expected to leak at

a greater rate in the reverse direction, it was necessary to supply enough actuator pressure to overcome the seal leakage and insure that the piston travel was sufficient to provide the required compression in the compliant seat. By bottoming the actuator piston on each stroke, a positive control was maintained on each valve cycle with no possibility of overloading the seat sealing surfaces.

3.1.3 Acoustical Monitoring Equipment

As a separate part of the cycle life-test program, an evaluation was made of using acoustical monitoring equipment for the determination of the valve mechanical condition and internal leakage rates.

The technique of using the acoustical vibration of an operating mechanism to determine the rate of failure was recently developed into a potentially useful tool. Many mechanical failures are determined by audio detection; for example, most failures of the normal automobile are first determined by detection of an unusual noise coming from the failing part. In most cases, the part has already failed when the acoustic level reaches the audible range of sound. With the acoustical signature method of testing, the normal acoustical patterns of a nominally operating part are determined and then changes from this baseline signature are used to detect potential failures in advance of the final complete failure of the mechanism.

Two acoustic signature analysis systems were employed for monitoring changes in the test valves on this program. One system, manufactured by Dunegan Research Corporation, consists of a transducer and preamplifier. The transducer active element was a PZT-5 ceramic which was ground for a resonant frequency of approximately 110 kHz. The preamplifier provided a fixed gain of 60 db and was used with and without internal frequency filtering. With filtering, the response was flat from 100 kHz to 300 kHz. Without filtering, the response of the transducer/preamplifier system was approximately 20 kHz to 500 kHz. The transducer was attached to the valve using a coupling which allowed the vibrations to be transmitted from the valve to the transducer. This system provides relatively high-frequency vibration information. Another system, consisting of an Endevco accelerometer and an Unholtz Dickie charger amplifier, was used to monitor the lower-frequency vibrations up to approximately 20 kHz. The output signals of these two systems was amplified for analysis as shown in Figure 3-4. Both types of sensors were mechanically attached to each of the valves at the inlet adapter flange.

By switching connections at the preamplifier, charge amplifier, and oscilloscope, signals from each of the four sensors (two in each valve) could be displayed as required. Photographs of the waveform were taken periodically during the testing and compared for indication of wear or damage.

The acoustic leak detection system is related to the acoustical signature process, but differ in certain key respects. With the acoustic leak detection system it is possible to detect the acoustic energy output from a leaking source, amplify the signal, and then calibrate this output against a known leak for measurement purposes.

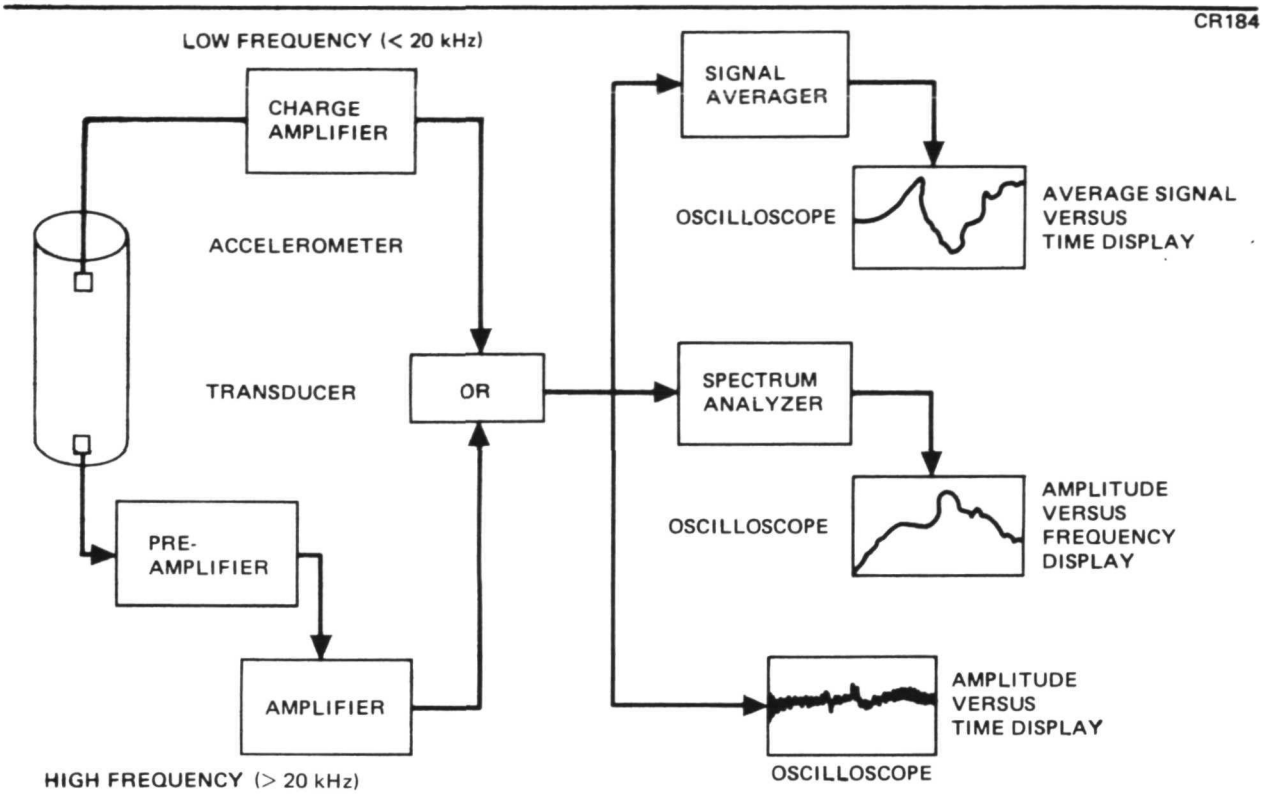

Figure 3-4. Acoustical Signature Instrumentation

The two types of leak detection systems, which were available at MDAC, were used for this program. Both sensors were mechanically mounted side by side, on a special mounting flange which was bolted to the inlet adapter. The first was the ultrasonic system which operates at frequencies higher than the normal acoustical range. With this arrangement the sensor was designed to be responsive to signals in the 36 to 44-kHz range which was the peak output of energy for a gaseous leakage through an orifice if the flow was in the turbulent region. The ultrasonic system was relatively insensitive to leakage in the lower laminar-molecular flow regimes. Since the normal leakage of the valve is in the laminar flow regime, no signal would be picked up by the ultrasonic equipment unless a gross failure occurred. It was expected that if the leakage entered the turbulent range, the ultrasonic system would have been able to detect this difference. A direct reading Delcon ultrasonic translator detector, Model 118, was evaluated for this service.

In addition to the ultrasonic system, the conventional sonic frequency equipment was found suitable for acoustical leakage measuring techniques under certain conditions. With this system, the lower frequency signals were not filtered out, so that a broader frequency range could be monitored. The output of the sonic equipment was somewhat lower than the ultrasonic equipment; however, it should have been useful for leakages which are in the molecular-laminar flow regimes. A direct reading Goldak Leak Hunter, Model 727, was evaluated for this program. The Goldak sonic system (with a contact type pickup) should be capable of providing direct readouts for the leakage rates anticipated for the cycle life tests and with proper calibration could have been more useful than the ultrasonic system.

3.1.4 Valve Refurbishment

The -1 and -501 test valves were disassembled and the poppets and seats from the two valves were sent to the vendor for relapping of the main sealing surfaces. The parts which were relapped consisted of two 5696031 (Part Number) Poppet Assemblies and one 5696013-2 Valve Seat and one 5696013-3 Valve Seat, the -2 Valve Seat being the unplated A286 seat and -3 Valve Seat being the gold plated A286 version. The four parts were optically inspected before relapping, and it was found that the poppet and seat from the -501 valve were in good condition even after storage for the 9 months which had elapsed since the completing of the testing accomplished on Contract NAS 3-12029 and reported in CR 72690 (Reference 4). The valve seat from the -1 valve was found to have developed some small pin holes in the unplated A286 material. This seat was therefore inspected with the interferometer and photographs were taken of the surface damage. Figure 3-5 is a microphotograph of a typical damaged area and Figure 3-6 is an interferometer photograph of the same general area.

These random pin holes were found to be 0.026 to 0.05 mm (0.001 to 0.002 in.) in diameter and not very deep. The pin holes were removed by the first lapping operation, without the seat width being increased to an unacceptable value. The poppet for the -1 valve had developed a minor leakage problem on the previous program and an attempt had been made to improve the flatness of the poppet by relapping the sealing surface at the MDAC Test Site using a copper lapping tool. This tool was not found to be acceptable and the relapping which was accomplished with the copper tool was not within the flatness or the smoothness specification. The work on the previous program was completed by substituting the -501 poppet shaft in the -1 valve assembly and setting the -1 poppet assembly aside for rework on this contract (Reference 4).

The two poppet assemblies were relapped by using a new AL_2O_3 lapping tool and using AL_2O_3 lapping compound. Both poppet assemblies were relapped to a surface finish of less than 2 microinches and both were flat and true within 6.25×10^{-5} mm (2.5 millionths in.) after relapping. It was necessary to remove more metal from the -1 poppet to obtain the proper flatness. It appeared that the poppet sealing surface had deformed to a slightly conical angle instead of being perpendicular to the poppet shaft centerline as specified; however, no waviness was noticeable around the circumference of the sealing area. No difficulty was experienced in bringing the poppet sealing surfaces back to the specified conditions.

The two seat-sealing surfaces were relapped using a diamond lapping compound and no difficulty in lapping was encountered on either valve seat. The A286 seat refinished to a surface finish of less than 1μ finish. Since the seat sealing surface is on the end of a flexible machined bellows, the flatness of the seat surface cannot be measured as readily as can the rigid poppet shafts. By using an optical inspection technique, it appears that both seat surfaces were within the specified flatness figures; however, it was necessary to conduct the Task 1 leakage tests before a final evaluation could be made. The seat width on the A286 seat was 0.31 mm (0.012 in.) after lapping and on the gold plated seat was between 0.18 mm (0.007 in.) and 0.25 mm (0.010 in.) [0.25 ± 0.05 mm (0.010 ± 0.002 in.)] is the design value.

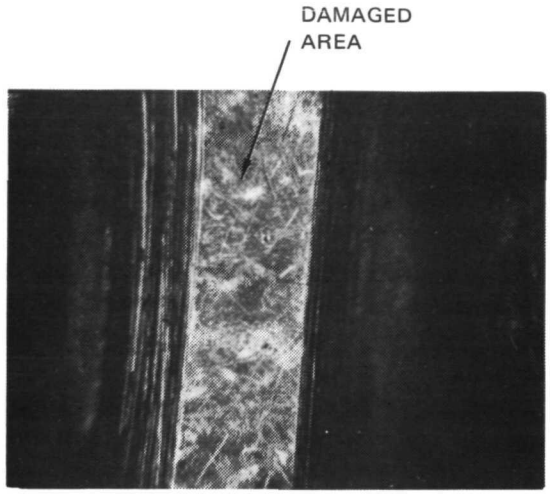

Figure 3-5. Microphotograph of -1 Valve Seat (A286) Damage (60X)

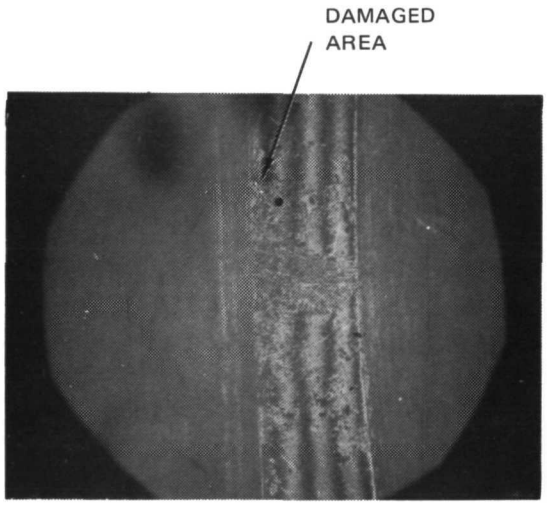

Figure 3-6. Interferometer Photo of Damaged Area of -1 Valve Seat (A286) (60X)

The two test valves were assembled and a leakage test was made to determine the internal leakage rates of each valve. Both valves were found to leak at an unacceptable rate. The -1 valve leakage was over 5 SCCM at 7 x 10^5 N/m^2 (100 psig) and the -501 was over 3 SCCM. The two valves were disassembled and inspected. It was found that the seat sealing surface on the A286 material used on the -1 valve had developed a new series of pin-hole deformations over the entire sealing surface. These pin holes were visible optically, using reflected light, without the aid of a microscope. Microscopic inspection verified the random nature of these small surface defects. Since these defects were not visible under microscopic examination before the valve was reassembled, it appeared that this pin-holing effort resulted when the full seat stresses were applied to the sealing surfaces during the leakage tests. The nature of the defects indicated that a form of intergranular corrosion had occurred at the surface during the storage period (after the fluorine tests). Since the valve seat had been ultrasonically cleaned after the relapping operation and before the microscopic examination, it appears that the very light pressures used in the relapping operation were not heavy enough to disturb the weakened surface; however, the surface failed under the 5.5 x 10^7 N/m^2 (8,000 psi) design stress during the leak test. This type of failure was probable since almost all metals show changes in the surface characteristics under exposure to atmospheric moisture after service in a fluorine system. Most metals, copper in particular, are normally bright and shiney when first removed from a fluorine system; however, discoloration starts taking place upon exposure to the atmosphere and complete discoloration occurs over a period of time. Even though the A286 material did not show a significant amount of discoloration, it appears that surface damage was occurring during the storage period.

The inspection of the gold plated -501 seat assembly revealed that no detectable surface damage of this seat had occurred during the storage period; however, the appearance indicated that the bumper clearance was insufficient, and the resulting interference did not permit the seat to load properly around the complete circumference.

No damage or defects of either of the Inconel 718 poppet assemblies were detected.

To correct the difficulties with the two seat assemblies, both units were returned for additional work. The first step of the extra rework on the -1 seat consisted of relapping the sealing surface until all of the pin-hole damage was removed. Enough material was removed to just eliminate the pin holes. This material removal resulted in an increase in the seat width to approximately 0.5 mm (0.020 in.) from the existing 0.3 mm (0.012 in.). Since the original flat sealing surface was placed on the edge of a radius portion of the seat, it was possible to calculate the depth of material removed. Assuming that the original radius was within design limits, a total of 0.008 to 0.010 mm (0.003 to 0.004 in.) was removed before all traces of the surface damage were removed.

The amount of material removal indicated that the surface damage was very shallow. However, sufficient material was removed to eliminate all clearance between the bumper and seat heights, and the final lapping was removing material from both the bumper and from the seat sealing surface. The next

step in the rework consisted of grinding a bevel on the inside angle of the seat (as shown on Figure 3-7) so that the seat width was returned to the original width of 0.25 mm (0.010 in.). After the grinding was finished, a new lapping tool was made which permitted lapping down the surface of the bumper without touching the seat sealing surface. This permitted the undercurring of the bumper height to the original value of 0.008 to 0.013 mm (0.0003 to 0.0005 in.). After the seat width and bumper height were returned to the original dimensions, a final light-lapping operation was used to dress the seat sealing surface. This final lap brought the sealing surface down to the specified 5×10^{-5} mm (2 μin.) AA finish, although the final surface did not have a theoretically circular lay.

The seat assembly for the -501 valve was refinished in one operation. This consisted of lapping the bumper surface down until the seat-to-bumper height was returned to the specified 0.008 to 0.013 mm (0.0003 to 0.0005 in.).

Both of the two test valves were reassembled at the A12 test site and the leakage rates measured. The -501 valve leakage rate was measured at 0.3 SCCM at 7×10^5 N/m^2 (100 psig) and the -1 at 1 SCCM at the same pressure. Both values were considered acceptable for the purposes of the Task 1 test effort.

3.1.5 Valve Modification and Pretest Checkout

The schematical arrangement of the Task I setup is shown in Figure 3-8. The actual test setup arrangement is shown in Figure 3-9 and the acoustical monitoring equipment is shown in Figure 3-10. The cycle counter arrangement consisted of two electrical actuated counters which were triggered by the signal to the actuation solenoid and a separate system which recorded the valve open position indicator traces. With this arrangement, the electrical counter provided an easily read total cycle count which was accurate for all valve opening commands; however, since it was possible that one of the valves could fail to operate even when commanded to open, a secondary count system was used. This secondary backup system consisted of recording the opening position indicator trace on a Brush recording instrument.

This backup system was not easily read since it required counting each of its 100,000 signal peaks individually for each valve (200,000 for double testing) and, therefore, this system was not used as the primary counting system. The secondary system could be easily scanned for discontinuities in the valve actuation traces, however, and if either valve failed to operate, it was possible to count the exact number of cycles completed before failure by counting individual signal peaks back to the start of the test period in which the failure occurred. By indexing the recording paper with the electric counter count at each leak check point, a minimum number of points required a hand count in case of a valve failure.

The instrumentation and equipment used on the Task I testing are shown in Table 3-2.

After completion of the basic cycle-life test setup, the two valves were modified to provide the required configurations for test No.'s 1 and 2 (Table 3-1). For these tests, the -1 valve was modified for double-acting actuation and

CR184

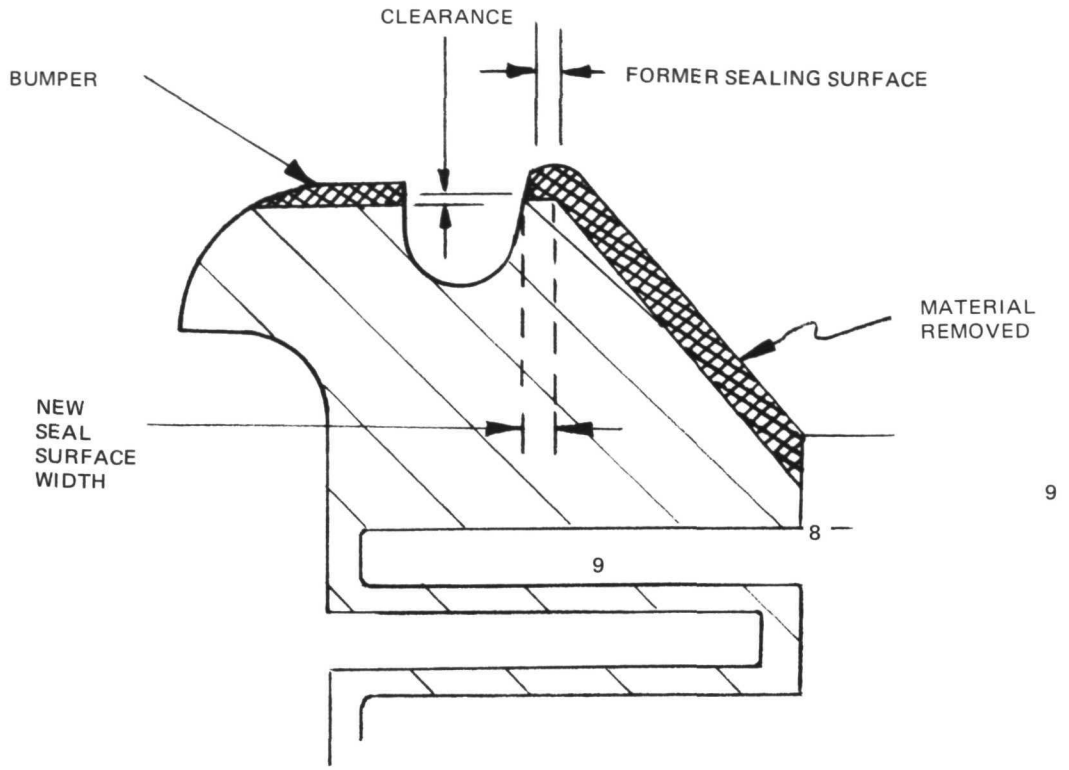

Figure 3-7. Valve Seat Refurbishment, −1 Valve

CR184

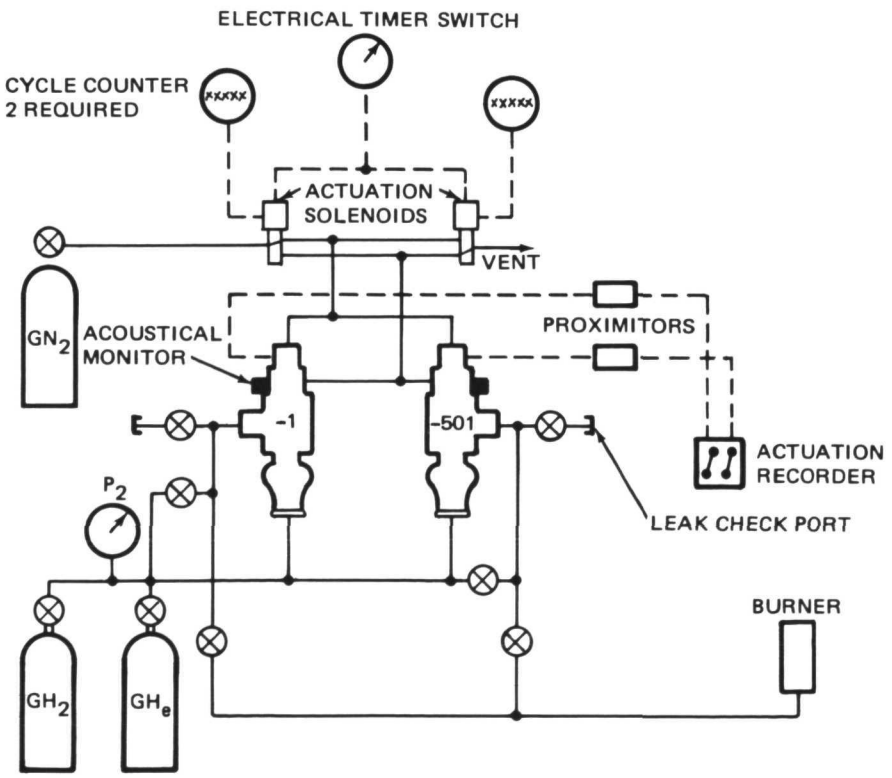

Figure 3-8. Cycle-Life Test Setup

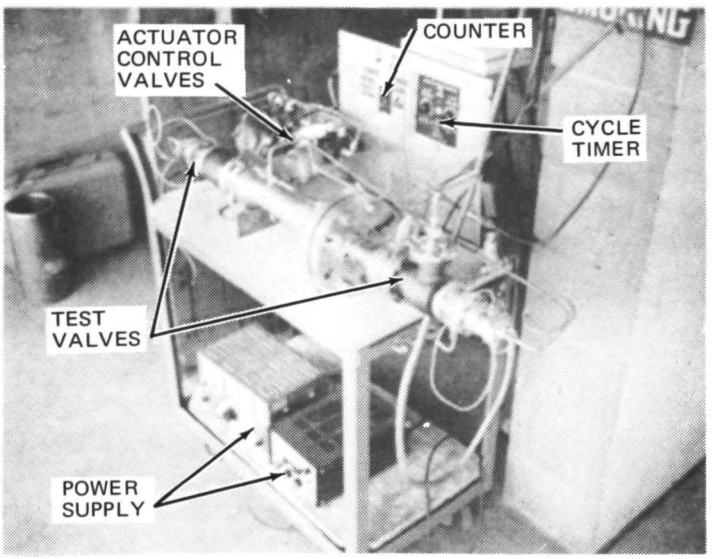

Figure 3-9. Test Setup of Task I Cycle Tests

CR184
N/A

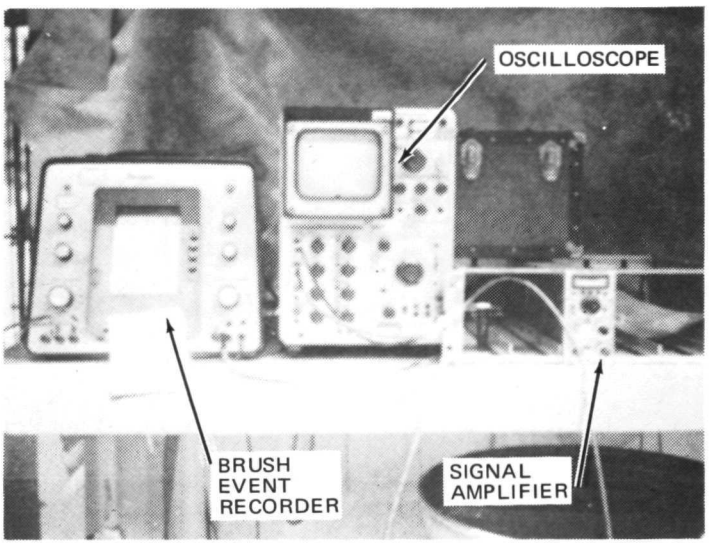

Figure 3-10. Acoustical Monitoring Instrumentation

Table 3-2

INSTRUMENTATION REQUIREMENTS – LIFE TEST

Parameter	Transducer	Range	Accuracy	Readout	Comments
Valve inlet pressure	---	0 to 1.7×10^6 N/m^2 (0 to 250 psig)	$\pm 1.7 \times 10^4$ N/m^2 (±2.5 psi)	Gage	
Valve outlet pressure	---	0 to 1.7×10^6 N/m^2 (0 to 250 psig)	$\pm 1.7 \times 10^4$ N/m^2 (±2.5 psi)	Gage	
Actuator supply pressure	---	0 to 4.1×10^6 N/m^2 (0 to 600 psig)	$\pm 4.1 \times 10^4$ N/m^2 (±6 psi)	Gage	
Valve poppet position (Open)	Proximity detector	---	---	Connector	Supplied with valves (Bently Nevada – Model 304)
Valve poppet position (Closed)	Proximity detector	---	---	Connector	Supplied with valves (Bently Nevada – Model 304)
Acoustic signature	PZT-5 Ceramic	---	---	Oscilloscope (Camera)	Amplitude versus time and frequency
Acoustic signature	Accelerometer	---	---	Oscilloscope (Camera)	
Ultrasonic leak detection	---	---	---	Gage	Delcon Ultrasonic Translator Detector, Model 118
Sonic leak detection	---	---	---	Gage	Goldak Leak Hunter, Model 727
Valve body temperature	Thermocouple (Cu-Cn)	61°K to 312°K (-350 to +100°F)	3°K (±5°F)	Meter	

shims were installed to limit the poppet travel in the opened and closed position. The -501 valve was left in the single acting actuator configuration and the only change in this valve was the installation of the valve opening travel limit shim. Since the two existing springs provided sufficient force to load the seat sealing surface to the proper stress level, the reverse actuation pressure was not required. Since no reverse pressure was required, it was not necessary to install the valve-closing shims because there was no way that the springs can load the seat to a value greater than was desired. The two valve assemblies were then given pretest internal leakage tests in their final test configuration. The following leakage rates were measured:

Upstream Pressure	Temperature -1 Valve		Temperature -501 Valve	
	Ambient	77°K	Ambient	77°K
1.7×10^5 N/m^2 (25 psig)	1.9 SCCM	10 SCCM	0.65 SCCM	0.8 SCCM
3.5×10^5 N/m^2 (50 psig)	4.4 SCCM	19 SCCM	1.3 SCCM	1.4 SCCM
7×10^5 N/m^2 (100 psig)	8.4 SCCM	42 SCCM	2.4 SCCM	2.4 SCCM

It should be noted that the thermal stabilization of the valves during the 77°K (-320°F) leakage tests was very poor apparently due to the effects of the mass of the test adapters which were mounted with each valve.

The test adapter used on the -1 valve has a much greater mass than that of the adapter used for the -501 valve and this fact may have accounted for some of the difficulty in getting stable leakage reading. Since the -1 valve was shimmed to reduce the seat stress during the reverse pressure actuation mode, the absolute values of the leakage measurement was not comparable to the leakage rates obtained under the normal design conditions.

The change in leakage rate with cycling should be significant, however, once the baseline off-design condition values were obtained. For the purposes of comparing changes in leakage rates over the test period, the respective ambient GHe readings at 7×10^5 N/m^2 (100 psig) was used as the baseline values. This gave a value of 2.4 SCCM for the -501 valve and 8.4 SCCM for the -1 valve. Both values are reasonable considering the surface finish existing on each valve and the loading condition imposed by the test setup. The final baseline reading is taken after approximately 1,325 cycles of operation had been completed by each valve in GHe for the purposes of checking out the test setup and the acoustical monitoring equipment.

The acoustical signature monitor equipment for the mechanical condition of the valves had received a preliminary checkout and acoustical signature traces of both valves obtained. The opening and closing traces of the accelerometer mounted on the -1 valve is shown in Figure 3-11. The upper trace shows the slower opening cycle and the lower trace shows the corresponding closing trace. The photos are taken with the oscilloscope set in the external triggered mode and with the camera shutter held open for one complete open-close cycle sequence. This method allowed the first trace taken to appear on the upper trace channel and the second trace to appear on the lower channel without regard as to which was the opening and which the closing cycle. While

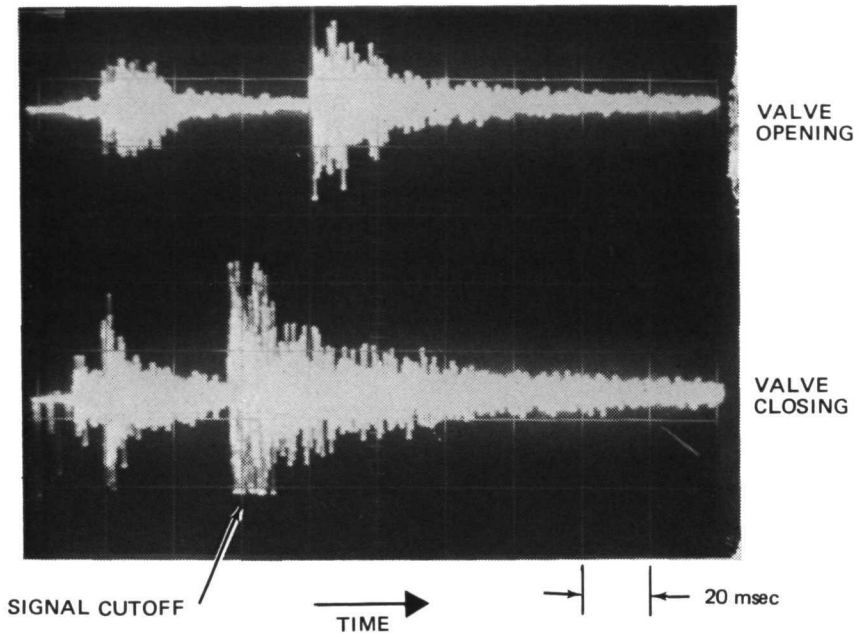

Figure 3-11. Accelerometer Trace of -1 Valve

either trace could have been in the top position on the film, there was no problem identifying the two traces due to the difference in time response between the opening and closing cycles. Since the valves open against the force of the return springs, the opening time is greater than the closing time interval and a greater time interval shows on the trace between the start and stop peaks on the signal. Each trace was sweeping from left to right in the photo with the start of the trace controlled by the electric signal to the actuation control solenoid. The time base used on Figure 3-11 gives 20 milliseconds per division. The trace shows a 20-msec actuation pressure buildup period and a 60-msec valve travel trace. The valves were operated at 8.6×10^5 N/m^2 (125 psig) actuation pressure without restricting orifices in the actuator inlet lines (normally driven at 3.1×10^6 N/m^2 (450 psig) with 1.27 mm (0.050 in.) restrictor orifices). This trace shows a very mild start-up transient, a very smooth valve motion and a relatively mild poppet stop transient. No indication of ringing in either of the bellows was indicated. The closing trace shows a shorter start-up transient which was normal (springs force and reverse pressure force both in the same direction), a shorter period of valve poppet travel and a somewhat more severe valve stop transient. It should be noted that the accelerometer used shows a signal cutoff characteristic on the valve closing stop transient which was not desirable. This trend is shown by the row of dots along the bottom of the stop transient trace.

The signature trace of the -1 valve taken with a Dunegan Research Corporation transducer (Model DRC-5140B-41) is shown on Figure 3-12. Note that in this case the closing trace is shown in the top trace position and that the

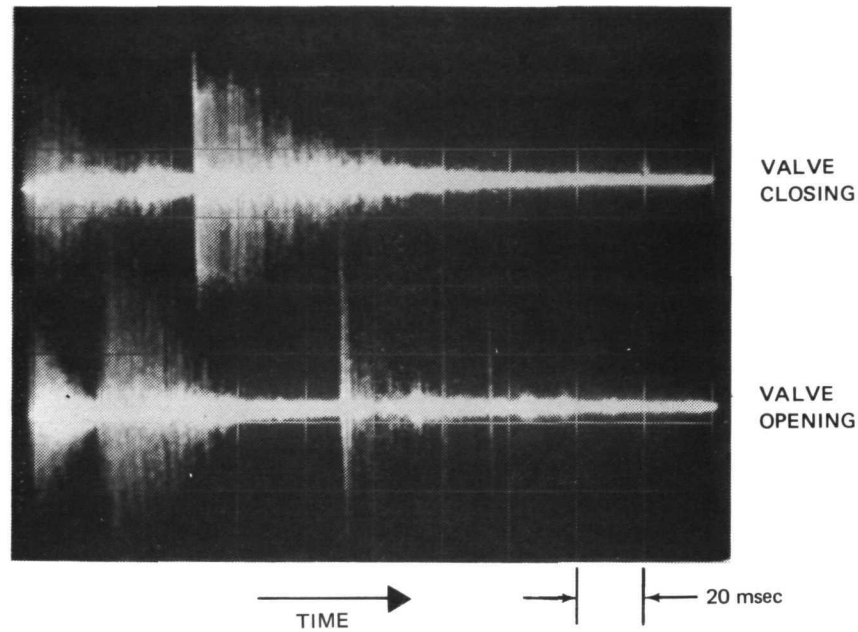

Figure 3-12. Transducer Trace of -1 Valve

closing trace envelope is very similar to the one obtained with the accelerometer. The opening trace shown in the lower position appears to differ considerably from the opening trace taken with the accelerometer (Figure 3-11). This indicates that the transducer is more sensitive to the changes in gas pressure and less sensitive to the mechanical range of frequencies. This is indicated by the amount of signal dispersion observed during the pressure buildup and valve travel phases as compared to the somewhat limited signal strength observed at the point the valve reaches the full-open end stop.

The accelerometer traces taken on the -501 valve are shown in Figure 3-13. Note that the opening trace (top of photo) is similar to the trace obtained on the -1 valve except that a resonant characteristic is observed at about 100 milliseconds after the full-open position is reached and also that the opening trace signal shows signal cutoff for this pickup. While the amplitude of the resonance did not appear to be very great, a frequency response analysis was made to identify the source of the disturbance. The closing trace is very similar for both valves; however, the -501 closed in a shorter time period. Since the -501 is operating in the single-acting mode and therefore does not contain the extra shaft seals required for operation in the double-acting mode, the difference in closing time interval was probably due to the difference in seal frictions between the two arrangements. The closing traces for both valves appear to be very smooth and no serious resonant conditions were indicated by these oscillograph traces.

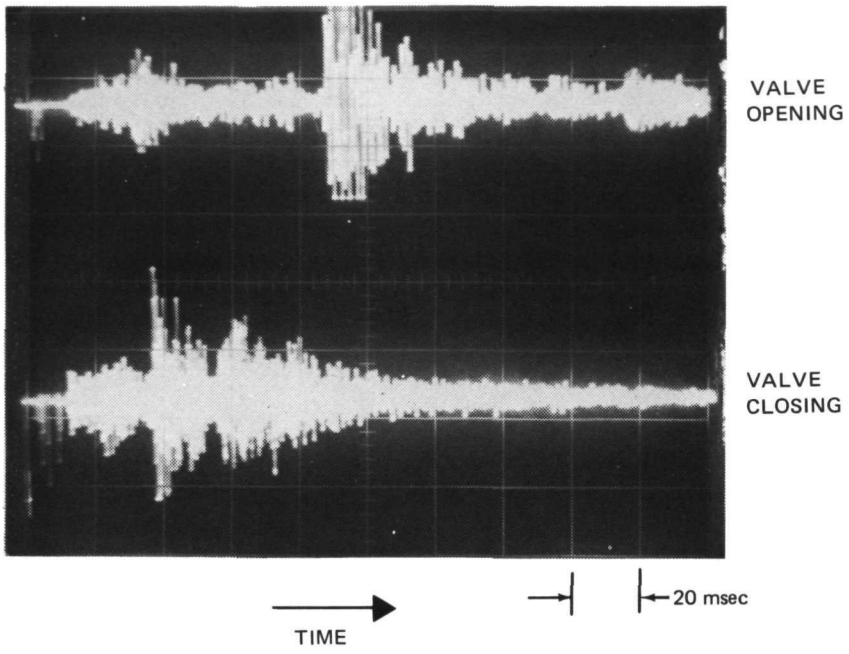

Figure 3-13. Accelerometer Trace of -501 Valve

The transducer trace for the -501 is shown in Figure 3-14. This trace shows the faster time response of the present -501 valve configuration and does not indicate the presence of any unusual harmonic disturbances.

3.1.6 Valve Cycle Life Tests and Results

3.1.6.1 Test No. 1 and 2

Test No. 1 and 2 were run concurrently at Unit 9, A12 location with GH_2. The No. 1 test was conducted using the -1 valve (A286-Inconel 718 combination) loaded to a relative stress level (RSL) of 4-percent. This relative stress level was obtained at an apparent seat stress of 2.7×10^7 N/m^2 (4000 psi). The -1 valve was cycled in the double acting mode with an actuation pressure of 8.6×10^5 N/m^2. The No. 2 test was conducted using the -501 (Gold Plate-Inconel 718) loaded to a RSL of 8-percent. This RSL was obtained at an apparent seat stress of 1.72×10^7 N/m^2 (2,500 psi). The -501 valve was cycled in the normal single acting mode with an actuation pressure of 8.6×10^5 N/m^2 (125 psig). A gaseous helium leakage reading was taken at the end of the checkout period for each valve. These readings were taken as the official start values for each valve and are shown as the 0 cycle numbers in Table 3-3. The system was then pressurized with GH_2 at 7×10^5 N/m^2 (100 psig) and the cycle testing started.

The leakage rate on the -1 valve increased almost 100-percent after the first valve cycle in GH_2 (but had not increased with 1,500 cycles in GHe

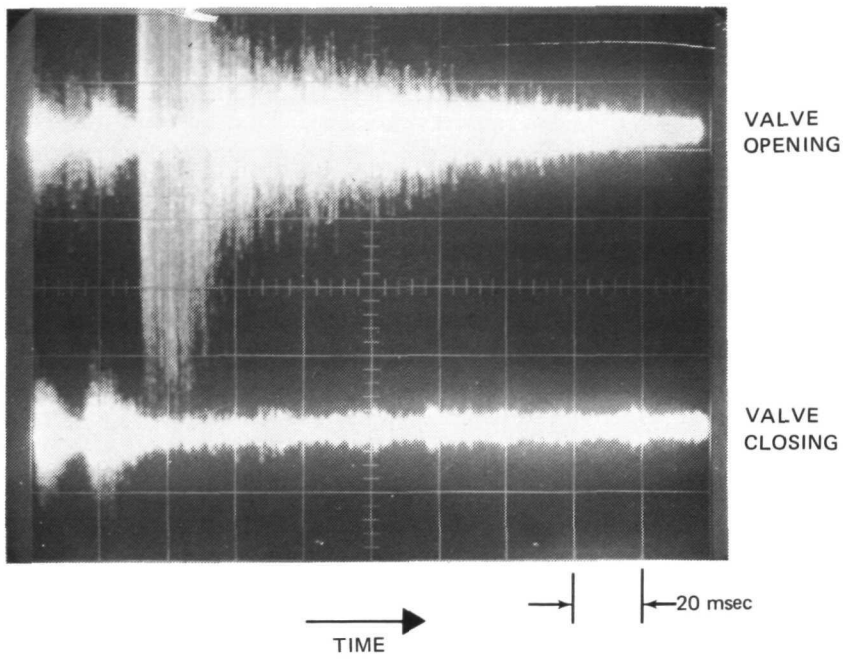

Figure 3-14. Transducer Trace of -501 Valve

during system checkout). The leakage rate of the -1 valve increased continually until 10,000 cycles were completed and then remained fairly constant until the readings were taken after 40,000 cycles. At 40,000 cycles, a large increase in leakage was observed and the leakage rate was found to be in excess of 10 times the start value. The -1 valve was removed for inspection. A quick inspection revealed that reactions had occurred in the sealing surface area of the poppet and seat and therefore the No. 1 test was terminated.

The -1 valve was disassembled and inspected after the excessive leakage rates were measured. It was found that a complete ring of black material surrounded the seat contact area of the poppet. This material appeared to be a "sooty" material which could be wiped off easily by rubbing the surface. After testing a small area with a cleaning rag, the remainder of the deposits was left intact and the valve poppet taken to the MDAC Chemical Laboratory.

The deposits were removed in the Chemical Laboratory and a series of chemical analysis was made. The first test was completed on the electron microprobe to check for the presence of residual fluorine in the deposits. No fluorine was detected.

An analysis of the electron shell spacing was made next (Electron Defraction) and this analysis indicated that the material which had a true crystalline form was the alloy A286. This result was anticipated from the visual damage which was detected on the seat sealing area and shown in Figure 3-15 and 3-16. In addition to the crystalline material detected, a

Table 3-3

TEST RESULTS OF CYCLE-LIFE TESTS – INTERNAL LEAKAGE AT 7 x 10^5 N/m^2 (100 psig) UPSTREAM PRESSURE AND AMBIENT TEMPERATURE

No. of Cycles	GHe Leakage Rate (SCCM) Test No.						
	1	2	3	4	4*	5	6
0	8.33	2.47	8.9	1.9	0.36	0.48	0.1
1	15.6	2.27	8.3	3.1	0.26	0.49	0.1
10	16.2	2.25	9.6	3.1	0.30	0.39	0.1
100	22.3	1.95	9.2	2.44	0.24	0.32	0.1
500	41.2	2.2	8.0	2.6	0.22	0.34	0.0
2,000	73.7	2.23	10.2	3.1	0.18	0.26	0
5,000	82.7	2.35	19.2	4.0	0.42	0.31	0
10,000	72.5	2.26	43.0	4.3	0.48	0.38	0
17,500	72.3	2.1	70.6	5.4	0.54	0.40	0
25,000	64.5	2.48	--	5.8	1.04	0.36	0
32,500	70	2.11	--	6.2	0.82	0.45	0
40,000	105	2.12	--	6.74	1.0	1.08	0
47,500		2.24	--	6.90	0.9	--	0
55,000	--	1.96	--	3.91	0.9	2.63	0
62,500	--	1.88	--	--	0.8	2.60	0
70,000	--	2.05	--	--	0.8	2.0	0
77,500	--	2.26	--	--	0.8	1.73	0
85,000	--	2.06	--	--	0.75	1.73	0
92,500	--	2.16	--	--	0.75	1.73	0
100,000	--	1.96	--	--	0.6	1.73	0

*Rerun

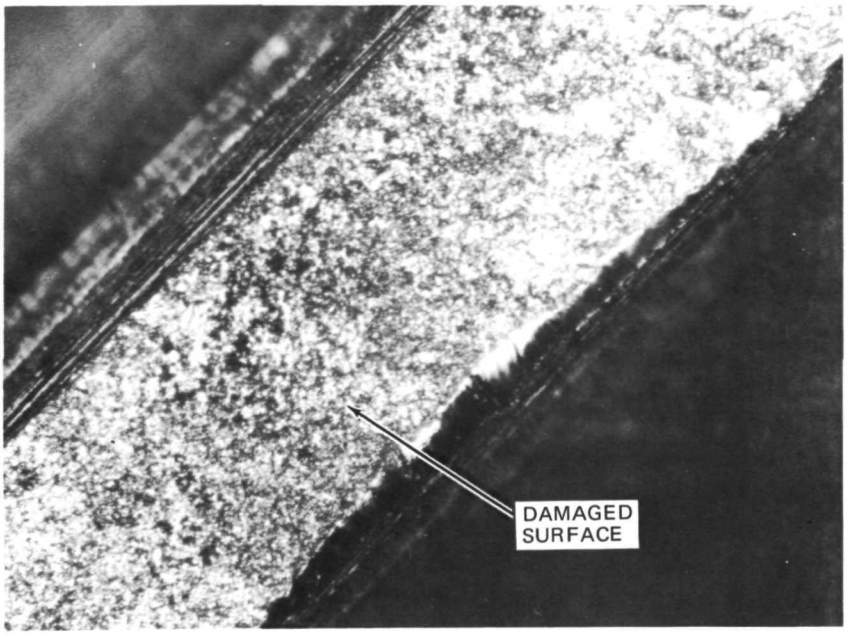

Figure 3-15. •1 A286 Seat after 40,000 Cycles on Test No. 1 • Typical Damage (160X)

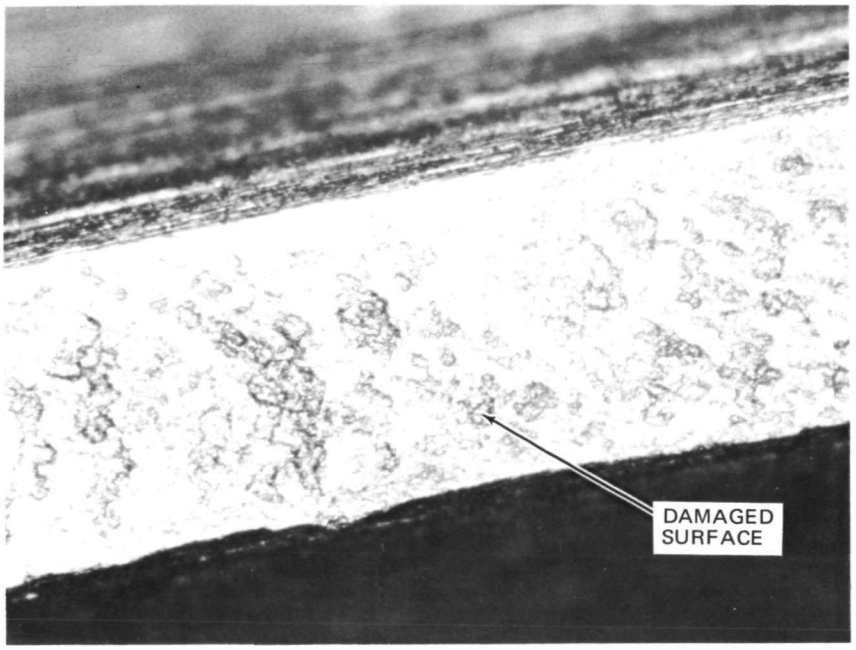

Figure 3-16. -1 A286 Seat after 40,000 Cycles on Test No. 1 - Area of Severe Damage (160X)

small amount of amorphous material was detected; however, the characteristics of this material did not match the characteristics of any of the anticipated reaction products and, therefore, the composition of this material was difficult to determine. The amount of amorphous material detected was so small that an insufficient quantity was available for further testing and there did not appear to be a practical method of determining the actual makeup of this material. It is possible that the amorphous material was actually the same material as the crystalline A286 material, but that it had been broken down to a size which was too small to show the normal crystalline characteristics. The interplanar spacing of the crystalline material was determined using photographs taken with the electron micrograph equipment. The final laboratory analysis is shown in the Appendix A. The failure mechanism observed in the -1 valve on Test No. 1 appears to be a combination of adhesive failure combined with a degree of surface fatigue. The damaged area shown in Figure 3-15 appears to have been the result of normal adhesive forces where the two material surfaces adhered to each other and loose wear particles were generated each time the surfaces were separated. In the case shown in Figure 3-15, the damaged area did not decrease the contact area to the extent necessary to produce a surface fatigue mechanism. The damage area shown in Figure 3-16 would appear to have developed the surface fatigue after a decrease in contact area occurred from the adhesive failure mechanism. When considering both the rate of change in leakage rate and the final surface damage it would appear that severe adhesive damage occurred at the start of testing and a progressive deterioration occurred during the first 5,000 cycles. Between cycles 5,000 and 32,500 the amount of adhesive wear appears to have remained relatively constant because the material removed from one surface tended to remain adhered to the material surface and little change in equivalent orifice (leakage path) opening occurred. Betweeen cycles 32,500 and 40,000, the surface fatigue failure occurred which produced the damage shown in Figure 3-16 and which produced the second rapid increase in internal leakage rates. This surface failure resulted in the leakage rate exceeding the original limit of 10 times the pretest value and the test was terminated at that point.

Since a total of 0.013 mm (0.0005 in.) was removed at the start of the program (to remove the effects of the previous LF_2 tests), it was not expected that enough residual F_2 could have remained in the seat material to have caused the reaction which occurred on the No. 1 test. However, the fact that the leakage increased significantly after 1 cycle in GH_2 and that the residual products appeared visually to be reaction products both tend to indicate that some form of F_2 related damage may have still been present in the material.

The first 100,000 cycle-life tests of the -501 valve were completed with no significant change in the measured internal leakage rate. The small change measured would indicate that the valve was improving through the testing and was actually leaking at a lower rate at the end of 100,000 cycles as compared to the start of the test program. The -501 valve was removed from the stand at the completion of cycle test No. 2 and the 77°K (-320°F) leakage test was performed. The thermal stabilization was considerably better on the post-test 77°K (-320°F) leakage tests than on the pretest leakage tests, and the post-test figure of 5.32 SCCM at 7×10^5 N/m^2 (-100 psig) was in good analytical agreement with the post-test ambient leakage test data.

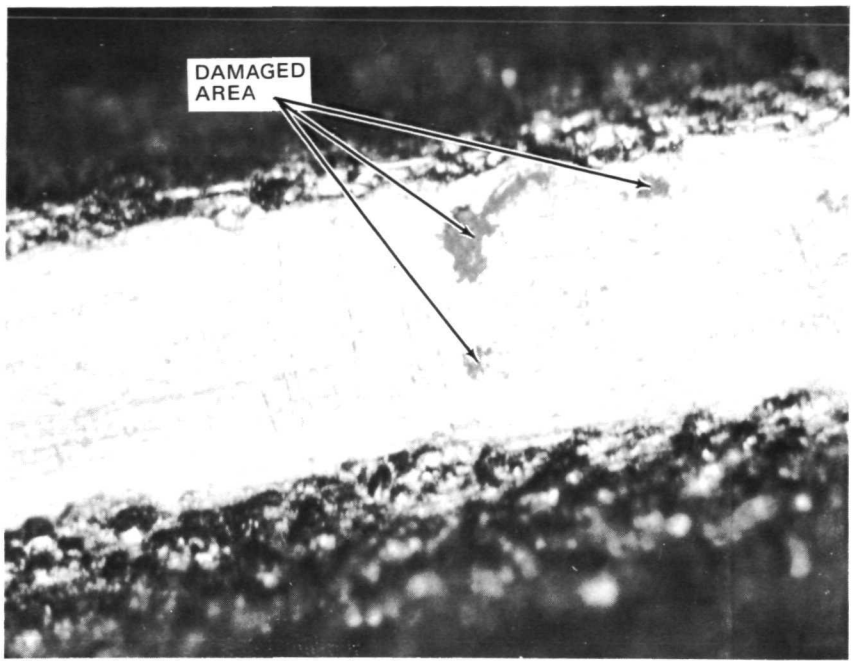

Figure 3-17. -501 Gold Plated Seat after 100,000 Cycles on Test No. 2 (160X)

The -501 valve was then disassembled and inspected. The complete valve was found to be in good condition and acceptable for further testing. A microscopic examination of the gold-plated seat revealed three small areas where the gold plating had separated from the basic seat material, as shown in Figure 3-17, but since these spots were all very vmall, 0.08 mm (0.003 in.), they are not expected to affect the suitability of the valve for further testing. The type of defect appeared to be a form of surface fatigue where the failure occurred in the subsurface layer of gold but was not confined to the material surface at the interface.

3.1.6.2 Test No. 3 and 4

The resurfacing of the poppet and seat assemblies was completed prior to the start of Tests No. 3 and 4. The poppet assembly of the -1 valve was found to have been worn only a very small amount during the No. 1 valve cycle test run. The Inconel 718 poppet was returned to the refinishing vendor and the poppet sealing surface relapped to a commercial surface finish. The final finish obtained was a multidirectional lay surface in the 2.5×10^{-5} to 5×10^{-5} mm (1 to 2 μ in.) range. The measured flatness was well within the 6.25×10^{-5} mm (2.5 millionth) (1/4 helium light band) value specified.

The first step in the refurbishment of the -1 valve seat consisted of smoothing the seat sealing surface out at MDAC using an Al_2O_3 plate with a 3×10^{-4} to 3.3×10^{-4} mm (12 to 13 μ in.) AA finish. This operation

revealed that approximately 80 to 85-percent of the seat circumference had only a small amount of wear while the remaining 15 to 20-percent of the area contained a number of relatively deep wear pockets.

After photographing the semifinished seat surface, a second operation was completed with the Al_2O_3 plate in an attempt to remove the deeper wear pockets. The depth of material which had to be removed was such that a problem was encountered with the hard nodular portion of the A286 material and an acceptable finish could not be obtained. The hard nodules would not smooth out and a series of undercut grooves was generated at the site of each hard nodule. The seat was then subjected to an extensive relapping process. The seat was smoothed to nominal 2.5×10^{5} to 5×10^{-5} mm (1 to 2 μ in.) finish while the seat width grew to a maximum of about 0.33 mm (0.013) in. Additional lapping would have widened the seat to the point that a complete remachining of the seat would be required to bring the seat dimensions back to an acceptable condition. The surface obtained without a complete remaching is within the specification for surface smoothness, however, a low spot existed in the area of greatest damage. The depth of this low spot measured about 2.5×10^{-4} mm (4 times the design limit). While it was expected that this low spot would result in a leakage rate in the valve which would be higher than normal, it was not expected that the change in leakage rate characteristics would change appreciably. After discussing this situation with the NASA-LeRC program manager, it was decided to accept the seat for testing without conducting the complete remachining process.

The post-test inspection of the -501 valve revealed that the basic valve was in good condition, however, definite signs of wear were detectable on both the poppet and seat-sealing surfaces. The seat assembly was resurfaced with the MDAC Al_2O_3 finishing plate and a smooth surface with no wear defects was obtained.

The -501 poppet (which cannot be resurfaced on the MDAC plate) was resurfaced and returned for testing. Approximately 0.005 mm (0.0002 in.) of material was removed from the Inconel poppet sealing surface. The -501 valve was reassembled and leak checked. The leakage after reassembly was greater than 5 SCCM at 7×10^{5} N/m^2 (100 psig) (ambient temperature GHe). Since this value was over twice the value measured for the valve before refurbishment, the valve was disassembled and reinspected. It was found that a fairly deep scratch was present across the gold-plated seat surface. While the shape of the scratch does not indicate how the scratch occurred, it is probable that it occurred accidentally during reassembly of the valve or that some form of contamination was present in the gas supply used to purge the valve before the leakage tests. A new 5-μ filter was installed in the GHe supply line in the A12 clean room to prevent the possibility of future contamination problems.

The scratch had a depth of about 0.008 mm (0.0003 in.) and as such was almost through the 0.010 mm (0.0004 in.) gold plating. Since no practical method would allow removal of the scratch without removing almost all of the gold plating, it was decided to return the valve seat to strip off the original gold plating and replate the sealing area. To preclude the possibility that the scratch had damaged the A286 substrate, the seat was refinished by MDAC using the Al_2O_3 surfacing plate. The scratch was completely removed using this method without passing through the gold plating

and an acceptable surface finish was obtained using this method. However, since most of the gold plating was removed in the scratch removal operation, the seat was returned to the vendor for replating. The replated surface was smoothed out using the Al_2O_3 surfacing plate, and the seat was returned to the A12 clean room for reassembly.

The poppet sealing surface was inspected after the leakage test and a number of small pin hole defects were detected in the sealing surface. The pin holes appeared to be in the area of the poppet which was loaded during the 100,000 cycle Test No. 2 and not in the exact location of the loaded area during the leakage test. The poppet was returned to the lapping vendor and an additional 0.02 mm (0.0008 in.) was removed from the poppet sealing surface. The total material removed after the No. 2 cycle test totaled 0.025 mm (0.001 in.) (the 0.005 mm (0.0002 in.) originally removed and the additional 0.020 mm (0.0008 in.)). The poppet measured acceptable flatness and the surface finish was in the 2.5×10^{-5} - 5×10^{-5} mm (1 to 2 μ in.) range. The poppet was then returned to the test site and the valve reassembled and leak checked. The leakage was found to be in the 5 to 6 SCCM range after reassembly. The valve was disassembled and reinspected. It was found that the bumper-to-seat clearance was insufficient to prevent the bumper from holding the seat off at the sealing surface on one side of the seat circumference. The bumper-to-seat clearance was increased by lowering the bumper height. After the proper height was obtained 0.010 mm (0.0004 in.), the seat sealing surface was given a light polishing lap and the part returned to A12.

After reassembly, the valve leakage was still measured at 5 SCCM and it was necessary to lower the bumper height again. The bumper-to-seat clearance was increased at MDAC to a clearance of approximately 0.02 mm (0.0008 in.) and the valve retested. Results showed a leakage of 2 SCCM and this value was considered accepted for cycle life test No. 4.

The cycle testing was then completed on both valves (Tests No. 3 and 4) through a total of 56,000 cycles with the results shown on Table 3-3. The -1 valve was operated with a relative stress factor of 8-percent 5.5×10^{-7} N/m^2 (8,000 psi apparent seat stress) and the -501 at 16 percent 3.3×10^{7} N/m^2 (4,800 psi). Both valves were operated in the double acting mode with shims installed to limit the compression of the compliant seat to the desired test condition. As mentioned previously, the -1 valve started with a somewhat high baseline leakage rate due to the slight low spot which existed in the A286 seat. As shown in Table 3-3, the -1 valve leakage rate was fairly constant for the first 500 cycles, then increased at a measurable rate for the next 15,500 cycles. Between cycle 8,500 and 16,000 the leakage rate increased at a rapid rate and the final reading was near the arbitrary failure limit. The testing was continued for an additional 200 cycles (16,200 cycles total) and the last leakage reading was attempted on the -1 valve. While the 1.75×10^{5} N/m^2 (25 psig) leakage reading was near the expected value, the 3.5×10^{7} N/m^2 (50 psig) and 7×10^{7} N/m^2 (100 psig) had increased into the unreadable range and the -1 valve was removed for inspection. The leakage rate change measured for the -1 valve on test No. 3 did not have the same leakage change characteristics as had been measured on test No. 1. (8-percent load versus 4-percent load.) The characteristics

of Test No. 3 did not indicate the same potential chemical reaction which had been suspected on the first test but instead produced a more normal characteristic for a highly loaded valve seat.

Note that a solenoid valve failed in the -1 valve test and 1,500 cycles of operation occurred on the -501 valve without the -1 valve being cycled. This difference of 1,500 cycles existed until the -1 valve was removed from testing.

The post-test inspection of the -1 valve indicated that severe adhesive wear had occurred at the poppet and seat interface, however, no surface fatigue characteristics were detected. The condition of the Inconel poppet is shown in Figure 3-18, and, while the surface damage appears to consist of material transferred from the seat to the poppet, it is in fact the other way around. The defects shown in Figure 3-18 consist of holes left in the Inconel by material removal. Apparently a small amount of A286 adhered to the Inconel poppet and was pushed into the harder material. The A286 then readhered to the A286 seat and was pulled back out of the surface. This condition results in the formation of pin holes in the hard Inconel surface. The corresponding seat damage is shown in Figure 3-19 and 3-20. In Figure 3-19 the adhesive damage has extended completely across the seat surface and considerable leakage would be expected at this location. Note that some undamaged surface is shown in Figure 3-20 and the eroded cavaties do not extend completely across the sealing surface. There was no indication of sliding between the poppet and seat at any location, however, there was some very small random scratches noted in several areas. These

CR184
N/A

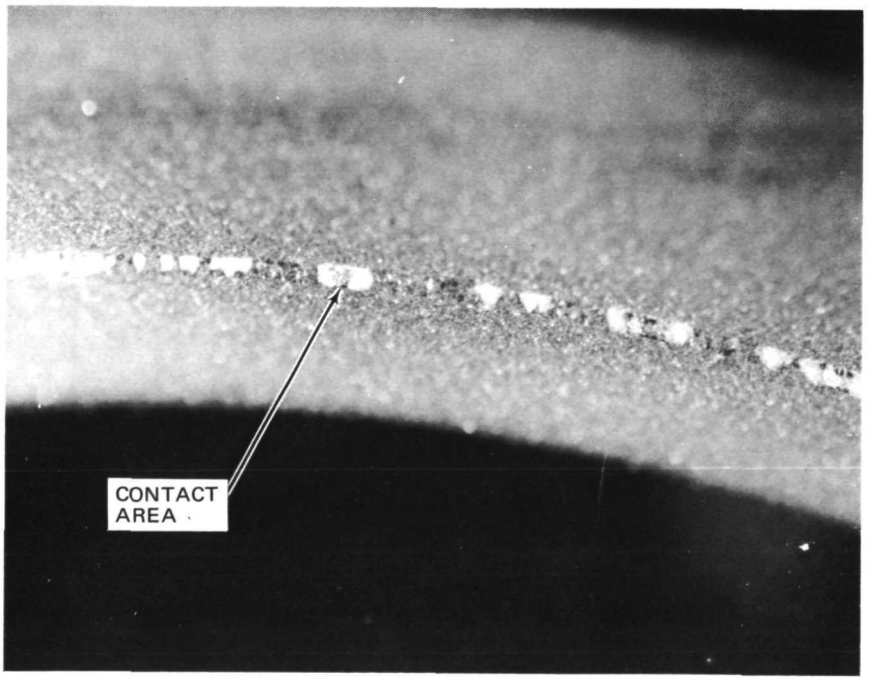

Figure 3-18. –1 Poppet after 16,200 Cycles on Test No. 3 (20X)

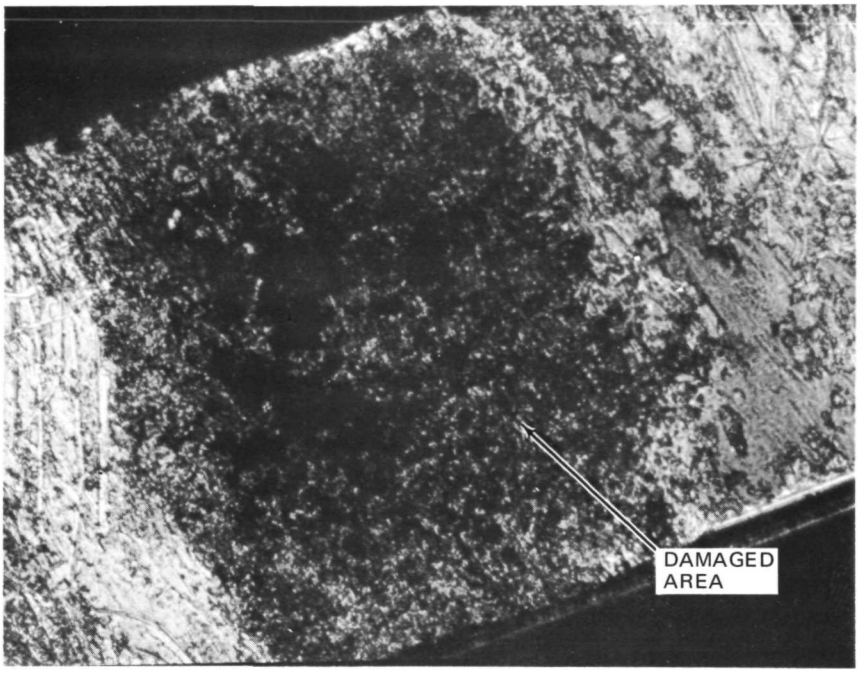

Figure 3-19. -1 (A286) Seat after 16,200 Cycles on Test No. 3 — Area of Severe Damage (160X)

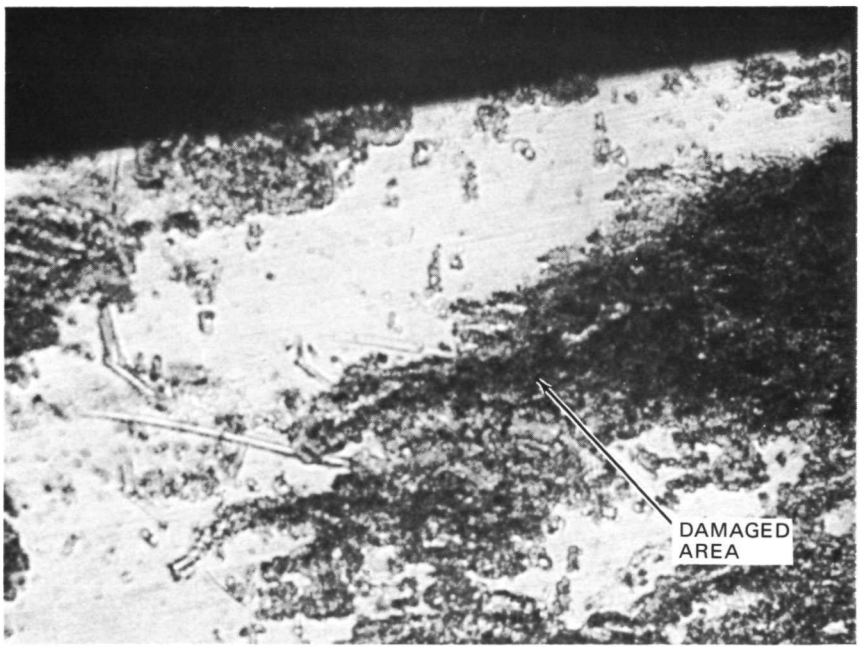

Figure 3-20. -1 (A286) Seat after 16,200 Cycles on Test No. 3-Area of Moderate Damage (160X)

random scratches appear to be caused by the heavy aluminum foil wrapping which is placed around the parts during the post-test handling procedures.

The -501 valve also showed the effects of increased seat loading during the No. 4 test. The -501 valve showed a gradual increase in wear rate (and leakage rate) for the first 47, 500 cycles at the 16-percent loading while no changes had been measured for 100, 000 cycles at the 8-percent loading. (Test No. 2.) When cycling was resumed after the leakage measurements at 47, 500 cycles it was found that the valve would not hold the locked up GH_2 pressure. A series of external leakage tests were conducted but no loose connection was found. The valve was then removed from the test stand and returned to the clean room for inspection. It was found that the poppet shaft seal bellows had cracked, and leakage was occurring between the main valve propellant cavity and the valve actuator. The -501 valve had accumulated approximately 150,000 cycles before the failure of the shaft seal bellows.

A visual inspection of the poppet and seat sealing surfaces indicated that detectable wear was occurring at the 16-percent loading. A considerable amount of gold plating had been extruded off of the seat sealing surface and a double ring of extruded material was observed at the inner and outer edges of the seat sealing surface. In addition, a detectable amount of gold plating was observed on the mating poppet surface where the gold had adhered to the Inconel and was then forced into the harder poppet material under these conditions of cyclic loading.

An attempt was made to continue Test No. 4 by installing the poppet shaft assembly of the -1 valve into the -501 valve. Photographs were taken of the seating surface of the -1 poppet and then the poppet was resurfaced to the pretest condition. This poppet assembly was then installed into the -501 valve. No resurfacing of the gold plated seat was attempted since such refinishing would affect the results of the first 47, 5000 cycles of operation. With the -1 poppet installed a pretest leakage measurement was made and this value was found to be near the original pretest value. The test was then restarted and continued to the next interval. At 55,000 cycles the leakage rate was found to be unreadable at 7×10^5 N/m^2 (100 psig). An additional 1,000 cycles was run to verify that the leakage had actually increased to the level found after 55,000 cycles. The leakage occurring at 56,000 cycles was at about the same level as that found at 55,000 cycles so the test was stopped at this point.

The seat surface of the -501 valve is shown in Figures 3-21 and 3-22. These photos show the presence of severe surface fatigue with the loss of large chunks of surface and subsurface material. Note also the presence of extruded gold along the upper surface of the seat area in Figure 3-22. This extruded gold appears to have been "coined" off the sealing surface and corresponds to the type of wear pattern observed at the 47, 500 cycle inspection. The severe surface fatigue was not observed at the 47, 500 cycle point and in all probability was not present at that time.

The measured leakage rates and visual inspection indicates that the seat failure observed in Test No. 4 consisted of two entirely different failure modes. It appears that from the first cycle to the 47, 500 cycle point a

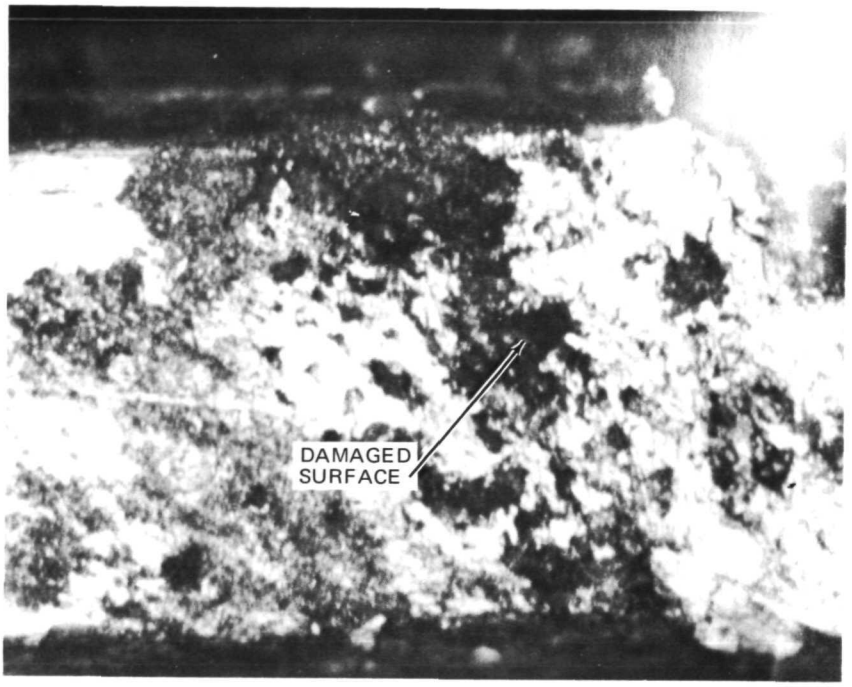

Figure 3-21. -501 Gold-Plated Seat after 56,000 Cycles on Test No. 4-Area of Severe Damage (160X)

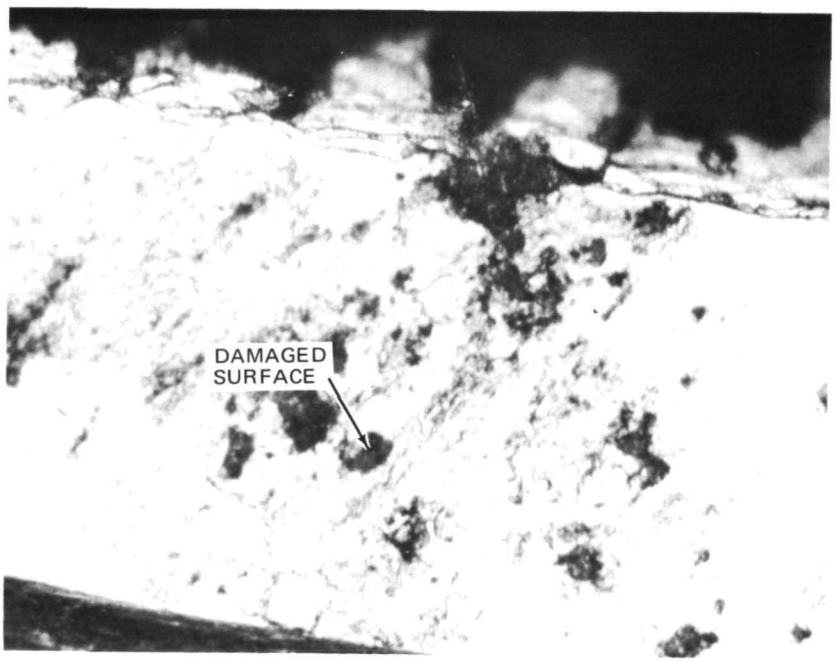

Figure 3-22. -501 Gold-Plated Seat after 56,000 Cycles on Test No. 4-Area of Moderate Damage (160X)

combination of adhesive wear and plastic flow deformation was occurring at a relatively slow rate and had the shaft bellows not failed, the valve would probably have been able to have completed the 100,000 cycles before the gold plating was completely removed from the seat sealing surface. In this case, the high and low spots on the poppet and seat were still mated and consequently the leakage rate was still under control. However, when the -1 poppet was substituted for the -501 poppet the wear deformatives were no longer in alignment. Under these conditions the high spots on the seat were absorbing all of the seat loading stresses and under this increased stress level the severe surface fatigue occurred.

The results of the first four-cycle life tests indicate that the most important characteristic of the poppet and seat material combination for service in GH_2 is the similarity of the materials and not just the RSF. A check of the two alloys used on the -1 valve, Inconel 718 and A286, shows that a majority of the alloying elements are common to both materials and therefore, the materials behave in the manner expected for "like and like" materials even though they are two different alloys. The key elements of each are shown in Table 3-4. It should be noted that the same three elements make up approximately 90-percent of both of these materials even though the percentage of each are different in the two materials.

Table 3-4

KEY ALLOYS IN -1 POPPET AND SEAT MATERIAL COMBINATION

	Inconel 718	A286
Fe	18 percent	53
Ni	52.5	26
Cr	19	15

Since the A286 is considered to be an iron-based super alloy and the Inconel 718 is a nickel-based super alloy, it would not be expected that the two materials would behave as similar materials. The results of Tests 1 and 3 indicate that in actual use the two materials do behave in the manner expected when similar materials work together. In contrast, the gold plating material is definitely dissimilar from the Inconel 718 and a completely different wear pattern is observed. This combination shows the expected characteristics of wear with unlike materials. It appears that for service in a gaseous media the adhesive force effects of different materials will have to be taken into account for wear rate prediction as well as the RSF.

A complete set of monitoring photographs were taken with the acoustical signature equipment during completion of test 1-4. The vibrational envelopes recorded remained constant throughout the testing, as shown in Figures 3-23 through 3-26. Since both valves remained in good mechanical condition throughout the testing, there was no occasion to obtain a trace of a valve malfunction. It was found that the photographs taken on the oscilloscope

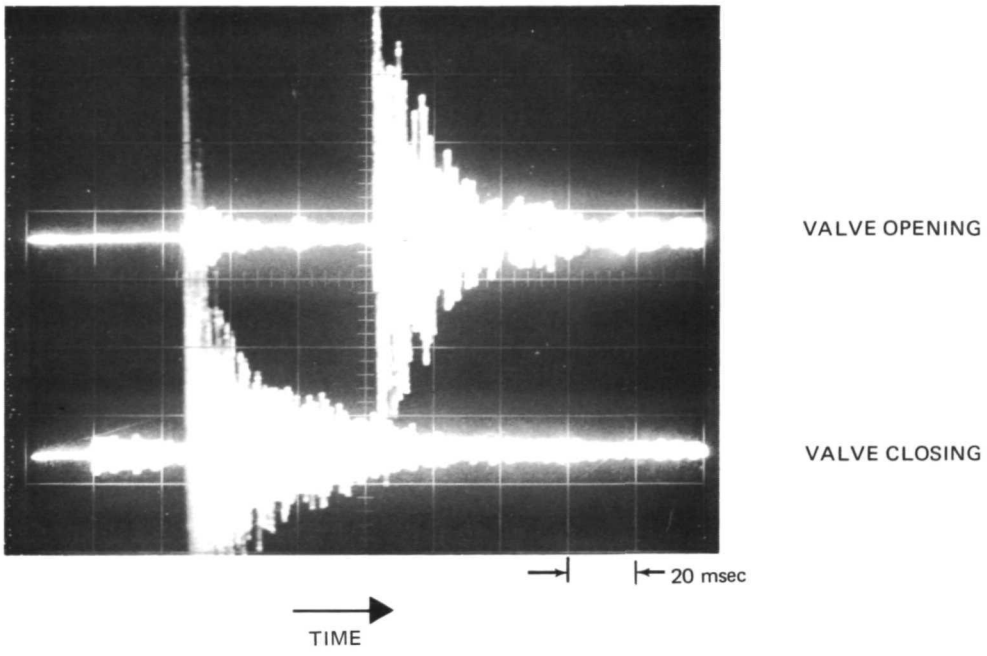

Figure 3-23. Accelerometer Trace of -501 Valve after 1,940 Cycles of Test No. 4

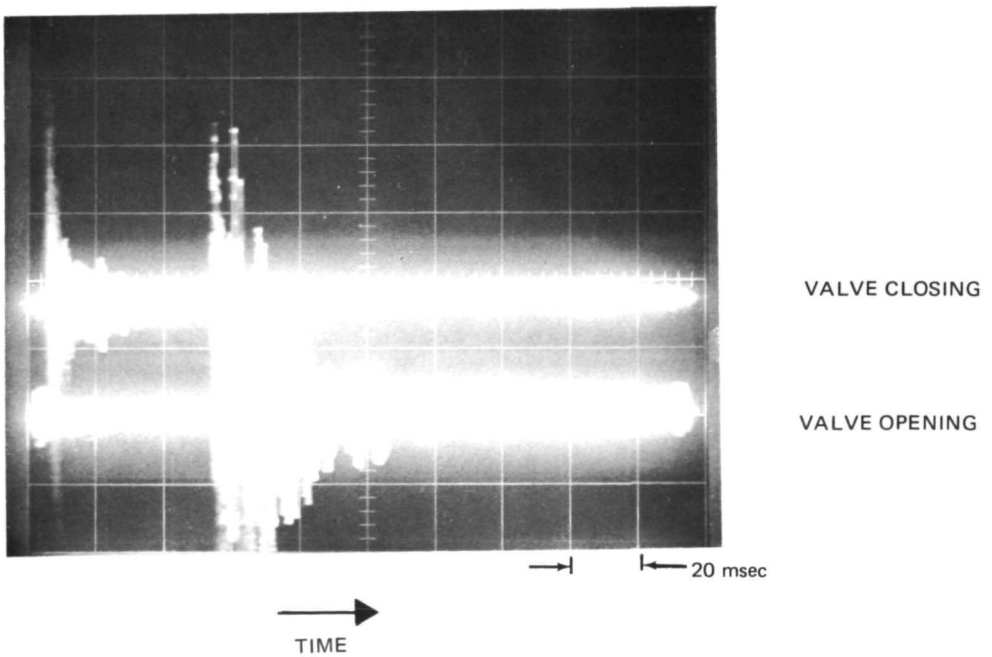

Figure 3-24. Accelerometer Trace of -501 Valve after 48,000 Cycles of Test No. 4

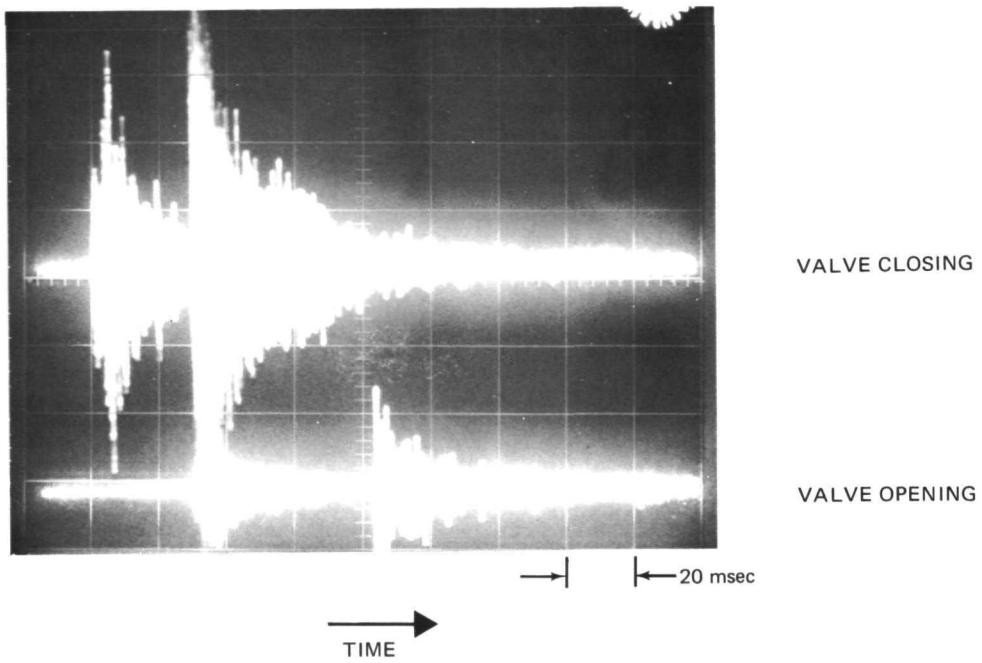

Figure 3-25. Accelerometer Trace of -1 Valve after 480 Cycles of Test No. 3

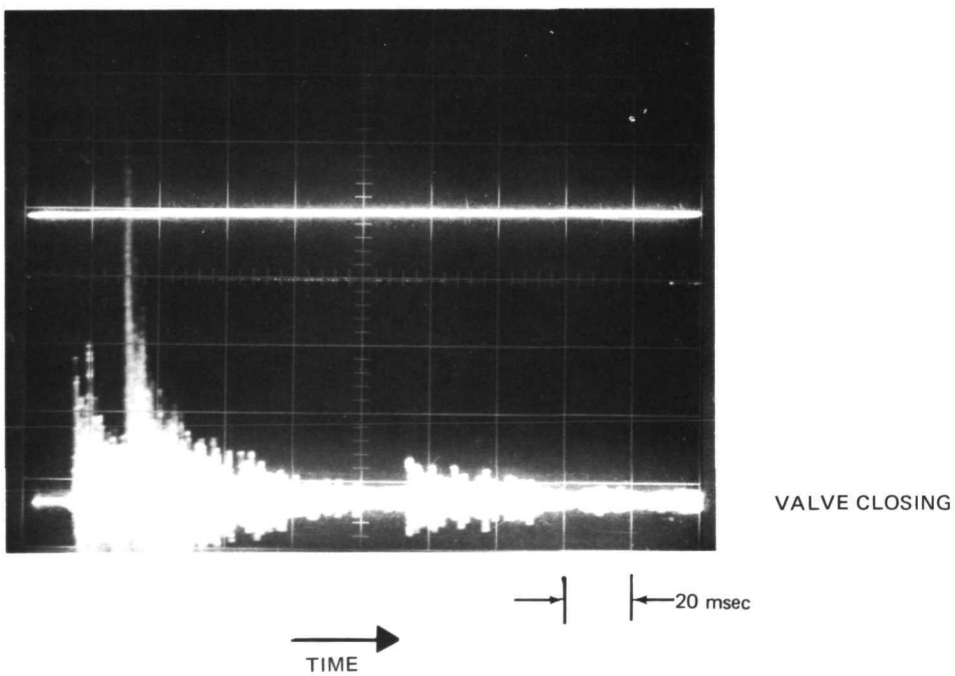

Figure 3-26. Accelerometer Trace of −1 Valve after 16,200 Cycles of Test No. 3

used for tests 1 and 2 were not adequate for a complete vibrational analysis. To cure this problem, it was decided to use a different type of oscilloscope for tests 3 and 4. The difficulty with the original oscilloscope selected was that a uniform horizontal sweep was obtained with the trigger impulse and this arrangement did not permit expansion of individual portions of the signal trace to be obtained for detailed analysis. An oscilloscope which had the special features needed for analysis (but not required for normal monitoring of the signal envelope) was used during the first part of tests 3 and 4. The expandable scale oscilloscope was incorporated in the second series of cycle life tests (No. 3 and 4), however, the results were still marginal for frequency spectrum analysis. To alleviate this difficulty it was planned to use a tape recorder to record the vibration signals on tests No. 5 and 6, and use the tape to provide a slow play back for vibrational frequency analysis. This type of analysis was of interest to determine the fundamental characteristics of the basic valve design and once this information was obtained, no further tape recordings are required. For routine acoustical monitoring of the mechanical condition of the valves, the two channel oscilloscope works in an acceptable manner and this instrument was used throughout the second half of the No. 3 and 4 test series. A check was made to determine if the shaft bellows failure occurring in test No. 4 was detectable on the acoustical monitoring instruments. No indication of this failure was detectable, however, since the failure consisted of a leakage type failure it is reasonable to assume that no mechanical failure indication would occur.

The Goldak sonic leak detector was used at the start of tests 1 and 2 and through the first 40,000 cycles of testing in an attempt to measure internal leakage rates with acoustic instrumentation. The sonic detector is sensitive to all of the background noise and was not capable of separating the acoustic energy generated by a small internal leak from the residual background noise. This was found to be true even when the -1 valve was leaking at a rate which was almost 50 times greater than was the -501 valve and both valves were monitored separately. Based on these results, the sonic leak detector was not acceptable for internal leakage determination when used in the present manner.

The Delcon ultrasonic detector was used during tests No. 3 and 4. No difference in reading was obtained between the valves during conditions of low leakage and during conditions of high leakage. It appears that the mass of the valve was such that the sound energy was absorbed within the walls of the valve cavities and no detectable signal was transmitted to the exterior of the valves. A quick check of potential sources of external leakages was made during the testing and the Delcon unit would pick up external leakage with no difficulty. In fact, relatively large signal changes were measured under the different conditions of external leakages without difficulty. Since no corresponding signal changes were measured for changing condition of internal leakages, it appears that neither method of acoustical leakage measurement is applicable for internal leakage rate under the present conditions. It may be possible to alter the valve design such that the acoustic detector is mounted inside the valve body cavity and in this way eliminating the loss of acoustical energy in passing through the valve housing. Such a modification was not within the scope of work on this contract.

3.1.6.3 Test No. 5

The valve seat from the -1 valve configuration (A286-INCONEL 718 combination) was removed from the valve and sent to a vendor for application of the Teflon S coating. A 0.025 mm (1 mil) coating (single coating) of the 958-203 Teflon S was applied to the sealing surface of the valve seat. A very light sand blasting operation was applied to the seat surface prior to the application of the plastic coating. Either sand blasting or a chemical treatment was required on a metal surface before coating so that a satisfactory bond could be obtained between the plastic coating and the metal surface. The light sand-blasting operation was selected for the valve seat due to the capabilities of the vendor (who normally uses the sandblasting method) and due to the uncertainty involved with the chemical treatment method. It was likely that a chemical treatment method would produce a surface which would be smoother than the surface obtained by sandblasting and the smoother finishes would make a better valve sealing surface. Unfortunately the effects of the chemical cleaning on the highly stressed A286 material was not known at the start of test No. 5.

The valve seat was returned to the A12 test facility clean room and installed in the valve. With the plastic coated seat installed, the valve was designated a -503 configuration. A pretest leakage test was made and the internal leakage was unacceptable for testing. The valve was disassembled and the seat removed for inspection. It was found that a very small blister existed in the plastic coating on the narrow sealing surface. The raised edges of this blister was removed and a reasonably smooth surface was obtained in the area of the blister. However, a small undercut area was accidentally made in the area next to the blister and additional work was needed before the seat was ready to test. This additional refinishing was accomplished by hand lapping this plastic surface on the 3×10^{-4} mm (12 μ in.) AA Al_2O_3 surfacing plate which had been under development at MDAC. The lapping was conducted directly on the plate without lubrication or lapping compound. It was found that this method works very well with the Teflon S and a smooth, flat surface was obtained in a very short operation.

The valve was reassembled and the leak test repeated. No leakage could be detected at 7×10^5 N/m^2 (100 psig) with GHe in the normal valve configuration and the valve was accepted for testing. The requirements of Test No. 5 include the reduction in seat compression required to provide the desired seating stress and this compression limitation was provided by installing shims between the actuator piston and actuator housing. When the shims were installed, a measurable amount of leakage occurred (as was expected) due to the load limiting feature of the shims. With the originally specified 2 mm (0.081) shims the leakage rate was higher than desired and a set of 1.7 mm (0.066 in.) shims were installed. These shims provided an acceptable leakage rate and the valve was installed on the test stand. It should be noted that Test No. 5 was conducted with the valve in the single acting mode and therefore the selection of shim thickness did not effect the seat loading stress under cyclic conditions but did limit the seat stress under each of the leakage test conditions (when a 7×10^5 N/m^2 [100 psig] was placed across the valve). Therefore the change in shim thickness did not change the normal test conditions but did change the leakage test conditions.

When installed on the test stand the valve leakage rates were measured with GHe at ambient temperature and found to be acceptable for testing (0.48 SCCM at 7 x 10^5 N/m^2 [100 psig]).

The No. 5 test of this test series was then completed through a total of 92,500 cycles. The leakage rates measured are shown in Table 3-3. The leakage rate of 55,000 cycles was higher than the readability range of the measuring equipment and the valve was removed for inspection at that time. The inlet adapter was removed from the valve and then the seat portion of the valve was submerged in Freon. With the outlet cavity pressurized at 15 psig, a steady stream of bubbles was observed at the root of the second convolution of the machined bellows portion of the seat assembly. No bubbles were detected at the poppet and seat interface. The valve disassembly was then completed and a microscopic examination made on the Teflon S coating. The seat sealing portion of the Teflon S coating was found to be unchanged from the start of the test and was in a condition suitable for further testing. The bumper portion of the coating had been damaged due to the increased misalignment which occurred with the collapse of the machined bellows.

To permit the continuation of Test No. 5 a temporary repair was made on the bellows assembly. The repair consisted of welding the failed convolutions together so that no leakage occurred through the bellows wall. This repair was accomplished by clamping the bellows in a compressed condition and then melting the edges of the two convolutions together on an electron beam welder. After completing this operation, a leakage test was made and it was determined that the weld material had cracked around the complete circumference of the bellows when the clamp fixture was removed. However, since enough material had been melted by the first welding operation it was then possible to secure a good weld between the two convolutions without using the clamping fixture. The second welding operation was completed and no further leakage occurred in the welded portion of the bellows. A visual check of the repaired bellows assembly indicated that several other convolutions were in the process of collapsing, however, the testing was resumed without further modification.

No rework of any kind was permitted on the Teflon S coating since reworking of this surface would have nullified the testing which had been completed prior to the bellows failure. The seat sealing surface was inspected with a microscope and one small area was found to have been damaged during the repair operation. This small area of damage resulted in an increase in the valve internal leakage rate; however, since the leakage was found to occur at the area of known damage it was not expected to affect the change in leakage rate with cyclic operation. This conclusion was verified when testing resumed after the 55,000 cycle point. As shown in Table 3-3, the leakage rate improved slightly from the 62,500 cycle point to the 85,000 point. At 92,500 cycles, a second convolution failed and severe leakage occurred through the bellows wall. Since it was not possible to obtain the normal internal leakage rate measurements with the failed bellows assembly, the valve was submerged in Freon and a bubble test made. The leakage rate of the seat sealing surface appeared to be unchanged from the 55,000 cycle observation and therefore it can be concluded that no surface deterioration had occurred with the Teflon S coating over the 92,500 cycles of operation which had been completed at the 50-percent RSF loading.

Upon completion of Test No. 5 a complete inspection was made into the condition of the machined compliant bellows portion of the seat assembly. The variation in bellows convolutions spacing were measured and are shown in Table 3-5. The variation in convolution spacing indicates that the bellows material had yielded to the point where additional repairs were not warranted. This A286 seat assenbly had accumulated the following number of cycles under controlled conditions.

870	at proof pressure in LF_2
40,000	at 7×10^5 N/m^2 (100 psig) in GH_2 (Test No. 1)
17,000	at 7×10^5 N/m^2 (100 psig) in GH_2 (Test No. 3)
92,500	at 7×10^5 N/m^2 (100 psig) in GH_2 (Test No. 5)
150,370	Total

Table 3-5

VARIATION IN BELLOWS CONVOLUTIONS

Convolution Number*	Clearance mm (in.)
1	0.36 (0.015)
2	Welded
3	0.36 (0.015)
4	0.18 (0.008)
5	0.18 (0.008)
6	0.22 (0.009)
7	0.25 (0.010)
8	0 to 0.12 (0 to 0.005 failed)
9	0.32 (0.013)
10	0.30 (0.012)
11	0.30 (0.012)
12	0.30 (0.012)
13	0.22 (0.009)
14	0.25 (0.010)

*Numbered from the seat sealing end.

The design stresses for this seat assembly were selected to provide a cycle life of over 10^6 cycles and this objective was not met for the actual valve testing sequence. Several reasons were believed to be responsible for the relatively early failure. They were:

A. The ringing effect found on valve closure produced more than one stress cycle in the material for each cycle of operation.

B. The cycle testing completed at the proof pressure condition (earlier program) created a severe loading condition for the seat bellows.

C. The post-test storage period after operation in LF_2 may have permitted structural deterioration of the A286 material.

D. The exposure to GH_2 on this program may produce a gradual deterioration to the A286 material even though this material is one of the best materials which can be used for this type of service.

The valve seat assembly was then returned to the vendor where the machined bellows portion of the -503 valve seat was removed from the present valve seat, and a new A286 machined bellows was welded into the assembly.

Before the actual remanufacture process was started, a recheck was made as to the suitability of using the A286 type of material for this application. This MDAC study indicated that the only material which would likely give better service for the present application would be Inconel 718, and since the Inconel is presently being used on the valve poppet assembly it was decided not to run identical materials on both sides of the valve seal closure interface. Accordingly, the A286 material was still the best known material for this application.

The remanufacturing of the valve seat consisted of cutting off the mounting flange and the poppet seat area from the present assembly and then welding these two flanges onto a new machined bellows (A286). The welding was accomplished using the TIG welder so that the costs of remanufacturing the seat assembly were minimized. While this repair could have been made by the electron beam welder, this procedure would have been considerably more expensive and since the electron beam welding was only a requirement for liquid fluorine service this additional cost was not warranted for testing in GH_2.

3.1.6.4 Acoustical Analysis—Test No. 5

A magnetic tape recording of the acoustical signature information was made on the -503 valve during the running of Test No. 5. The signals from the Endevco accelerometer and the Dunegan transducer were both recorded simultaneously. Two sets of recordings were made, one at normal operating pressures, and the other at higher than normal operating pressures. The signals were recorded at 3 m (120 in.)/sec tape speed in the FM recording mode in order to record frequencies up to 150 kHz, the resonant frequency of the Dunegan transducer. A 1-kHz calibration signal was also recorded for later reference.

This recording was then played back at a reduced tape speed of 9.5 cm (3-3/4 in.)/sec and the signals transferred to an oscillograph recorder whose chart speed could be adjusted as high as 2 m (80 in.)/sec.

In reviewing the oscillograph traces, several observations could readily be made. Since the oscillograph showed the pulse received from the valve opening and the pulse received from the valve closing for several such cycles, very accurate timing information was obtained. The time between opening, closing, and then opening again compare favorably with the times obtained using other methods of testing.

The signature for both the opening and closing of the valve appears to consist of three comparatively distinct regions. The first portion of this signal consists of a low-amplitude pulse approximately 12 msec long. This portion of the signal was immediately followed by a very sharp increase in the signal to a high amplitude which then exponentially decays in approximately 0.060 second. The final portion of this signal consists of a long tail of small-amplitude, low-frequency vibration. This low-frequency vibration is most noticeable for the valve-closing signature. The vibration continues during the entire time from valve closing until valve opening, a time of approximately 1.3 seconds. This signal indicates that a beat frequency is present.

An attempt was made to count the number of cycles present in the first and last regions of each signal as displayed on the oscillograph. The precursor signal displayed a predominant frequency of 185 Hz. The final section of the signal displayed a predominant frequency of 266 Hz.

The resonant frequency of the two actuator return springs and the shaft seal bellows was then calculated. The theoretical resonant frequency of both return springs was found to be the same number even though the springs are considerably different in size. A value of 248 Hz was calculated for both return springs. The approximate resonant frequency of the shaft seal bellows was calculated to be 198 Hz. The test results are therefore showing that both the springs and the shaft seal bellows are excited on each operating cycle. A beat frequency between these two fundamental frequencies was detectable on the oscillograph traces. Assuming that two possible beat frequencies exist and that these two represent the sum and difference of the two fundamental frequency, values of approximately 50 Hz and 450 Hz would be expected for the beat frequencies. The beat-frequency pattern shown on the traces indicates that the predominant frequency is lower than the fundamentals and therefore it is expected that a significant beat frequency of approximately 50 Hz is being generated on each valve operating cycle. The conversion of this beat frequency vibration into stress cycles in the shaft seal bellows will depend on the amount of dampening of this beat frequency vibration.

The vibration spectrum analysis was completed as part of test No. 5 and the results are in good agreement with the valve design analysis. The key component resonant frequency data include:

	Calculated (Hz)	Test Results (Photo) (Hz)	Spectrum Analysis (Hz)
1. Actuator Spring—inner	248	266	230
2. Actuator Spring—outer	248	266	230
3. Poppet Shaft Seal Bellows	198	185	150

The anticipated vibration energy peaks would, therefore, be expected to occur as follows:

1. Springs—fundamental	230 Hz
2. Springs—second harmonic	460 Hz
3. Bellows—fundamental	150 Hz
4. Bellows—second harmonic	300 Hz
5. Beat frequency (minus = 230 - 150)	80 Hz
6. Beat frequency (plus = 230 + 150)	380 Hz
7. Beat frequency (minus: second harmonic)	160 Hz
8. Beat frequency (plus: second harmonic)	760 Hz

The vibration characteristics were determined for both the opening and closing motion of the test valve with both a high and a low actuation supply pressure. Each of the valve motion traces was separated into three parts. These three parts consisted of a starting motion, an operating motion, and a stopping motion. Each of these separate operations were then studied to determine the source of the measured energy peaks. The "stop" portion of the opening mode was found to consist of the following energy peaks:

1st Peak	High Pressure	Bellows Fundamental
	Low Pressure	Bellows Fundamental
2nd Peak	High Pressure	Bellows 2nd Harmonic
	Low Pressure	Bellows 2nd Harmonic

In addition to the energy peaks, the intervening null points were found to consist of the following:

1st Null	High Pressure	Minus Beat Frequency
	Low Pressure	Minus Beat Frequency
2nd Null	High Pressure	Spring Fundamental
	Low Pressure	Spring 2nd Harmonic

The valve closing "stop" condition consisted of the following:

1st Peak	High Pressure	Bellows Fundamental
	Low Pressure	Bellows Fundamental
2nd Peak	High Pressure	Plus Beat Frequency
	Low Pressure	Bellows 2nd Harmonic
1st Null	High Pressure	Minus Beat Frequency
	Low Pressure	Minus Beat Frequency
2nd Null	High Pressure	Bellows 2nd Harmonic
	Low Pressure	Spring Fundamental

The vibrational traces for the opening and closing stop conditions are presented in Appendix B.

The results of this study indicate that the single-ply shaft seal bellows is generating a significant amount of vibrational energy and the resonance of this part is resulting in the bellows being subjected to a number of peak loading stresses on each operating cycle. Since the valve operating sequence for the Task I tests was set for valve cycling at the rate of 1 Hz, it is possible that the bellows was being stressed at up to 150 cycles for each operating cycle. It was thought that the increased number of cyclic stresses would account for the poppet shaft seal bellows failure which were apparently occurring prematurely during the cyclic testing. This failure problem could be solved by the use of either a multiply bellows or a welded-type bellows. Both of these alternate type bellows have better vibrational dampening characteristics than the single-ply hydroformed bellows and would be selected for all applications other than with liquid fluorine or similar high energy oxidizers. The single-ply bellows was selected for the 1T32095 valves originally due to the LF_2 constraints and would not be selected for use with either hydrogen or oxygen.

While there are several ways of dampening a single-ply bellows, none of these methods appeared to be warranted on this test program.

3.1.6.5 Test No. 6

The valve seat assembly for the -503 valve was refurbished and returned to MDAC. This seat assembly was refurbished by machining a new bellows assembly and then welding the existing mounting flange and seal portion of the old assembly onto the new bellows. The first two machined bellows assemblies were rejected before the respective machining operations were completed by the vendor. The third unit was completed without difficulty and was acceptable for use in the final valve assembly. The new bellows was fabricated from the same type of material (A286) as used on the original bellows assembly. The final assembly of the reworked part was made using a TIG welder. This welding operation resulted in an out-of-parallel condition between the mounting flange and the seal portions of the final assembly. This condition was corrected by taking the seat assembly to a specialist machine shop where the seal portion of the seat was remachined. After the out-of-parallel condition was corrected, the sealing portion of the assembly was coated with a Teflon S coating. This coating was found to be acceptable mechanically, but

the seat-to-bumper clearance height was not great enough to prevent contact of the bumper portion of the seat under normal operating conditions. Therefore, the coating was removed from the bumper contact area and a 0.012 mm (0.0005 in.) cut made to lower the bumper height dimension. The seat was then returned for removal of the original plastic coating and recoating of the part again with new material.

This last coating was applied after the bumper area had been masked off and no coating was applied to the bumper surface in the final configuration. The seat was returned to MDAC and the sealing surface was smoothed out using the 3×10^{-4} mm (12 μ) Al_2O_3 finishing blocks. The valve was reassembled and installed in the cycle test rig. The initial leakage rate was measured at approximately 0.1 SCCM of GHe at 7×10^5 N/m^2 (100 psig) and after 500 cycles of operation, no leakage was detectable. The -503 valve completed the scheduled 100,000 cycles of operation on Test No. 6 without further indications of leakage. (Table 3-3).

The test was conducted with the valve operating in the double acting mode and with the seat sealing surface loaded to an apparent seat stress of 2.74×10^7 N/m^2 (4,000 psi) (90 percent RSF). No difficulty was encountered during this test run and the valve was found to be in excellent shape with little wear on the Teflon S sealing surface. Visual inspection of the Teflon surface indicated that some flattening and smoothing of the surface has occurred from the 10^5 cycles of operation, however, no apparent damage to the surface was detected. Some transfer of the black Teflon material onto the mating Inconel 718 surface was detected and several areas of the Inconel 718 were found to have pitted during this test. These pits were removed by relapping the poppet sealing surface. This operation removed approximately 0.008 to 0.010 mm (0.0003 to 0.0004 in.) of material before the pits were removed. In one case it appeared that a single grain of Al_2O_3 had become embedded into the Teflon and during testing this particle caused damage to the mating Inconel surface. However, except for this one area the remaining pits appeared to have been caused by the Teflon S coating material. While there is no explanation at this time as to the reason the harder Inconel pitted without damage to the Teflon S, it would appear that a Teflon S coated poppet and seat arrangement should be investigated.

3.1.6.6 Rerun of Test No. 4

As a result of the design review conducted at this stage of the program, it was decided to conduct a rerun of the Test No. 4 of the Task I effort. This rerun was to determine if the gold plating failure which had occurred on the original No. 4 test was due to the lack of hardness of the gold plating or was the result of the schedule testing conditions. The -501 valve seat was refurbished (after completing the portion of the Task II effort scheduled for this valve) and a rerun of Test No. 4 was completed. This test was conducted with the valve operating in the double acting mode and with the relatively high reverse actuator pressure of 1.3×10^6 (190 psig). The valve completed 32,500 cycles without difficulty, however, when the leakage check was attempted at 40,000 cycles it was found that gross leakage was occurring. The valve was disassembled and it was determined that a crack had started in the seat machined bellows. This same type of failure had occurred with the -1 valve on an earlier cycle life test after a total of 156,000 cycles of operation had been completed.

The variation in leakage rates measured (as shown in Table 3-3) would indicate that a very small crack may have started early in this test run and part of the leakage may have been due to the crack. The total accumulated cycles of operation on this valve was approximately 196, 000 (about 40, 000 cycles more than was obtained with the -1 valve before the seat bellows failure occurred).

The failure which occurred on this assembly consisted of a relatively small leakage area in the root of the third convolution from the mounting flange end of the assembly (opposite from the seat sealing end). This defect could have been a very small crack or could have been due to a pin-holing effect through the A286 material. The location of the defect was such that the failed portion could not be viewed under a microscope in a manner that would allow inspection of the failed area. The location of the failure was determined by capping both ends of the assembly with plastic caps and then pressurizing the bellows with GHe while the unit was submerged in Freon.

Repair of the assembly was made by cutting a set of spacers which were inserted into the convolution cavity and TIG welding these spacers to the two adjacent convolution edges. This repair effectively sealed the leaking area by blocking in the failed convolution and thereby forming a solid ring in the bellows. This repair appeared to be very satisfactory, however, the bellows assembly was then one active convolution less than it was originally.

The valve was reassembled after the repaired bellows was returned, and an internal leakage test conducted. The internal leakage rate was found to be approximately 1 SCCM on the reassembled valve. This value compares favorably with the 1.04 SCCM measured after 25, 000 cycles and the 0.82 SCCM measured after 32, 500 cycles. The testing was therefore resumed with the cycle counter set at the 40, 000-cycle figure.

In an attempt to prevent further damage to the -501 valve during the remainder of this test run, a set of orifices were installed in the actuator pressure lines. A 1 mm (0.040 in.) orifice was installed into the valve opening pressure line and a 0.9 mm (0.035 in.) orifice in the valve closing line. These two orifices reduced the valve actuation time response considerably and no mechanical ringing of the valve was observed during valve actuation with the arrangement. The cycle rate of the valve was reduced in proportion to the valve time responses so that a complete valve seat loading could occur during each valve cycle. The cycling rate was reduced to approximately 20 per minute from the previous 35 to 40 per minute.

At the end of the Task I testing, the -501 valve was used to obtain a series of high speed movies of the valve poppet opening and closing functions. A series of four test runs were made at 1, 000 frames per second with valve actuator pressures of 8.6×10^5 N/m^2 (125 psig) and 1.7×10^6 N/m^2 (250 psig). The movies were taken through a glass container which was placed on the valve inlet in place of the normal test adapter. The movies revealed that the valve opened in approximately 25 msec and closed in 9 to 15 msec. The motion was very smooth in all cases and no bouncing or chatter was detected on valve closure. The film was studied on a frame-by-frame basis in the Data Reduction Facility at MDAC and the following information was indicated.

Valve Motion Characteristics

Valve Actuator Pressure	8.6×10^5 N/m^2 (125 psi)	1.7×10^6 N/m^2 (250 psi)
Total Opening	4.8 mm (0.187 in.)	6.5 mm (0.257 in.)
Closing Velocity (Max)	1.2 m/sec (4 ft/sec)	1.5 m/sec (5 ft/sec)
Seat Compliant bellows Compression on Impact	0.7 mm (0.027 in.)	1 mm (0.040 in.)
Closure Seat Stress	1.7×10^7 N/m^2 (2,500 psi)	2.6×10^7 N/m^2 (3,800 psi)

The normal seat stress for the -501 configuration is 3.3×10^7 N/m^2 (4,800 psi), therefore the closure stresses measured were lower than the normal design stresses. The lower contact stresses were indicated further by observing the movies at normal speed. It was noted that the poppet closes on the compliant seat with a steady motion and then stops for several milliseconds while the momentum is absorbed. After this pause, the springs force the poppet down on the seat to full compression in a second separate motion. This 2-stage closing motion, wherein the seat compression is lower during the contacting point in the closure cycle, indicates that the seat stresses were also lower on closure contact. This 2-stage motion is visual on all of the closure cycles recorded.

3.1.7 Summary of Task I Test Results

The final test data plotted graphically for the Task I effort are shown in Figure 3-27. It should be noted that these data have not been normalized for initial leakage rates. The change in leakage with cycles will show the data of greatest interest. It should be noticed that the rerun of test No. 4 does not show the same loss of leakage control as was observed on the original test No. 4. This trend would indicate that the gold plating used on the original Test No. 4 was softer than the present plating, as had been expected. These data confirm the performance predicted for the hard gold-plated surface and indicate that the soft gold hardness measurements obtained by MDAC after the original Test No. 4 run was completed were a true indication of the hardness of the gold plating used for that test. Note that the original test specimen had been certified as hard gold plating by the vendor but measured in the soft gold range by MDAC. The specimen was apparently plated with soft gold.

The results of the complete Task I effort indicate the following:

A. The Inconel 718-A286 material combination is not acceptable in GH_2 when loaded in the 2.7×10^7 to 5.4×10^7 N/m^2 (4,000 to 8,000 psi) seat stress range.

B. The Inconel 718-Soft Gold material (Class 1, Grade A) had a cycle life of 25,000 cycles when loaded at 3.3×10^7 N/m^2 (4,800 psi) seat

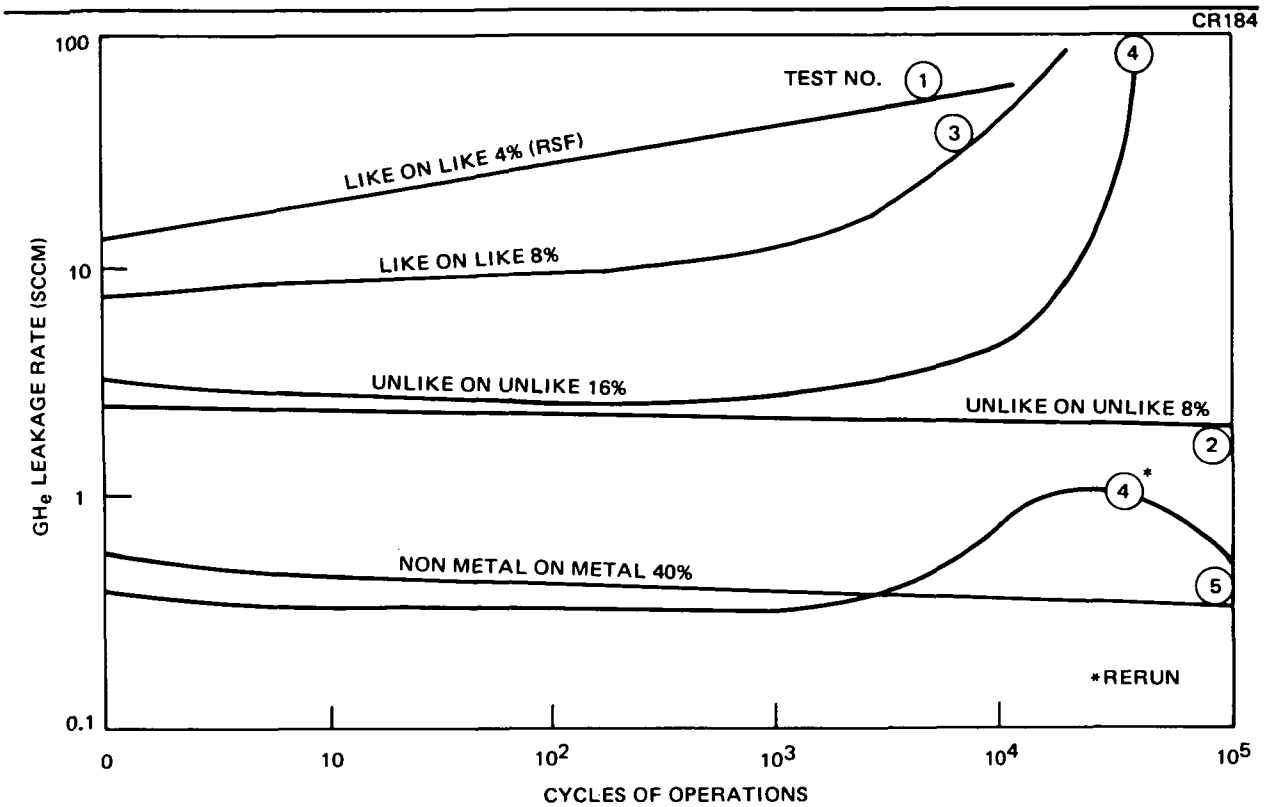

Figure 3-27. Cycle Life Characteristics in GH_2 Environment/Ambient Temperature/7 x 10^5 N/M^2 (100 psig)

stress in GH_2. This combination would appear acceptable for a design cycle life of 10,000 cycles (with a safety factor of 2.5) at this load level.

C. The Inconel 718-Hard Gold material (Class 1, Grade C) is acceptable for 100,000 cycles of operation at seat loading in the 1.7×10^7 to 3.3×10^7 N/m^2 (2,500 to 4,800 psi) seat stress range in GH_2.

D. The Inconel 718-Teflon S (958-203) material is acceptable for 100,000 cycles over the 1.2×10^7 to 2.7×10^7 N/m^2 (1,800 to 4,000 psi) seat stress range in GH_2.

E. The acoustical monitoring equipment used for mechanical signature monitoring gave encouraging results, and this system merits further investigation.

F. The acoustical monitoring equipment used for internal leakage monitor did not produce useful results and no further investigation of this equipment is recommended.

G. The RSF was found to be significant within each different class of sealing materials; however, it does not appear to be adequate for the completed generalization of the wear characteristics. Since the adhesive energy coefficient is significantly different between the different material groups, it appears that consideration must be given to both the RSF and the adhesive energy functions for valid wear predictions.

3.2 TASK II. VALVE CONTAMINATION TOLERANCE TESTING

A series of test were conducted to evaluate the contamination tolerance of the basic (1T32095) valve sealing closure design configuration and two of the three poppet/seat material combinations that were tested in Task I, Cycle Life Testing. The selection of the two best poppet/seal material combinations were made by MDAC based on the results of the Task I testing. The material selected were the Inconel 718/Hard Gold Plate and the Inconel 718/Teflon S combinations (operating with a RSF of 16 percent and 90 percent respectively).

The contamination tolerance testing consisted of full-flow tests (valve held fully opened during testing) and valve cyclic tests (valve fully opened and closed) at full-flow conditions.

The full-flow tests were performed to determine the damage to the valve-closure sealing surfaces from particulate contaminants impacts (hits) at high flow velocities with the valve fully opened. This series of tests included two full-flow tests which were performed on the -501 valve with ambient gaseous nitrogen containing a measured amount of solid contaminants. The contaminants selected consisted of particles in the 25 to 75-μ range for the first test and the 70 to 200-μ range for the second test. The particle material selected was aluminum oxide (Al_2O_3) particles which were harder than the poppet and seat materials.

A series of cycling tests were performed to determine the damage to the sealing closure surfaces from particulate contaminants trapped between the poppet and seat during cyclic operation. This series of tests were conducted as follows:

A. A series of seal closure contamination tolerance tests were performed on each of the valves (-501 and -503) with GN_2 test media containing a measured amount of particulate contaminants. The GN_2 flow rate was a nominal 1.1 kg/sec (2.5 lb/sec).

B. The valves were then tested using LN_2 as the fluid media. The LN_2 flow rate was 3.8×10^{-3} m^3/sec (60 gpm).

During these tests, the valve was repeatedly cycled opened and closed to determine whether particles were trapped on the sealing surfaces. The cycling rate was a nominal 1 Hz.

3.2.1 Component Design Evaluation

The evaluation of the contamination damage tolerance of propellant shutoff valves was made using two existing (1T32095) poppet-type shutoff valves. These pneumatically actuated valves were of the flat-on-flat sealing surface design and were described in detail in References 2 and 4. The original valve design was made with the objective of obtaining reliable operation with some degree of propellant contamination and the contamination tolerance features shown in Figure 3-28 were incorporated in the original design. This sketch shows a cross section of the main internal sealing interface of

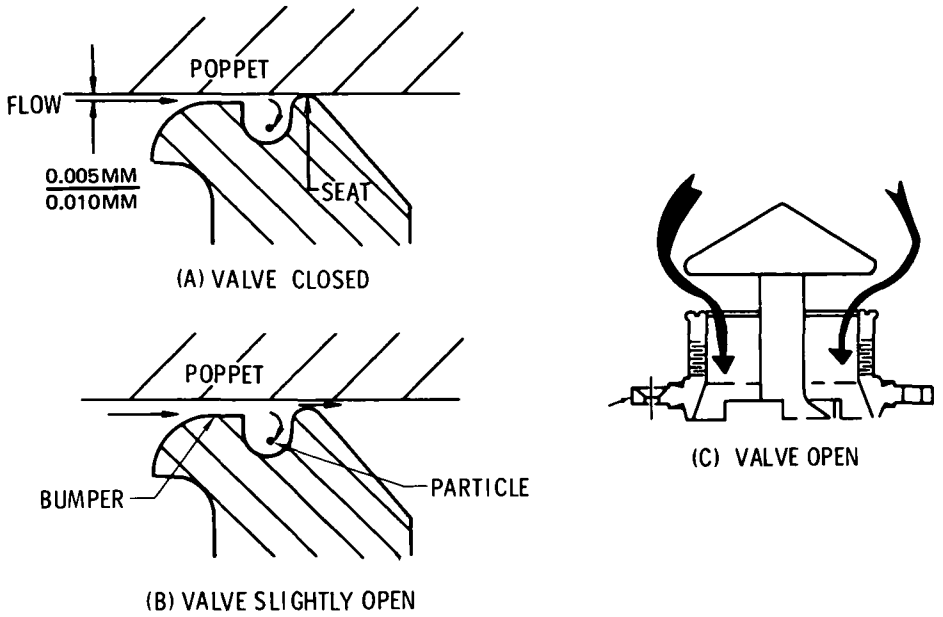

Figure 3-28. Contamination Entrapment Features of Valve Seat Design

the poppet and seat. Several features of this design have the capability of providing acceptable contamination damage avoidance characteristics during the valve closing operation. Note that with the valve poppet slightly off the seat but in the process of closing (Figure 3-28B) the bumper-to-seat clearance becomes so small that large particles are stopped in the bumper zone and cannot reach the seat sealing area. In addition to this shielding arrangement, the contamination trap placed between the bumper and the sealing surface provides an increase in flow area which permits smaller particles to fall out of the flow stream and separate into the contaminant trap. Further, since the velocity across the seat sealing surface is quite high at the point of seat contact, the jet effect of the flow stream tends to keep the seat sealing surface free of contamination particles. The valves made with this design arrangement were tested successfully with a liquid fluorine propellant earlier and no contamination damage occurred during that test program (Reference 4).

However, the propellant used on the previous testing was filtered through a MDAC developed 10-μ filter during the propellant loading process and therefore the lack of contamination damage could be attributed to the basic valve design or to the degree of cleanliness of the propellant and piping. To evaluate the actual tolerance of the 1T32095 valves to contamination, a new test setup was developed, with the capability of injecting controlled amounts of prepared contamination into the flow stream under actual valve operating conditions.

Two valve configurations were tested during the original design evaluation portion of the effort. These two configurations were identical mechanically; however, a different seat coating material was used for each valve. The -501 valve had a 0.012 mm (0.0005 in.) plating of 23+ carat hard gold MIL-G-45204, Type 1, Class 5, Grade C, while the -503 had a 0.025 mm (0.001 in.) (nominal) coating of a Teflon S (958-203) material (Reference 5). The basic substrate seat material was A286 and the mating poppet surface was Inconel 718 in both configurations.

3.2.2 Test Planning and Setup

Task II consisted of a series of 11 tests, (GN_2-LN_2, full flow and cyclic with the -501/-503 valve configuration), as shown in the test matrix (Table 3-6). These tests were conducted at the A-12 test facility using the basic test setup shown in Figure 3-29. The LN_2 setup was similar to the GN_2 setup shown except that the LN_2 storage tank was used in place of the GN_2 pressurant supply.

This test setup operated in an open-loop mode, under real operating conditions, and with controlled contaminant injection. There are several important advantages associated with the use of this type of system. In general, this open-loop system using full-size components, with rated flow rates and duty cycles, and offers the closest approach to the actual conditions occuring in a real flight situation. The disadvantages of this type of system are limited to the problems associated with the effects of injector injection rates on contaminated flow rates (average per liter) and to the disposal of the test media used during each test. As discussed later, the test media was changed to GN_2 from GH_2 for this program to minimize the media disposal safety hazards.

The injection rate control problem was not solved completely during this program due to the modification required on the injector system during the early part of the program. By developing the injector system, to improve the control of particulate injection rate, the tests conducted during the latter portion of the test effort were generally satisfactory for injection of 1 to 10 grams of test material. The injector used would require further development to handle the injection of 0.1 to 1 gram of material in a controlled manner.

Notwithstanding the limitations noted, the open loop system used for the contamination tolerance testing on this program represents a significantly better arrangement for component testing than have the various systems used in the past (References 6 and 7).

The test plan specifies GN_2 for the gaseous test runs in place of the originally specified GH_2. This change was made after a study was conducted to evaluate the relative merits of each media. The GN_2 was selected for the following two reasons:

1. The heavier GN_2 would retain the injected contaminant particles in suspension for a longer time period under the conditions of

Table 3-6

VALVE CONTAMINATION TOLERANCE TEST MATRIX

Test No.	Valve*	Test Fluid Media	Contaminant Particle Size**	Cycle Rate/ Sec	Instrumentation or Test Objective
Full Flow Tests					
1	-501	GN_2	None	-0-	Leakage, flow rate
2	-501	GN_2	25 to 75	-0-	Leakage, physical damage
3	-501	GN_2	75 to 200	-0-	Leakage, physical damage
Seal Closure Tests					
4	-1	GN_2	25 to 75	1 Hz	Leakage, physical damage, cycling
5	-1	GN_2	75 to 200	1 Hz	Leakage, physical damage, cycling
6	-501	GN_2	25 to 75	1 Hz	Leakage, physical damage, cycling
7	-501	GN_2	75 to 200	1 Hz	Leakage, physical damage, cycling
8	-1	LN_2	25 to 75	1 Hz	Leakage, physical damage, cycling
9	-1	LN_2	75 to 200	1 Hz	Leakage, physical damage, cycling
10	-501	LN_2	25 to 75	1 Hz	Leakage, physical damage, cycling
11	-501	LN_2	75 to 200	1 Hz	Leakage, physical damage, cycling

*The valves designated for testing are subject to substitution of the new valve configuration, if required.

**Micron

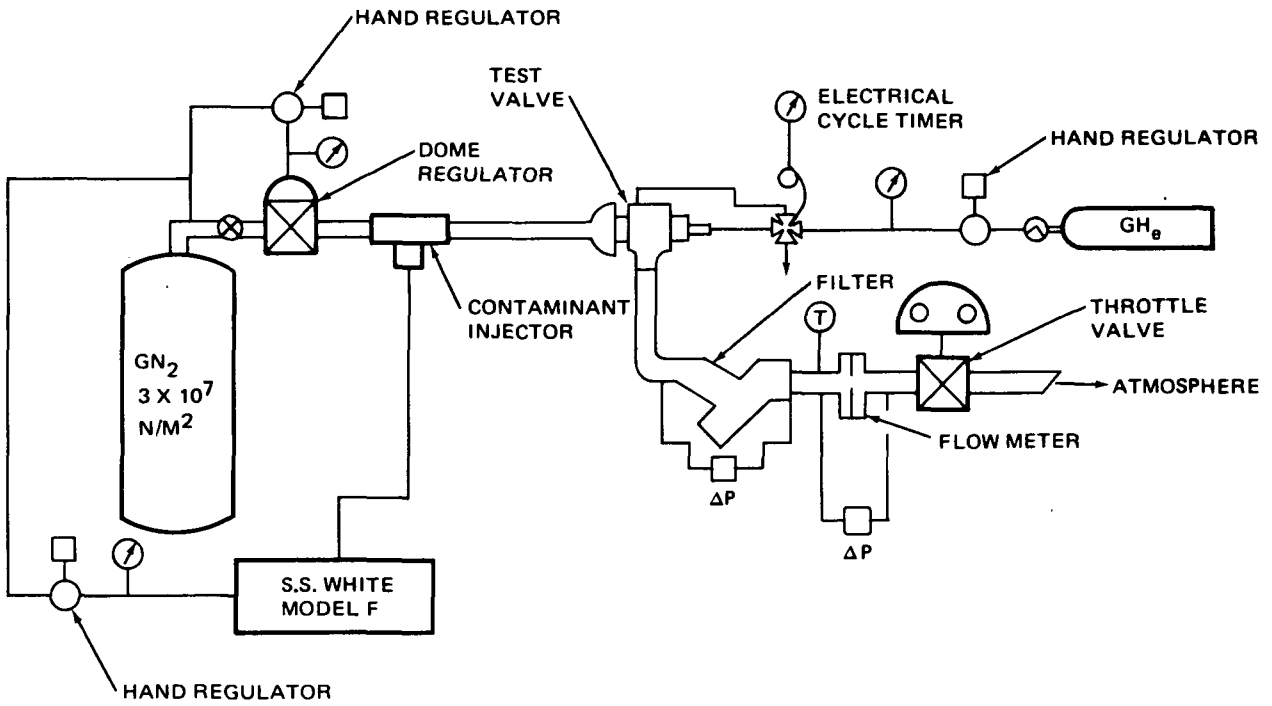

Figure 3-29. Full-Flow Test Setup

these tests and therefore a greater number of particles could pass through the valve on each test run.

2. The safety hazard was greatly reduced with the GN_2 media.

The contamination mixture selected consisted of Al_2O_3 particles in a random size range within the two specified size ranges. The number of particles per gram were calculated using a log normal size distribution for each of the two size ranges. The Al_2O_3 particles were selected for the following two reasons:

1. These particles are hard (Knoop 1450-1750) and therefore they meet the basic hardness requirement.

2. These particles are relatively light in weight (specific gravity 3.4 to 3.5) and will therefore be retained in the fluid stream longer than would particles with greater density. While both of these powders are readily available, they do not have the uniformity of shape needed for accurate grading and counting operations. The present powder has particle shapes ranging from nearly spherical to those which are long and thin. The latter particles do not lend themselves to accurate grading and counting procedure and hence introduce some degree of uncertainty into the test results.

The test powders selected for the controlled contamination tests were size graded Al_2O_3 particles. The powders were obtained by passing a supply of Alcoa T60 dust through a set of standard sieves. Two sizes of powders were used for testing. A fine powder was obtained by adding the T60, which passed through a 200-mesh sieve, with an equal amount of S.S. White Airbrasive powder No. 3. A coarse powder was obtained from the T60 by collecting the particles which passed through a 60 mesh sieve but which did not pass through a 200-mesh sieve.

A modified S.S. White Model F Airbrasive unit (Reference 8) was selected to inject the particulate into the pressurized flow stream.

The modifications to the unit consisted of:

A. Substitution of a particulate mixing chamber orifice plate with larger orifices.

B. Adapting the hand held nozzle assembly to permit rigid mounting in the test flow loop.

C. Installing a nozzle with a larger throat size so that particles in the 75 to 250 μ size range could be injected.

To operate successfully at the desired pressure level of 7×10^5 N/m^2 (100 psig), the chamber relief valve setting was readjusted on the injector unit. The actual test setup for the GN_2 tests is shown in Figure 3-30.

CR184
N/A

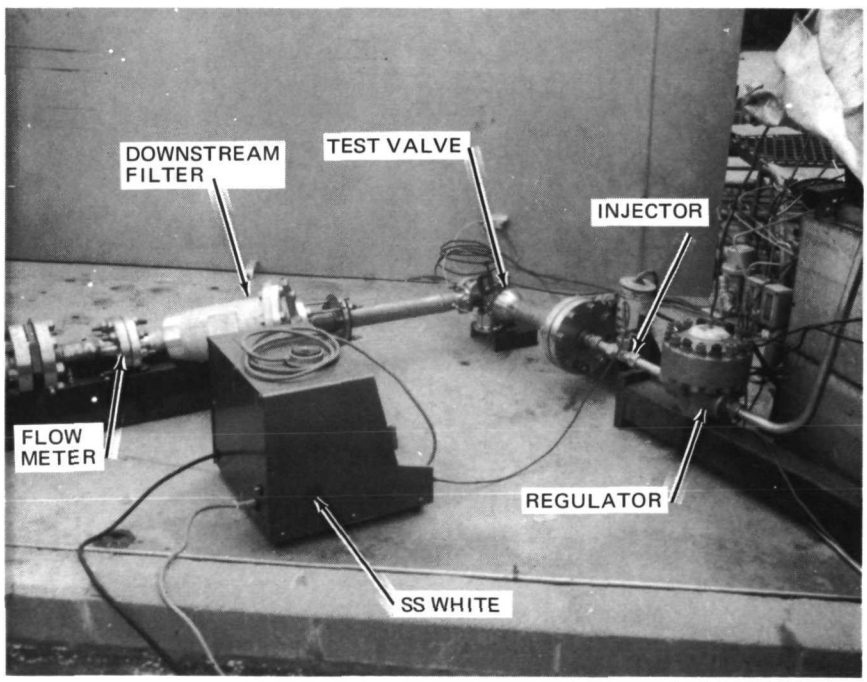

Figure 3-30. Test Setup for Task II Testing

3.2.3 Contamination Tolerance Tests

3.2.3.1 Test Preparations

The -501 valve was refurbished for use on the Task II testing effort. The refurbishment included stripping the gold plating from the valve seat and replating the surface with a new layer of gold. The wear characteristics measured on Test No. 4 of Task I indicated that the gold plating hardness might not be as hard as was originally specified. Consequently, a hardness test was made at MDAC of the worn gold plating before the part was returned for replating. The measured hardness values were in the 85 to 90 Knoop range which indicates a very soft, Class A plating (24 carat gold). A check was then made, and the records indicated that the part was treated in a hard gold (23+ carat) plating solution; no explanation for the soft condition could be found. The plating solution used was specially formulated and, while the solution is similar to several commercial solutions, it was not the same mixture. To gain additional information on the gold plating characteristics, a separate test disk was plated in the same solution as the new plating which was put on the valve seat for the Task II testing. This disk was tested at MDAC after plating and found to be in the hard Class C range (176 Knoop). To obtain accurate hardness readings on these very thin platings — 0.01 mm to 0.012 mm (0.0004 to 0.0005 in.) - with the Knoop testing machine it is necessary to section the part and make hardness readings on the plated surface parallel to the substrate. Since it is impractical to section the valve seat, an accurate hardness reading was not possible.

The replated seat was reassembled in the valve for the Task II testing and a preliminary leak check made in the A-12 clean room. This check indicated that the leakage values were acceptable for further testing.

The initial modifications to the contamination injection unit were completed and calibration runs of particulate injector rates were performed. The initial flow rate calibration tests showed an injection rate of 2.5 grams/minute with the nozzle at ambient pressure and the mixing chamber pressurized to 3.5×10^5 N/m^2 (50 psig) [i.e., a 50-psi differential]) when injecting the large size particles. Since this injection rate was within the desired range the injector was placed in a closed pressurized plenum chamber. A calibration run made at 7×10^5 N/m^2 (100 psig) receiver pressure and 10.5×10^5 N/m^2 (150 psia) mixing chamber pressure (the S. S. White unit is limited in operation to approximately 10.5×10^5 N/m^2 (150 psia) or 9.3×10^5 N/m^2 (135 psig). This arrangement produced a 1.2×10^5 N/m^2 (35 psi) differential which was found to be sufficient to produce an injection rate of about 2 grams/minute.

The first test was completed without contaminant injection so that the system flow control valve could be set for the test condition of 1.1 kg/sec (2.5 lb/sec) flow rate at 7×10^5 N/m^2 (100 psig) upstream pressure. This condition was established. The system was then checked with the test valve cycling and it was determined that the upstream pressure regulator operates slower than the test valve during cycling operation and the upstream pressure to the test valve overshoots to about 1×10^6 to 1.4×10^6 N/m^2

(150 to 200 psig) momentarily on each valve closing cycle. This overshoot does not affect the valve operation, but it does result in a complete loss of pressure differential across the injection unit. It was previously determined that when the injection pressure differential drops to a low value the particulate flow stops in the nozzle section and the injection nozzle becomes "plugged" with particulate. When this plugging occurs, the nozzle may remain plugged even when the downstream pressure is returned to normal and the correct pressure differential is reestablished. While this condition could become a serious problem during the cyclic portion of the test program it was minimized by selecting the valve cycle sequence such that the valve remained in the closed position for a minimum time interval and therefore minimize the time that the injector was exposed to high back pressure. It would appear that this problem caused some variation in the amount of particulate injected within a fixed time interval of cyclic operation.

3.2.3.2 Full Flow Testing – 501 Valve Configuration

After establishing the system flow dynamics, the first full-flow test was conducted. Since the injection system was completely charged with the large size particles of Al_2O_3 (75 to 250 μ) the initial test run was test No. 3 instead of test No. 2 (Table 3-7). The test run was made with a flow time of 30 sec and an injection time of 1 sec. After completing the run, the system was disassembled and inspected for particulate injection. No evidence of particulate injection was found so the test was repeated with a 60-sec flow time and a 10-sec injection time. Post-test inspection indicated that there was still no contaminate injection occurring during the test run. To correct this difficulty, the injection system was modified and the test repeated. The modification consisted of enlarging the mixing chamber particulate inlet holes to a No. 64 drill size from the No. 68 drill size. The test run was then repeated with a 60-sec flow and with a 60-sec injection period.

The post-test leakage test was attempted after this run, however, the internal leakage had increased to a point above the readability range of the testing apparatus. The post-test inspection revealed that approximately 13.5 grams of particulate was injected in the 1 minute run. This figure is considerably greater than the 0.25 grams which had been selected for the full flow run. Of the 13.5 grams injected, 6.5 grams was recovered from the filter housing and duct work and 0.5 grams from the 10-μ filter element.

While this test was much more severe than had been scheduled, it did provide some very useful data. The results (shown in Table 3-7) indicate that the valve design was not optimum for full flow contaminate runs.

The test valve was disassembled at the completion of the test and inspected for damage. It was found that the upstream portion of the poppet and the shaft deflector (which protects the shaft seal bellows) had suffered considerable damage of the type produced with a sandblasting machine. (The cover plate for the filter housing was also damaged in this manner.) The valve seat sealing surface was stripped of almost all of the gold plate and had suffered considerable impact damage as shown in Figure 3-31. The bumper area of the seat was damaged to a lesser extent as shown in Figure 3-32.

Table 3-7

TASK II – CONTAMINATION TOLERANCE TEST RESULTS

No.	Type	Media	Valve[b]	Contaminant			Pretest Leakage (SCCM)	Post Test Leakage	Leakage Change
				Size (μ)	Weight Injected (Gms)	Injection Rate (Mg/Liter)			
1	Calibration	GN_2	-501	--	0	--	--	--	--
2	Full Flow	GN_2	-501	25 to 75	1.5	--	1.1	2.24	1.14
3	Full Flow	GN_2	-501	75 to 250	13.5	--	1.1	(c)	--
4	Cyclic	GN_2	-501	75 to 250	1.0	--	0.2	0.4	0.2
5	Cyclic	GN_2	-501	25 to 75	1.5	--	2.24	3.3	1.1
6	Cyclic	LN_2	-501	25 to 75	2.0	33.9	0.2	0.1	(-0.1)
7	Cyclic	LN_2	-501	75 to 250	1.5	56	0.24	45	44+
8	Cyclic	LN_2	-503	75 to 250	0.9	20	0.1	0.4	0.3
9	Cyclic	LN_2	-503	25 to 75	3	100	0.0	21	21
10	Cyclic	GN_2	-503	25 to 75	2	--	0.9	0.66	(-0.2)
11	Cyclic	GN_2	-503	75 to 250	1	--	1.1	(c)	--
8[a]	Cyclic	LN_2	-503	75 to 250	1.5	--	0.04	1.0	0.96

(a) Rerun.
(b) -501 Hard Gold Plated Seat
-503 Teflon S Coated Seat
(c) Value too high to measure.

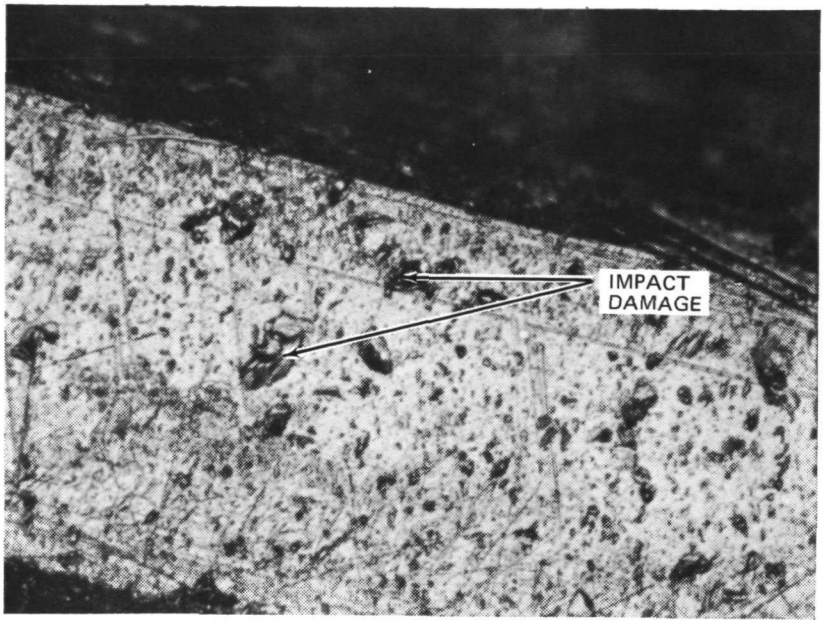

Figure 3-31. -501 Valve (Hard Gold-Plated) Seat Sealing Surface after First Contamination Test (160X)

The gold plating was not removed from the bumper area; in fact, the only place that lost the gold plating was the seat sealing surface. The bottom of the contamination trap groove suffered little or no damage on this overly severe run, and this location would appear to be a more desirable location for the seat sealing surface than the raised seat location of the present design.

The sealing surface of the poppet suffered very little damage, however, some of the shine was removed from this surface as shown in Figure 3-33.

The valve refurbishment operation was started by lapping the seat sealing surface down so that a new gold plating could be applied. After lapping this surface until the seat width had increased from 0.25 mm (0.010 in.) to 0.5 mm (0.020 in.) without removing all of the surface damage, it was decided that the valve seat seal surface will require remachining before an acceptable surface can be obtained.

The second full-flow test was completed using the 25 to 75-μ size particles. A total of 1.5 grams of particulate was injected during this test. The leakage rate changed from 1.1 SCCM pretest to 2.2 SCCM post test. Post-test inspection indicated that four significant hits had occurred on the seat sealing surface. Three of these hits caused only minor damage and would probably not have affected the leakage rate to a measurable extent. The fourth "hit" had resulted in the embedment of a small Al_2O_3 particle in

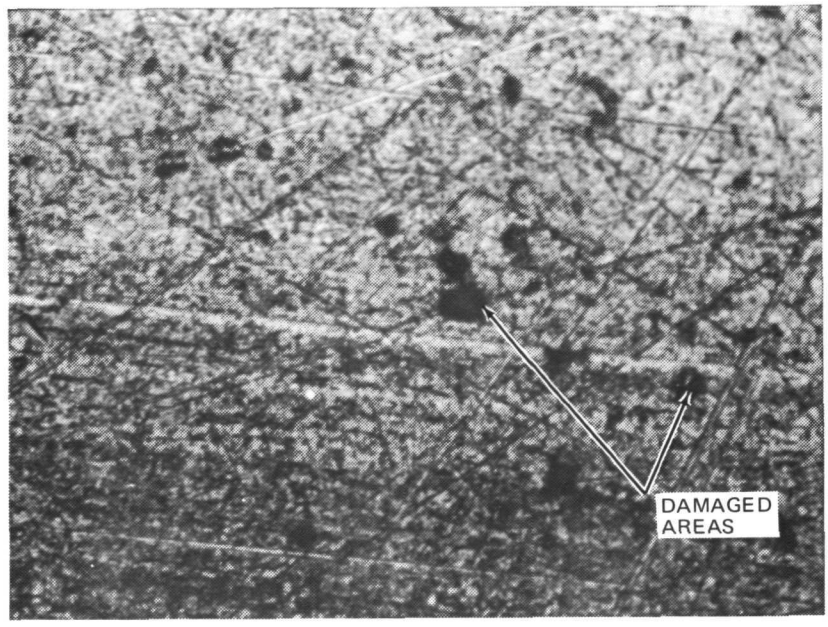

Figure 3-32. -501 Valve Bumper Surface after First Contamination Test (160X)

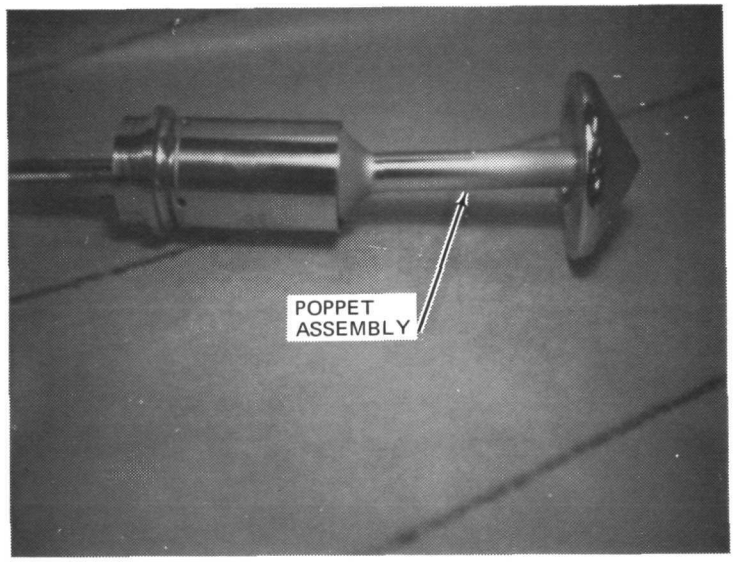

Figure 3-33. -501 Valve (Inconel) Poppet Assembly after First Contamination Test

the gold plating and this particle remained embedded at the point of impact. This embedded particle was not completely embedded and apparently was preventing the proper loading on one side of the valve seat. This slight unloading of the seat sealing surface on one side of the seat appears to have caused the relatively small increase in leakage rate measured on this test. The embedded particle was in the 25 μ size range and appears to have been about 0.025 mm (0.001 in.) in diameter. Since the -501 valve seat has a gold plating which is less than half this amount 0.01 mm (0.0004 in.), it is understandable why the particle could not be embedded to a depth that would not have increased the leakage rate. Based on the results of this test, a gold plating of 0.025 mm (0.001 in.) would be indicated as an improvement in valve damage tolerance. However, since Test No. 1 indicates that better full flow performance would be expected by moving the raised seat portion of the sealing surface to the poppet (and mating this surface with a submerged surface in the seat assembly), it appears that no change in gold plating would be required for the modified valve design. The present design and the proposed redesign are shown in Figure 3-34.

3.2.3.3 GN_2 Cyclic Flow Tests -501 Valve Configuration

The two cyclic flow contamination tests with GN_2 on the -501 valve were completed using the test setup shown in Figure 3-30. These tests consisted of testing with both the large and small particle sizes. On test No. 5, (Table 3-7) the valve was cycled for 10 complete cycles while 1.5 grams of 25 to 75 μ size Al_2O_3 was injected. The leakage increased from 2.2 SCCM (pretest) to 3.3 SCCM (post test). The post-test inspection revealed very little seat/poppet damage and no single area of substantial damage - the random minor damage apparently causing the relatively small increase in post test internal leakage.

The valve poppet and seat were refinished after this test. The poppet was relapped using conventional methods. The seat was refinished by MDAC using the 3×10^{-4} mm (12 μ) Al_2O_3 surfacing plate without using any lapping compound. The valve was reassembled for test No. 4. The pretest leakage rate was measured at 0.2 SCCM with GHe at 7×10^5 N/m^2 (100 psi). Test No. 4 was conducted in two parts due to a reduced injection rate of particulate during the first 10 cycles. A total of 1-1.5 grams of 75 to 250 μ size particles were injected during two test runs of 10 cycles each (20 cycles total). The post-test leakage rate was 0.4 SCCM.

Since the minimum specified amount of particulate is something less than 0.5 grams per test, the testing on tests 3-5 was complete with 2 to 3 times the required amount of particulate. By considering the amount of leakage increases measured and the amount of particulate injected, it would appear that the contamination tolerance features of the present valve design were working as anticipated. However, the data from the full flow test which had 13.5 grams of particulate injected indicates that further improvements in the design could be made by modifying the valve.

3.2.3.4 LN_2 Cyclic Flow Tests -501 Valve Configuration

The two contamination tolerance tests scheduled for the -501 valve in LN_2 were then completed. The first liquid test conducted with the 75 to 250 μ size particles was completed using the same injection equipment used

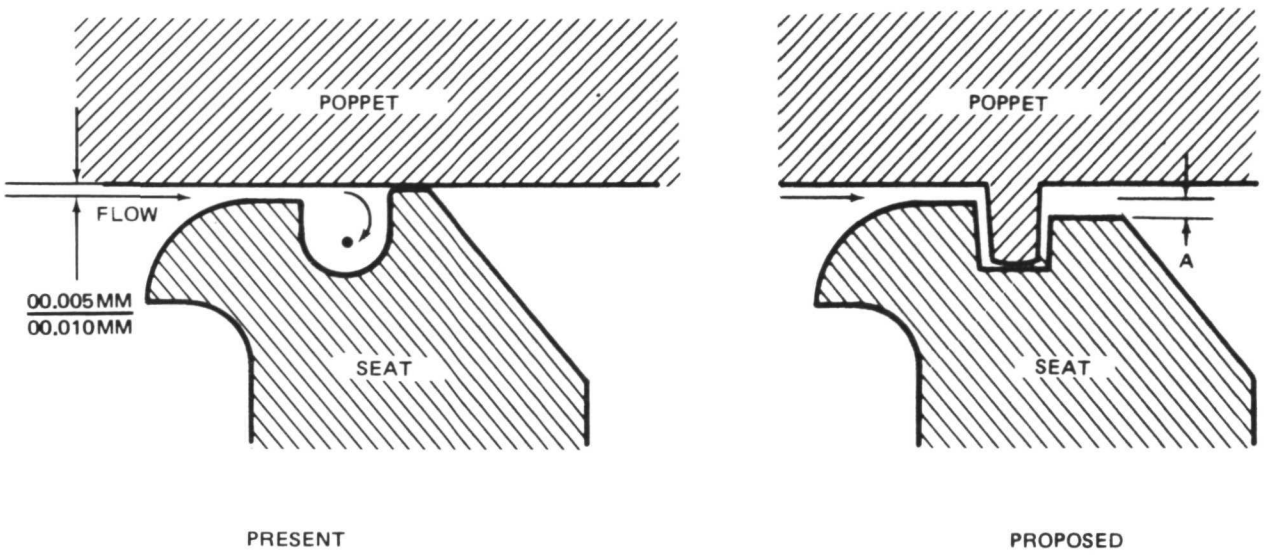

Figure 3-34. Present Design and Proposed Redesign Seal Closure Configuration

for the gaseous testing portion of this program. The test setup for LN_2 testing is shown in Figure 3-35. The pretest internal leakage was found to be approximately 0.24 SCCM (GHe at 7 x 10^5 N/m^2 100 psig) (Table 3-7). Test No. 7 consisted of 20 to 25 cycles of operation with a total of 1.5 grams of contaminate material being injected, (56 Mg_2/liter rate). The post-test leakage was found to be 45 SCCM at 7 x 10^5 N/m^2 (100 psig). The valve was disassembled and inspected for damage. The seat surface was found to have suffered moderate impact damage from the particles; however, no damage areas were found which went completely across the seal width as shown in Figures 3-36 and 3-37. The length of the worst damage extended for only 25 to 30 percent of the total seal width, and this reduction in seat width would not account for the increase in internal leakage rate. Three areas of damage were found where an entire Al_2O_3 particle, or some portion of the particle, was embedded into the gold plating or where some portion of a particle was still embedded in the plating. A relatively large number of small damaged spots was also detected on the mating Inconel 718 poppet sealing surface. The increase in leakage rate appeared to be due to the partially embedded particles holding the sealing surfaces apart and not from the impact-damaged areas observed. These results indicate that the thickness of the gold plating is insufficient to permit complete embedment of the large contamination particles used for this test. It would appear that the plating thickness should be increased to about 0.025 mm (0.001 in.) from the present 0.01 mm (0.0004 in.) for service where particles in the 75 to 250-μ size range is possible.

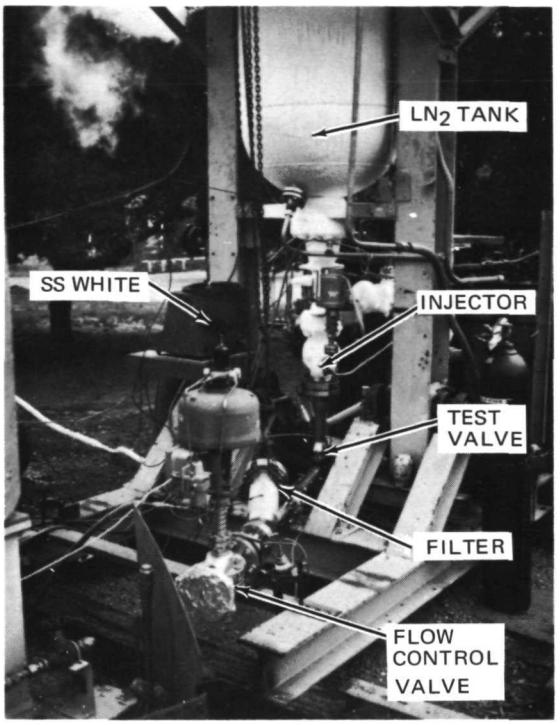

Figure 3-35. Test Setup for LN_2 Contamination Tolerance Tests

The seat assembly was replated and refinished for the next test. Test No. 6 was conducted with the smaller 25 to 75-μ particles. The pretest leakage was measured at 0.2 SCCM and the post-test leakage was 0.1 SCCM (Table 3-7). A total of 20 cycles of operation was completed and 2 grams of material were injected into the valve (at the rate of 33.9 mg/liter).

The reduction in leakage rate measured would be attributed to the "wearing-in" of the sealing surface as a result of the 20 cycles completed on the test and an additional 50 cycles completed in system checkout. The results of this test indicate that the present gold-plating thickness is sufficient to handle particles in the 25 to 75 μ size range and that the contamination avoidance characteristics of the valve are functioning in the proper manner.

Excellent results were obtained on the LN_2 tests even though the valve was installed in the vertical plane such that all of the injected material was allowed to fall in a vertical direction directly into the valve and potential particulate separation from the flow media was eliminated. This condition represents the most severe test condition possible.

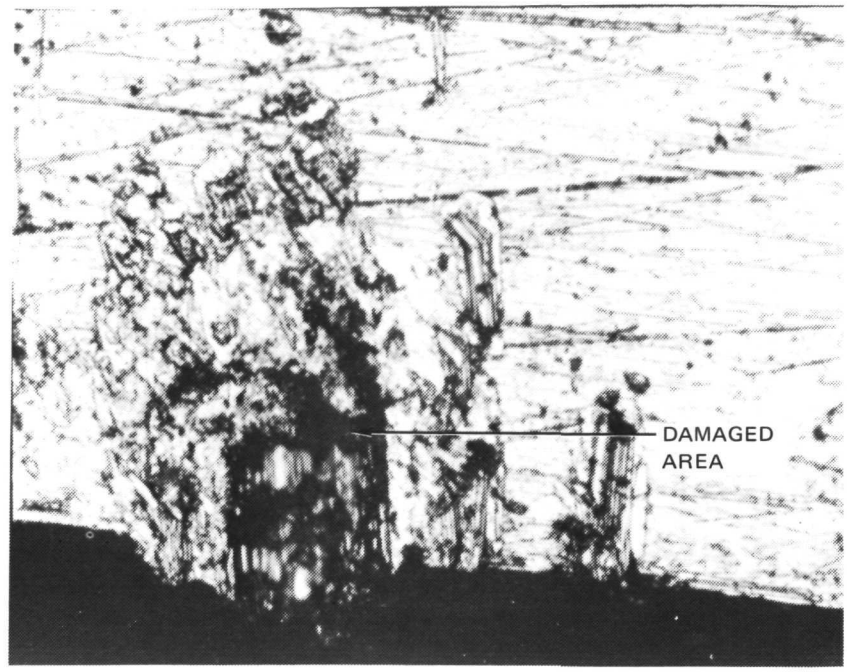

Figure 3-36. Contamination Damage on Gold Plated Seat (75–250μ Particles in LN_2) (250X)

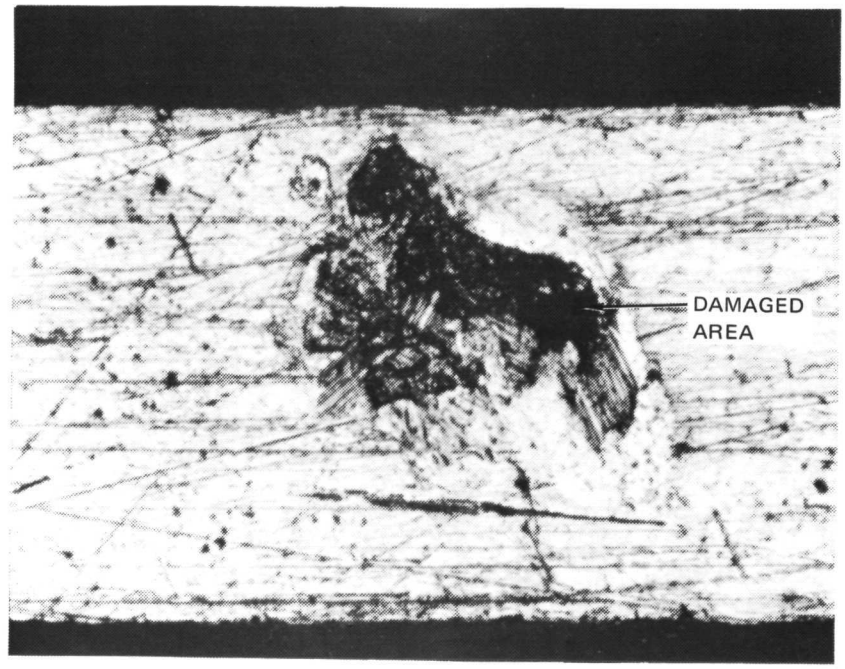

Figure 3-37. Contamination Damage on Gold Plated Seat (75–250μ Particles in LN_2) (250X)

3.2.3.5 LN_2 Cyclic Tests -503 Valve Configurations

The first contamination tolerance test with the Teflon "S" coated -503 valve configuration was then completed. This test was conducted using the same test setup used on the last test made with the -501 valve. The -503 valve poppet was relapped. No damage was detected on the Teflon S coated valve seat so no rework of the seat assembly was made in preparation of the Task II testing. A very light lapping operation was conducted by MDAC using the 3×10^{-4} mm (12 μ) Al_2O_3 lapping blocks to ensure that a smooth Teflon "S" surface existed for the next test. This surface condition was verified when the pretest leakage rate was measured at 0.1 SCCM of GHe at 7×10^5 N/m^2 (100 psig (Table 3-7). A total of 0.9 grams of particulate was injected during the 10-second, 10-cycle test run (Test No. 8). The contamination was injected at a rate of 33.9 mg/liter of LN_2 flow.

Post-test inspection of the valve closure interface indicated that little or no damage had occurred to the Inconel 718 poppet and only mild damage had occurred to the Teflon "S" coated seat (Figure 3-38). The damage to the seat surface consisted primarily of a single spot where a channel had been created by particulate impact (Figure 3-39). This channel extended for approximately 95 percent of the distance across the seat sealing surface 0.25 mm (0.010 in.), and most of the observed leakage occurred at this one spot. The post-test leakage rate was 0.4 SCCM which is well within the valve design specification and, except for the one damage spot mentioned above, the leakage rate would probably not have changed a measurable amount from the pretest leakage condition.

The next test was conducted using the 75 to 250-μ size particles. A recheck was made of the valve log books entries and it was determined that Test No. 8 had been run with the same size powder (75 to 250 μ or powder No. 2). As a result, the running of this test was essentially a rerun of test No. 8. The internal leakage rate was found to be higher after test No. 9 (1 SCCM) than had been found after Test No. 8 (0.4 SCCM), however, this was not considered to be an excessive difference when the nature of the test is considered. While refurbishing the valve for Test No. 9, it was found that the shaft seal bellows was cracked at the last convolution on the inner end of the bellows assembly. The poppet assembly was then taken to the original supplier of the valve for estimation of cost and schedule for repair of this assembly.

This bellows assembly originally had 20 convolutions and since the end convolution was the one which failed, it was decided that the simplest repair would consist of removing the end convolution and rewelding the remaining 19 convolutions back in place on the shaft. The actual repair removed the two end convolutions and the remaining 18 convolutions were welded into place. The welding was completed satisfactorily and the assembly returned to the A-12 test site. Since the shaft seal was now shorter than when originally installed, the shaft travel was reduced to compensate for the shorter bellows. A 2.5 mm (.1 in.) shim was placed in the actuator piston cavity to reduce the total shaft travel in the open position. To further improve the duty cycle on the shaft bellows a 0.8 mm (0.035) orifice was

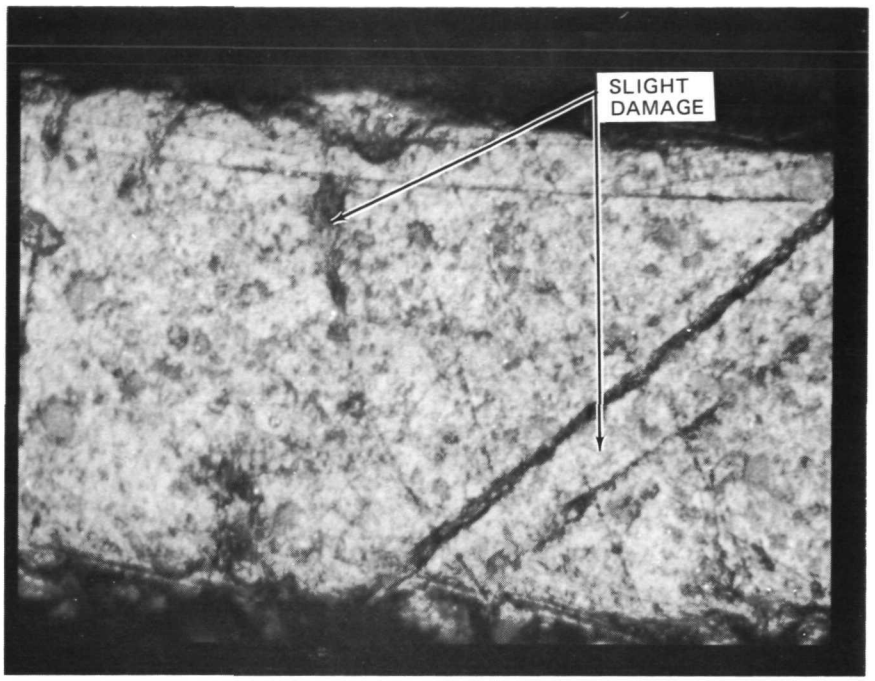

Figure 3-38. Typical Damage to Teflon S Coated Seat on Test No. 8 - LN_2 (75-250μ) (160X)

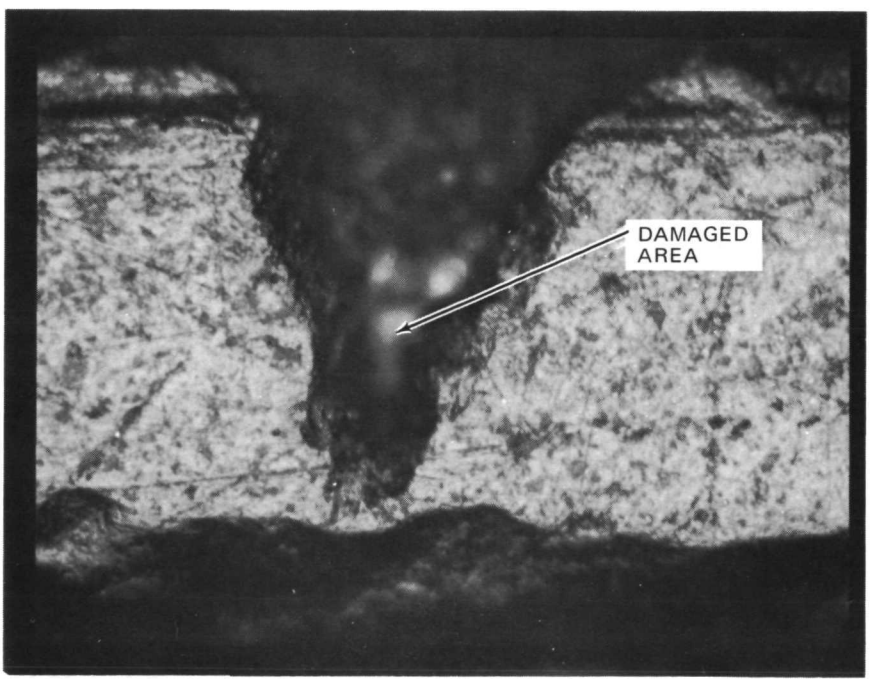

Figure 3-39. Chipped Area of Teflon S Coated Seat on Test No. 8 (160X)

placed in the actuator pressure inlet such that the time response of the valve was reduced and a very slow poppet travel was obtained. When this arrangement was tested with LN_2 it was found that the time response was too slow to provide good cyclic control and the restricting orifice was replaced with a 1 mm (0.040) orifice. This arrangement proved to be satisfactory and was used on test No. 9.

Test No. 9 was completed on the -503 configuration (Inconel 718-Teflon S) using the small No. 1 powder (25 to 75 μ). The pretest leakage was less than the minimum detection rate for the water displacement measuring system and a value of 0 SCCM at 7 x 10^5 N/m^2 (100 psig) GHe was recorded. The test was conducted in the LN_2 flow loop. The powder injection was greater than anticipated and a total of 3 gms was injected during the 7 seconds of injection time (~100 mg/liter rate). The damage to the seat sealing surface was greater than had been anticipated. The post-test leakage rate was 21 SCCM at 7 x 10^5 N/m^2 (100 psig)(Table 3-7). The post-test inspection revealed several areas of moderate surface damage including damage spots of about 75 μ in size (Figure 3-40). In addition to the spot damage detected, one area was found with a severe "channeling" type of failure (Figure 3-41). At the location of the channel failure site, the center portion of the Teflon was removed along the centerline of the seat face while most of the edge material was still intact. This particular area of damage appears to be the area of greatest leakage.

The high leakage rate measured on Test No. 9 was probably due to a combination of three things. These were:

1. The unusually high injection rate.

2. The injection system may not have been completely purged of the No. 2 powder and apparently several larger particles were injected along with the smaller No. 1 powder.

3.2.3.6 GN_2 Cyclic Tests -503 Valve Configuration

Test No. 10 was completed after the test setup was returned to the Pad 1 test area for GN_2 testing. The poppet surface was relapped before this test and 0.0025 to 0.005 mm (0.0001 to 0.0002-in.) of material was removed before an acceptable surface was obtained. The Teflon S coating was removed from the assembly and a new coating provided. This new coating was then smoothed out using a 10^{-4} mm Al_2O_2 finishing blocks (at MDAC) and a pretest leakage test completed. This test showed an unacceptably high internal leakage rate and the valve was disassembled for further rework. The surface contact between the Teflon S and the poppet sealing face was found to be very light in certain portions of the seal area. It appeared that the light sandblasting operation, which was required for the A286 surface before the Teflon S was applied, had caused uneven erosion on the A286 surface in some areas. The lapping operation was resumed on the Teflon S and, before a flat sealing surface could be attained, the height of the Teflon S was reduced to the same height as the seat bumper land height as shown in Figure 3-42. To correct this condition the seat was placed in a lathe, and the bumper height was reduced using fine emery paper. After the bumper height was reduced, the

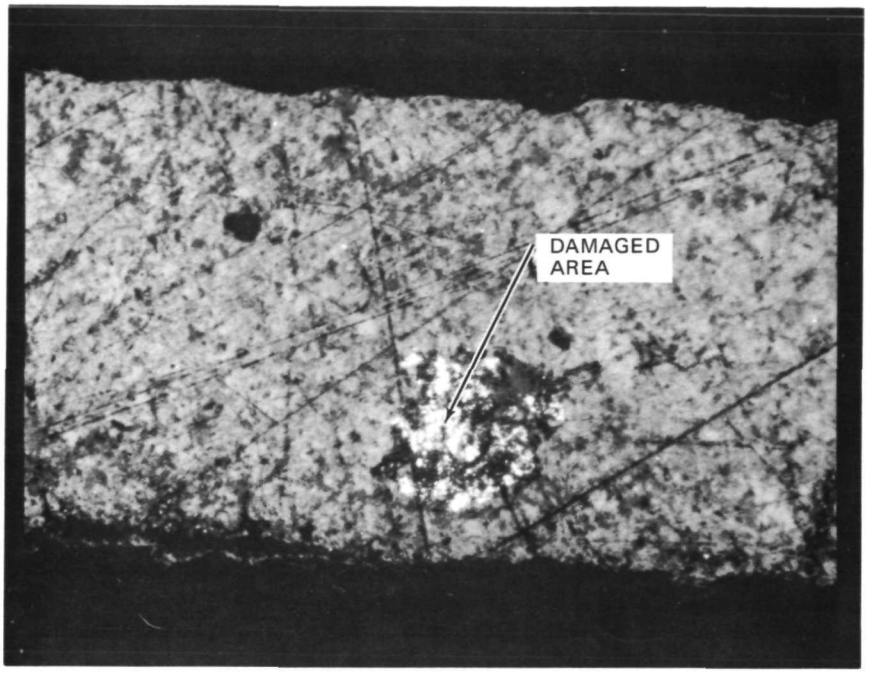

Figure 3-40. -503 Valve (Teflon S Coated) Seat Surface with Large Damage Area on Test No. 9 (160X)

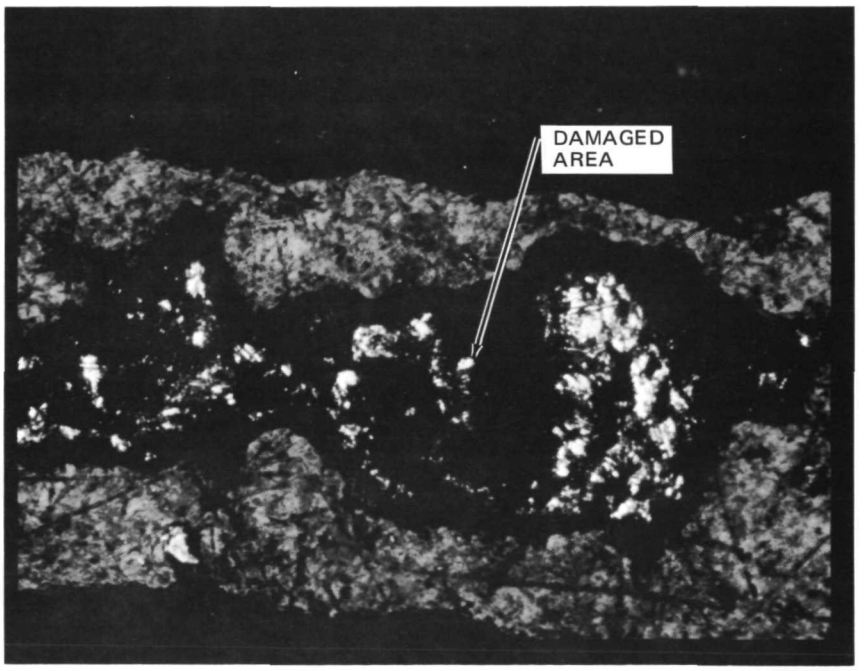

Figure 3-41. -503 Valve (Teflon S Coated) Seat Surface with Channel Erosion on Test No. 9 (160X)

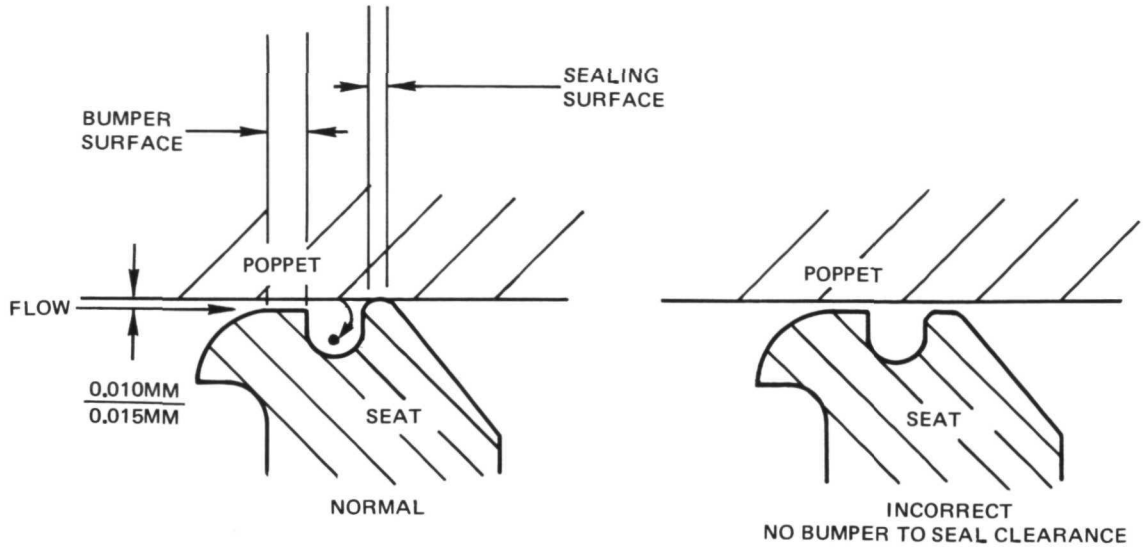

Figure 3-42. Seat Design Showing Seat and Bumper Clearance

lapping of the seat was continued until a flat sealing surface was obtained around the complete circumference of the seat. The extensive lapping operation resulted in the Teflon S coating becoming very thin in some areas (Figure 3-43) and also in the final bumper to seat height being considerably less than the specified 0.012 mm (0.0005 in.). The pretest leakage test was repeated at this point and a value of 0.9 SCCM was obtained (7×10^5 N/m^2 GHe). Since no further improvement could be expected without completely redoing the Teflon S coating the valve was accepted for testing. Test No. 10 was run with the injection of 2 grams of No. 1 powder. The post-test leakage test indicated an internal leakage of 0.66 SCCM (Table 3-7) which was less after testing than in the pretest condition. The posttest inspection indicated that no significant damage had occurred on the Teflon S surface (Figure 3-44) and the seat and the interface between the bumper and the poppet. It would appear that the bumper to seat height clearance at the time of testing was very small and the contamination particles were trapped between the bumper and the poppet instead of the sealing surface between the seat and the poppet.

Test No. 11 was conducted after refurbishment of the valve seat. The poppet was not refurbished because there was no apparent damage in the area where the sealing contact is made. The seat assembly was completely refinished in preparation for the final test in this test series. The seat sealing face and the bumper contact height was made flat and true by finishing the entire end surface of the valve seat on a piece of 400-grit emery paper.

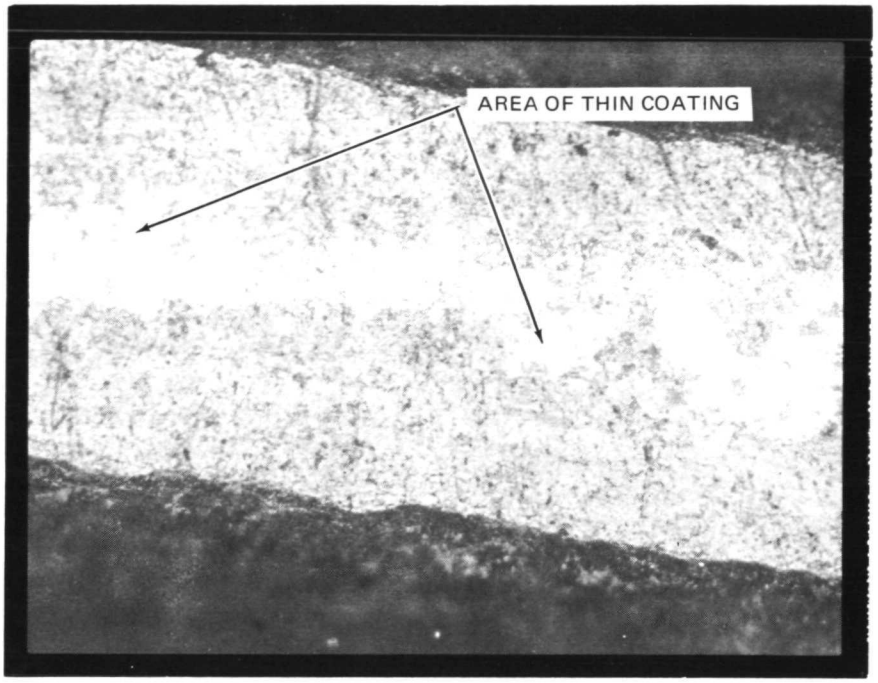

Figure 3-43. -503 Valve (Teflon S Coated) Seat Surface with Areas of Thin Coating - Pretest for Test No. 10 (160X)

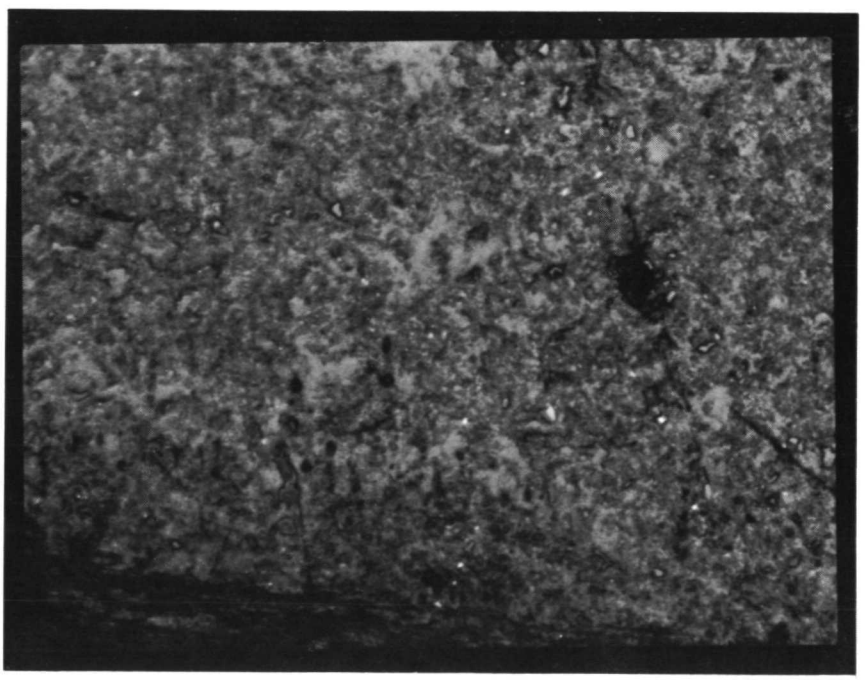

Figure 3-44. -503 Valve (Teflon S Coated) Seat Surface after Test No. 10 - Without Damage (160X)

The emery paper was supported by a surface plate so the flatness of the seat surface could be maintained. The seat surface was refinished until a sealing surface of uniform width was obtained around the complete circumference of the seat sealing surface. The bumper height was then reduced slightly using a special lapping tool and diamond lapping compound. The seat was then taken to the vendor for a new Teflon S coating.

The new coating was applied and the seat was returned to MDAC. This sealing surface was then smoothed out using the 10^{-4} mm (4 μ) Al_2O_3 finishing block. The results obtained were similar to the seat condition encountered on the No. 10 test, i.e., the seat sealing surface was not flat after the Teflon S coating was applied. It appears that the light sandblasting operation is too severe for this type of application, and the chemical surface preparation method should be investigated for future Teflon S coating application.

The seat was flattened to an acceptable value by extensive refinishing with the Al_2O_3 refinishing block; however, this was accomplished with a decrease in the bumper-to-seat standoff height clearance (as in test No. 10).

An attempt was made to make an accurate measurement of this standoff height clearance, however, the results were not completely satisfactory. The microscope, which has been used for the pretest/post-test optical inspection of the test parts, was calibrated for a depth of focus reading. The calibration was made using two metal discs which had a difference in thickness of a measured 0.025 mm (0.001 in.). The micrometer screw had to be turned through 40 divisions to change the focus from one disc to the other disc when both are placed side by side and with a 160X lens installed in the microscope. After this preliminary calibration was completed the seat surface was inspected using the same setup. The results of this measurement indicated that the bumper height and the seat sealing surface height were within 0.006 mm (0.00025 in.) under the worse case and in some areas no clearance could be measured. This technique of measurement is not completely satisfactory for measuring the height differences when a plastic is involved due to the difficulty in obtaining a good reference surface on the plastic finish. The present readings were made by focusing on the plastic surface so that the greatest percentage of the surface was in focus, however, this does not necessarily mean that the reference surface is the highest point in the actual surface. The same difficulty would be expected if rough metal surfaces were inspected, however, good results would be expected with this method when inspecting very smooth surfaces.

The valve seat was accepted for testing and the pretest leakage measurement taken. A value of 1.1 SCCM (Table 3-7) was obtained for pretest condition (Test No. 11). The test was completed using 1 gram of No. 2 powder (75 to 250 μ) in GN_2. The posttest leakage rate was too high to measure with the water displacement equipment. The posttest inspection indicated that little or no damage had occurred on the Teflon S surface (as shown in Figure 3-45). Considerable damage had occurred to the Inconel 718 surface of the poppet. Most of the poppet damage had occurred in one area of the poppet and in a position that would correspond to the poppet-to-bumper interface instead of the poppet-to-seat interface. Some additional damage had occurred in the area where the poppet and seat make contact, however, this damage appeared to be considerably less than the one area of poppet to

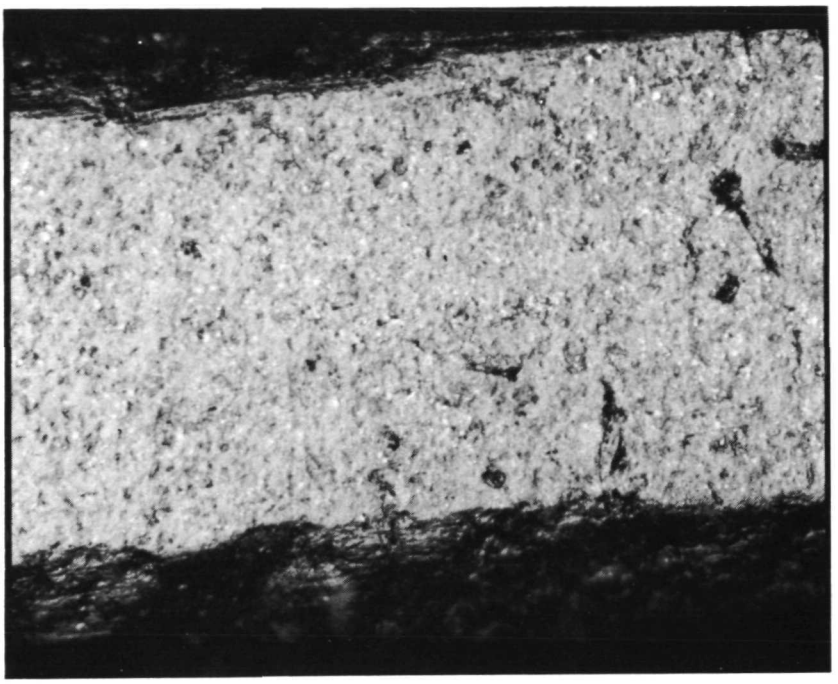

Figure 3-45. -501 Valve (Teflon S Coated) Seat Surface after Test No. 11 - Without Damage (160X)

bumper contact. The results of the post test inspection indicate that the high post test leakage rate was due to the inability of the poppet to make contact (the poppet was held off of the seat sealing surface in one spot). These results indicate that the present valve design is very sensitive to the bumper to seat stand off height dimension for good contamination damage tolerance control. However, this dimension cannot be reduced below a critical value unless the bumper and/or the poppet is provided with a surface which has the same embeddability characteristics as that used on the seat sealing face. Since the present -503 does not have a Teflon S coating on either the bumper contact surface or on the mating Inconel 718 poppet surface, it is not feasible to reduce the bumper to seat clearance dimension to the desired value without creating a potential interference problem of the type encountered on both Tests 10 and 11. These results indicate that the poppet and seat surface (both sealing and bumper) should be coated with the Teflon S coating for the maximum contamination damage tolerance.

3.2.4 Conclusions and Recommendations

The conclusions that can be made from the complete Task II testing effort include:

A. The present contamination injection system is capable of injecting particles in the < 250-μ size range in a somewhat controlled manner. The present system is sized to handle larger quantities of particles than used on the present test program. For injection of 1 gram

or less per test a modification to the particle mixing chamber in the injection unit would produce more consistent results than does the present design.

B. The contaminant damage avoidance features of the 1T32095 valve design are inadequate under steady state full flow conditions. This condition should improve by reversing the position of the raised portion of the sealing surface so that the sealing surface will be raised on the poppet and submerged on the seat assembly. (This modification was tested on the Task III effort.)

C. The Inconel 718/Gold Plate (-501) configuration is tolerant of contaminant particles of 75 μ or less with the present 0.012 mm (0.0005 in.) thick gold plating (MIL-G-45204B, Type I, Grade C, Class 5) during cyclic operation.

For service with contaminant particles in the 75 to 250 μ size a class 6 plating would be recommended. This thicker plating 0.036 mm (0.0015 in.) would provide improved embaddability characteristics when compared to the Class 5 plating. Since the effects of this thicker gold plating on valve cycle life is not known, a Task I cycle life test (10^5 cycles) would be recommended if the thicker gold plating is investigated.

D. The Inconel 718/Teflon S (-503) configuration has acceptable contaminant damage tolerance to particles of 75 μ or smaller under cyclic operations. The present configuration does not have adequate damage tolerance to particles in the 75 to 250 μ size range. This lack of tolerance is due partly to the fact that the Teflon S coating is too thin to properly embed the larger particles when the Teflon S surface is made smooth enough to meet the leakage control specification. This condition could be improved by substituting a chemical cleaning procedure for the precoating process in place of the normal sandblasting operation so that less substrate damage would occur to the metal surface and hence less cleanup of the Teflon S surface would be required to obtain a flat uniform sealing surface. Further improvements would be expected by coating the poppet with Teflon S as well as the seat assembly.

This Teflon S/Teflon S configuration would provide a total plastic coating thickness of 0.037 to 0.05 mm (0.0015 to 0.002 in.) and improved embeddability characteristics would be expected. While this combination is not presently scheduled for evaluation on the Task III effort, it should be considered for future evaluation.

E. The contaminant particle mix used for the Task II testing consisted of either a sieved T60 Alcoa Al_2O_3 powder or a combination of this powder with a No. 3 Airbrasive powder. While both of these powders are readily available, they do not have the uniformity of shape needed for accurate grading and counting operations. The present powder has particle shapes ranging from nearly spherical to those which are long and thin. The latter particles do not lend themselves to accurate grading and counting procedure and hence introduce some degree of uncertainty into the test results. The

present test powders are recommended for use on all preliminary screening tests, while a replacement set of powders of more spherical shape would be recommended for those tests where an absolute performance evaluation is required.

3.3 TASK III. CONTAMINATION AVOIDANCE CONCEPTS

The Task III effort consisted of an analytical and experimental investigation of methods that can be used to improve the contamination damage avoidance characteristics of propulsion components. Two methods of improvement were investigated on this program. The two methods selected could have been either two component design improvements, two auxiliary device evaluations or one design improvement and one auxiliary device evaluation. After studying the potential merits of various potential methods of improvement, the third approach was selected (one method of valve design improvement and one auxiliary device evaluation). The results of Task I and Task II were used in the analytical portion of this task.

The valve redesign method selected consisted of evaluating the reversed seat/poppet configuration (-505) of the 1T32095 valves. The auxiliary device selected for testing was a venturi type dynamic separator. Both methods were subjected to a series of preliminary tests. Both methods behaved in a predictable manner and offered significant improvements in the contamination damage avoidance characteristics of propulsion feed system components.

3.3.1 Analysis

The results of the tests made with the test valve operating in a cyclic mode (1 Hz) show that the damage tolerance characteristics of the basic valve were reasonably good for the small size particles but somewhat less satisfactory when the larger particles were injected. It should be remembered that the type of testing used on this program was designed to represent a worst-case situation, and the particulate addition constituted a mild sandblast condition. As would be expected, the test runs that produced high post test leakages were generally found to be caused by particle entrapment on the seat when the seat coating material was too thin to imbed the trapped particles properly.

The basic valve design was redesigned to improve the damage tolerance characteristics based on the results of the testing completed with the original valve configurations. To improve the performance of the valve under full-flow conditions, it was necessary to redesign the sealing interface so that the seat sealing surface was submerged below the height of the protective bumper as shown in Figure 3-46a. This lowering of the seat face into a submerged position prevents the high velocity particles from impacting directly on the seat sealing surface and thereby causing erosive damage to the sealing surface. To help reduce the problem of inadequate embedding characteristics, the seat surface coating on the redesigned valve was changed to the 0.025 mm (0.001 in.) thick Teflon S coating from the original 0.012 mm (0.0005 in.) thick gold plating.

The second method of improving the contamination damage avoidance characteristics of the propulsion fluid systems consists of providing a suitable

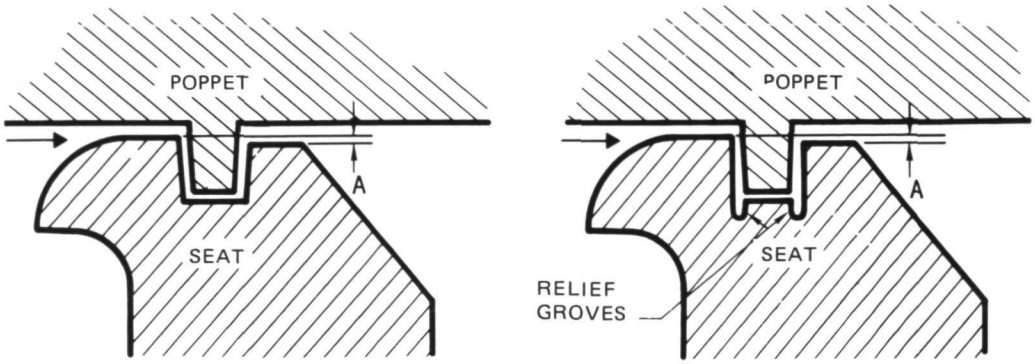

(A) PRESENT (-505) – REDESIGNED (-1)

(B) PROPOSED (-507)

Figure 3-46. Recommended Modification of -505 Configuration

device to remove the contamination particles from the propulsive fluids. A study was undertaken to investigate devices, other than conventional filters, which would be suitable for this service. The design objectives for this separation device were:

A. Minimum pressure drop across the device.

B. Constant pressure drop under all conditions of particle entrapment.

C. Capable of operation in a zero-g environment.

The approach taken started with the fundamentals of particle separation under dynamic conditions. This analysis (Appendix C) consisted of a study of the momentum characteristics of various particles in various flow fields to determine the minimum turning angle required to direct a contamination particle effectively into a retention device. The analytical model selected and the assumption used are shown in Figure 3-47. The results of this preliminary study are shown in Figure 3-48 on a nondimensional basis. Note that in the Reynolds number term the velocity, diameter, and density all refer to the contaminant particle and not to the fluid stream while the viscosity is for the flowing fluid. Using the data shown in Figure 3-48, an investigation was made into the various possible methods where a contaminant particle could be directed into a retention device with the least amount of pressure lost to the flow fluid. The four configurations studied in detail are shown on Figures 3-49 to 3-52. The final version of the contamination avoidance device studied consisted of the venturi type separator configuration. The pressure loss analysis for these configurations is presented in Appendix C. The final configuration consisted of a single stage screen baffle combined with a venturi conditioning section (shown in Figure 3-52). It

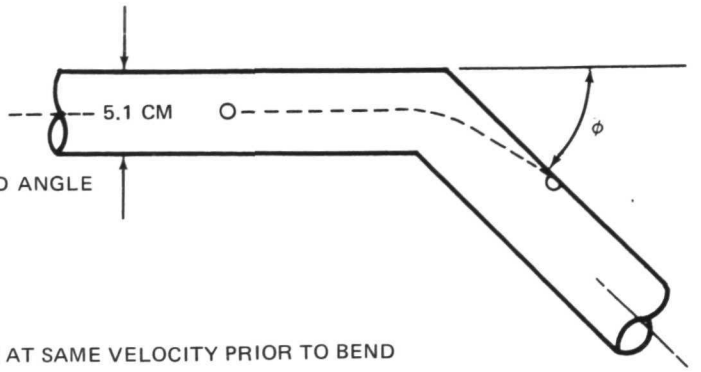

THE DUCT DIAMETER IS 5.1 CM AND THE BEND ANGLE (ϕ) IS VARIABLE

- ASSUMPTIONS
  - PARTICLE IS SPHERICAL
  - PARTICLE AND FLUID ARE TRAVELLING AT SAME VELOCITY PRIOR TO BEND

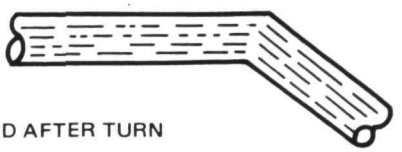

- GAS STREAMLINES ARE PARALLEL TO DUCT WALL BEFORE AND AFTER TURN
- THE ONLY FORCE ACTING ON THE PARTICLE IS DRAG FORCE DUE TO THE CARRIER FLUID
- BOUNDARY LAYER EFFECTS ARE NEGLECTED

Figure 3-47. Analytical Model of Separation Device

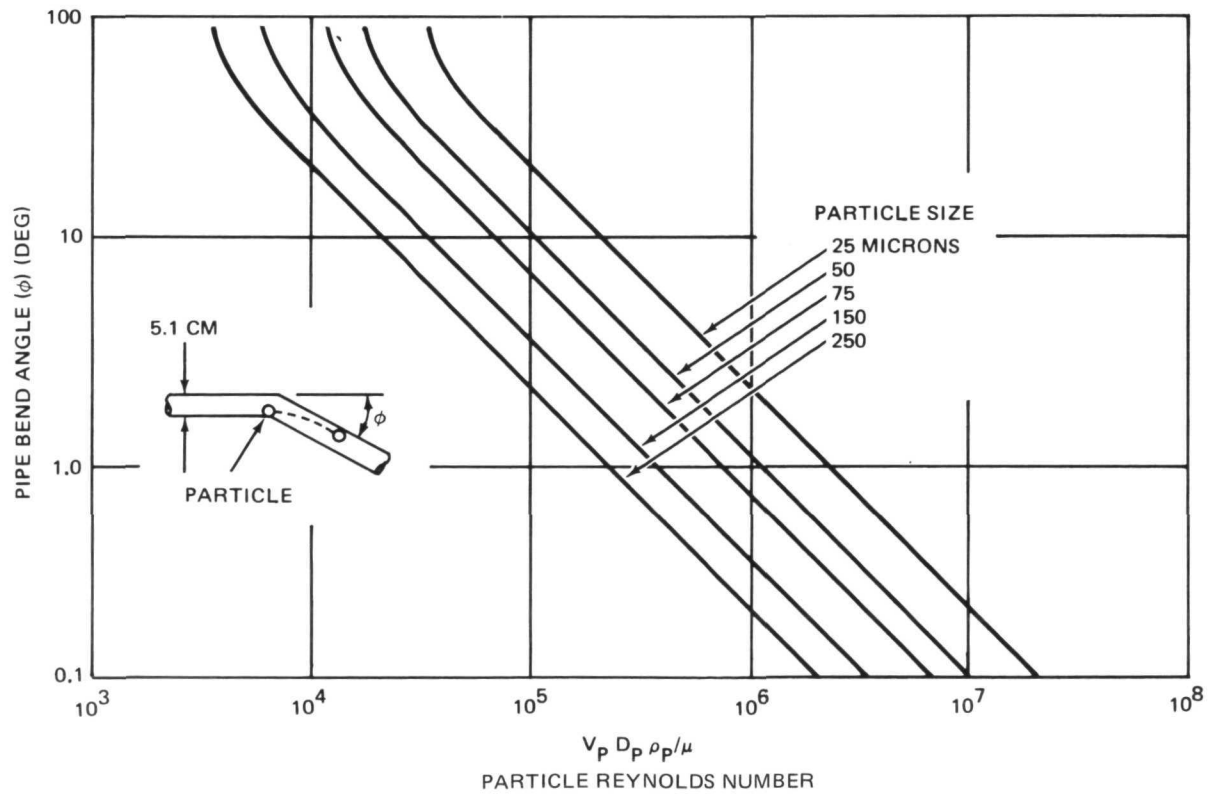

Figure 3-48. Minimum Pipe Bend Angle Required for Particle Impact on Pipe Wall

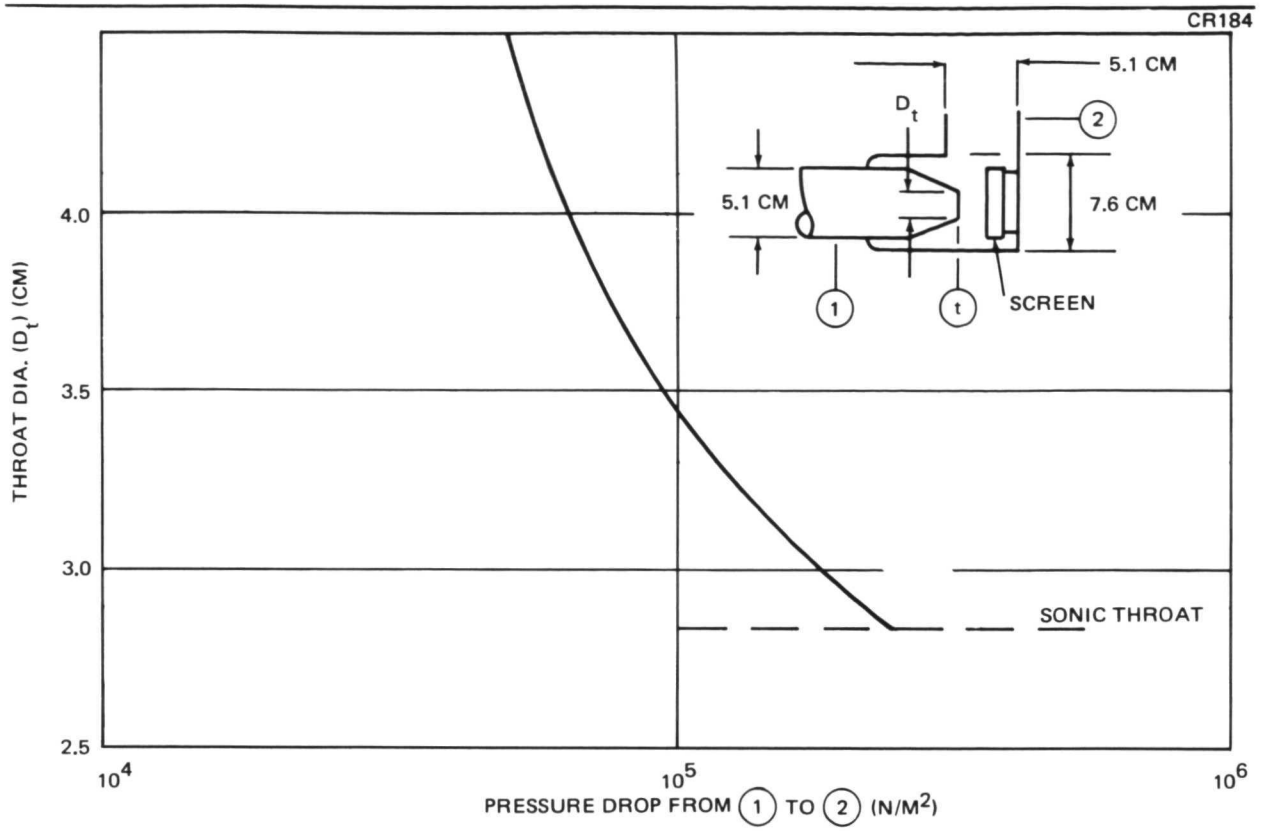

Figure 3-49. Pressure Drop for Nozzle and Plenum System

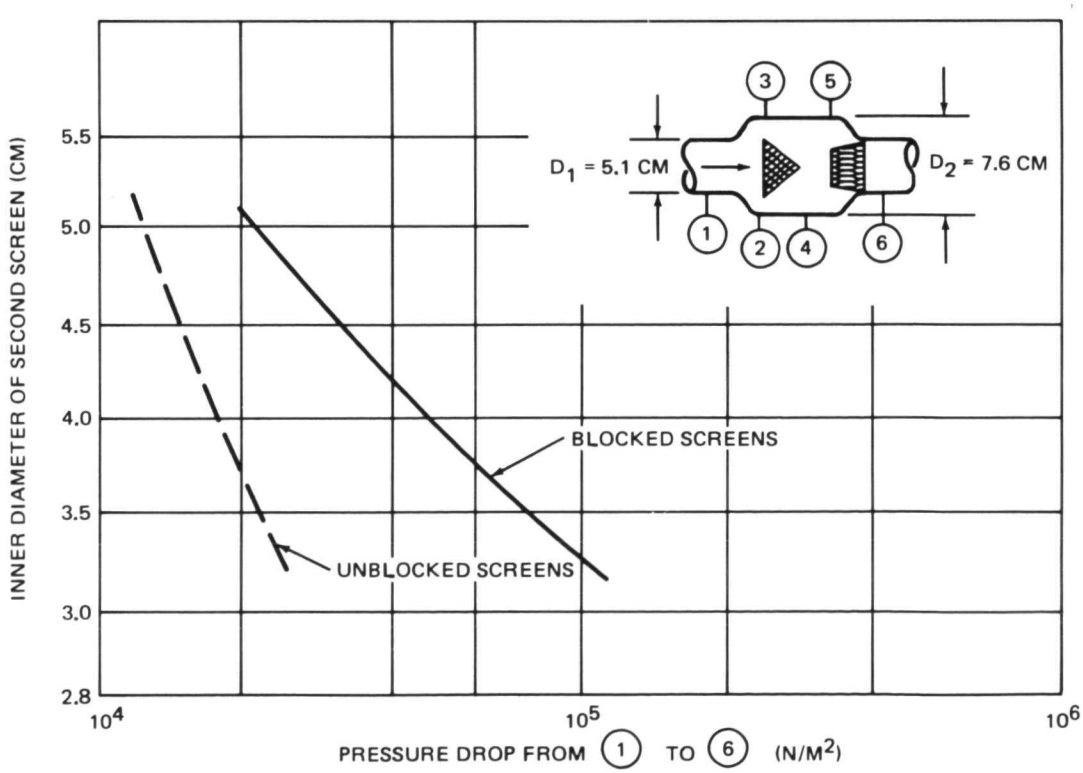

Figure 3-50. Pressure Drop for Conical Screens and Plenum

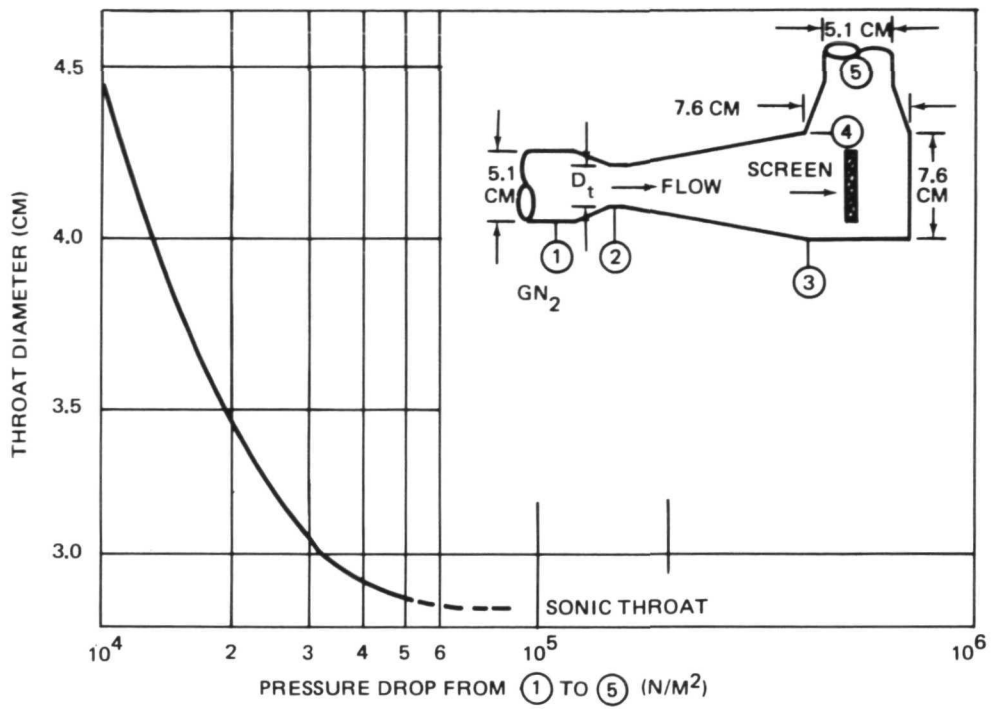

Figure 3-51. Pressure Drop for Venturi and Plenum System

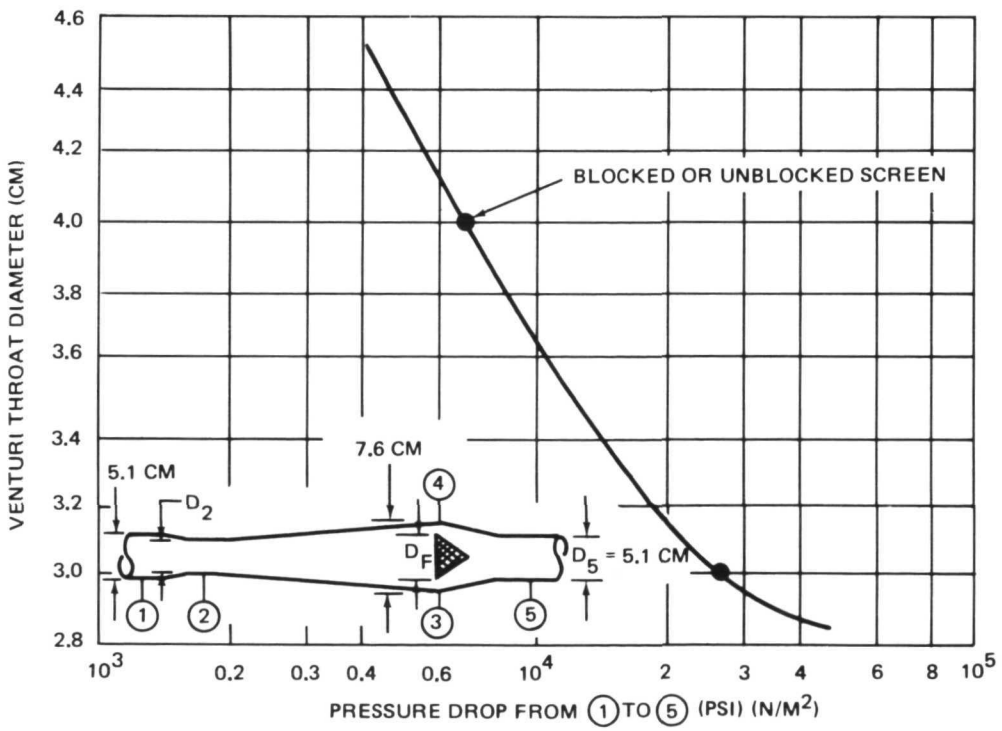

Figure 3-52. Pressure Drop for Venturi Type Dynamic Separator

should be noted that the pressure drop across this design is not affected significantly by the blocking of the openings in the screen separator, and, therefore, this arrangement cannot cause a system failure due to a flow obstruction. The calculated pressure drop of 7×10^3 N/m^2 (1 psi) with a 7×10^5 N/m^2 (100 psi) supply pressure (1 percent) will apparently meet the original design goals established for this study. The fact that a flow rate (secondary) is established through the particulate collector (screen) should result in the wedging of the particles into the material such that they will be entrapped into the screen mesh, and they should remain entrapped in the wedged position even in a zero-g environment. The entrapment feature was enhanced by using a two-ply screen configuration as shown in Figure 3-53.

The venturi conditioning section was used to distribute the particles into the center of the flow stream at a point just upstream from the particulate separator such that the particles impact on the separator before they can be deflected around the separator screen. With this arrangement, a trade-off exists between the venturi throat size, the distance downstream of the trap assembly, the diameter of the trap, flow velocity and density and the particle sizes which are to be separated. The analysis covering the gaseous flow regime with spherical particle sizes up to 250 μ was completed.

In compliance with the New Technology clause of this contract, a disclosure was made on the proposed contamination avoidance device configuration.

CR184

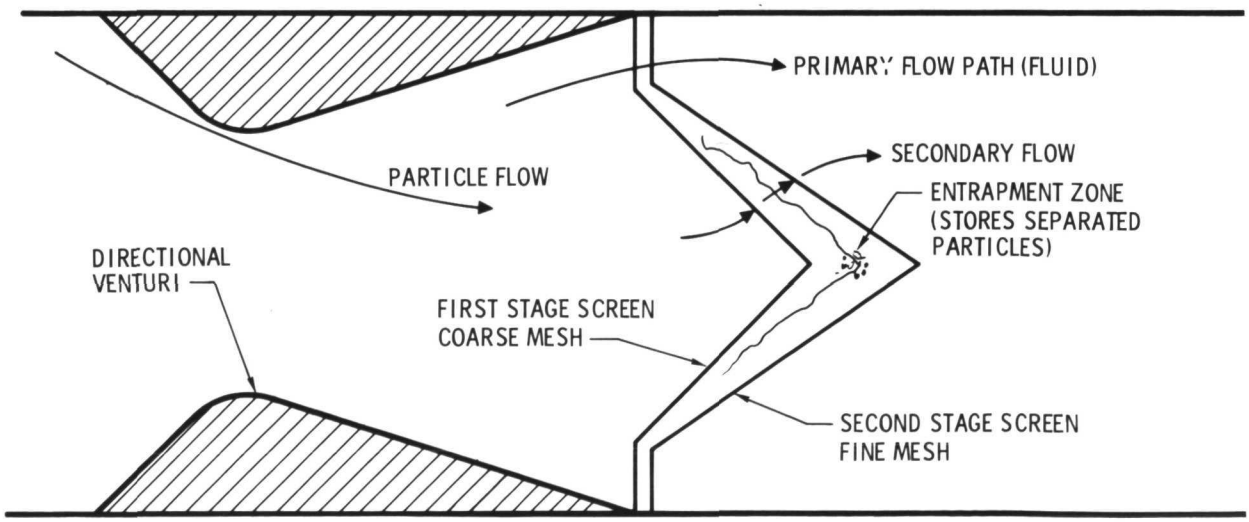

Figure 3-53. Basic Dynamic Separator Design

Note that the pressure drop in the final design does not change appreciably with increased screen blockage due to the fact that the area around the screen trap is sufficient to permit the fluid to pass with little additional pressure drop. The venturi section of this design is used to direct the particles into the center of the flow stream such that the particles strike the screen traps before they can be deflected around the screens. The predicted pressure drop shown in Figure 3-52 was based on the performance of the venturi only, and the value shown assumes an ideal exit cone angle. The particle separation efficiency of this arrangement would be expected to improve if the screens are brought closer to the venturi throat; however, the venturi cone exit angle will increase as the distance is reduced, and the pressure recovery of the venturi section will be reduced. Hence, a greater ΔP will occur across the separator. The tradeoff between separation efficiency and pressure drop can be made after other system requirements are established, however, lacking these specific system requirements, a typical model was selected for testing on this program.

Dimensions of the design fabricated for testing were somewhat arbitrarily selected on a first-try basis. A venturi throat size of 3.5 cm (1.4 in.) diameter was selected from a tradeoff between separation efficiency and pressure drop. The value used favors the pressure drop requirement, and a rather low operating efficiency would be expected with the small size (low inertia) particles. The throat to trap distance selected was 12.7 cm (5 in.). This value results in an exit cone half angle of 0.16 rad (9°) with the 5.1 CM trap size selected, which is somewhat larger than the optimum 0.12 rad (7°) angle, and favors separation efficiency at a slight loss of pressure recovery in the venturi divergent section. The trapping section design presents a greater problem. The design selected consists of using two conical screens mounted together as shown in Figure 3-53. The screen type of trapping arrangement was selected over a solid wall configuration so that the secondary fluid flow through the screens could be used to help retain the particles in the trap. This arrangement permits the momentum of the flow stream to force the particles to be trapped through the first screen but not through the second screen. Since no equivalent momentum can be established in the reverse direction, due to the high pressure drop through the fine screen, the particles are trapped between the two screens and should tend to remain there, even under zero-g conditions. The upstream screen selected was a 60-mesh screen while the downstream screen was a 400-mesh size. These sizes were picked such that particles smaller than 250 μ could pass through the first screen but that particles larger than 37 μ would not pass through the second screen. The material chosen by MDAC for the screens was 200 nickel with the wires sintered together. Unfortunately neither the 60-mesh nor the 400-mesh wire, which had been selected, was available in the nickel material and therefore the closest sizes available were substituted. The coarse mesh screen available in the nickel 200 material was a 100 by 100 mesh (150 μ) and the fine mesh was a 250 by 250 mesh (58 μ).

3.3.2 Test Planning and Setup

Task III tests consisted of the six GN_2 tests of the -503/-505 valve configurations shown on the Test Matrix in Table 3-8. The test setup is shown in Figure 3-54. These tests were conducted at Pad 1 of the A-12 test facility, using the same equipment used for the Task II tests. The contamination

Table 3-8

CONTAMINATION AVOIDANCE DEVICE TEST MATRIX

Test No.	Valve	CONTAMINANT			Cycle Rate (cps)	Test Objective
		Particle Size (μ)	Powder No.	Weight Injected (Grams)		
Full Flow Tests						
1.	-505	25 to 75	3*	5	0	Leakage, physical damage
2.	-505	75 to 250	4**	5	0	Leakage, physical damage
Cyclic Valve Tests						
3.	-505	25 to 75	3	1	1	Leakage, physical damage
4.	-505	75 to 250	4	1	1	Leakage, physical damage
Dynamic Separator Tests						
5.	-503	25 to 75	3	10	0	Leakage, physical damage, weight of removed contaminants
6.	-503	75 to 250	4	10	0	Leakage, physical damage, weight of removed contaminants

NOTE: All tests accomplished with GN_2 at 7×10^5 N/m^2 (100 psig) inlet pressure.

*Powder No. 3 consisted of a 220 grit Al_2O_3 abrasive powder sieved through a 200 mesh sieve.
**Powder No. 4 consisted of a 50-50 mixture of 100 grit and a 120 grit Al_2O_3 abrasive powder.

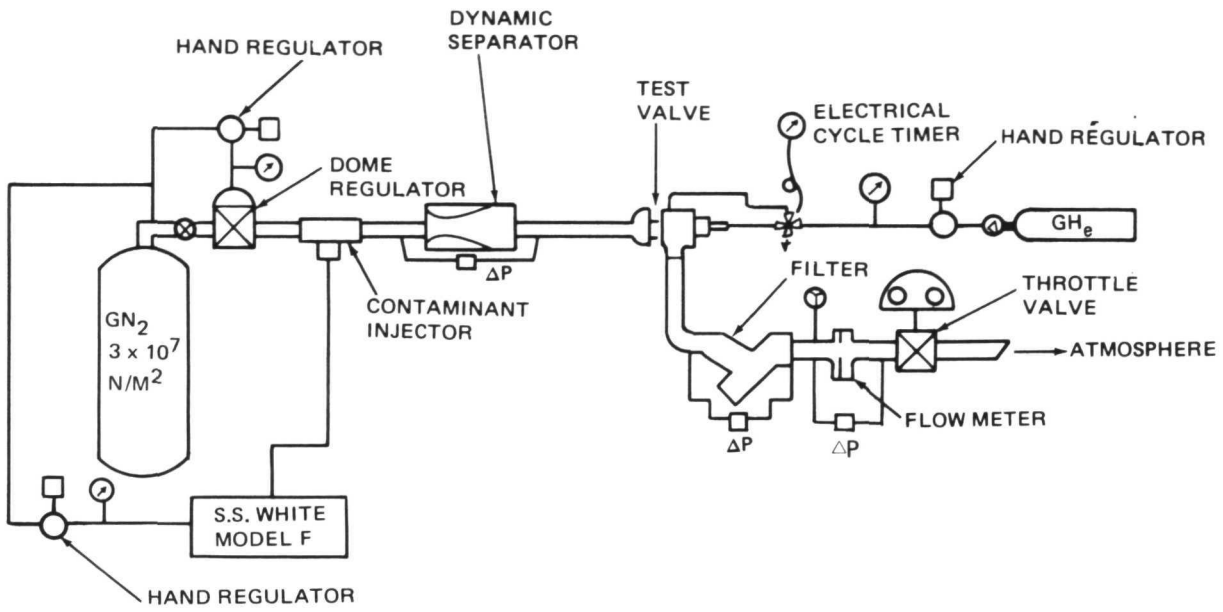

Figure 3-54. Dynamic Separator Test Setup

powders used for the Task III tests are different than those used for the Task II testing. This change was made to obtain Al_2O_3 powders that had a greater percentage of particles in the desired size range. Test samples of the previously used powders (No. 1 and 2) were rated using a Fisher Model 95 Sub-Sieve Sizer instrument, and both powders showed an average particle size which was smaller than the average obtained by adding the specified portion of powder obtained from the powder sieves. It was concluded that the number of long thin particles found in the T60 powder was high enough to prevent proper sizing in a conventional sieve arrangement and a relatively higher number of undersize particles were trapped on the larger sieve pans. This was true even when the powders were sieved from a 48 hour period and the screens unblocked with compressed air at one hour intervals.

The results of this investigation indicate that powders 1 and 2 were graded correctly for the maximum size of particles, but did not reflect the proper size of the minimum size particles. To improve this situation a search was conducted for a new source of test powders. The powders selected for the Task III tests have been obtained from the F. W. Davis Co., Los Angeles, and have been size graded for use in making abrasive grinding wheels and abrasive paper. The range of particle sizes for each powder are shown in Table 3-9. These powders were composed of Al_2O_3 particles which were supposed to be cubical. A microscopic examination indicated that a number of grains had been fractured during the handling operation, and some long thin particles were in these test powders. However, the grain size ranges

Table 3-9

PARTICLE SIZE DISTRIBUTION FOR TEST POWDERS

Test Powder	Percentage by Size Range (microns)									
	300-212	212-180	180-150	150-125	125-106	106-90	90-75	75-63	63-53	<53
No. 3								55	34	11
No. 4	1	6	27	33	26	6	1			
No. 5				37	48	13	2			

for the new powders appeared to be much more uniform than was observed with the earlier test powders, and it was anticipated that more predictable test results would be obtained with the new powders.

Task III testing was completed using the internal leakage rates of the test valves as the criterion for evaluating tests. This arrangement was straightforward for the testing of the redesigned valve configuration (-505) for tests No. 1 through 4. However the requirements for the separator tests were not as directly associated with the internal leakage rates of the downstream valve as was the case with the redesigned valve. To optimize the limited amount of testing required using the dynamic separator, it was decided to use the unmodified -503 valve for these tests (5 and 6) so that the potential improvements of valve internal leakages (with contaminated flow) of the redesigned -505 valve would not obscure the effects of the dynamic separator. Since both valves were available for testing, the requirement to use both valves was not a handicap. However, the installation of the dynamic separator into the existing flow test loop without removing the test valve caused some difficulty. Since neither time nor money was available to make a new test setup it was necessary to install the separator into the system without extensive modifications to the existing setup. This was accomplished by using 1.57 radians (90 degrees) elbows at the inlet and outlet of the separator. This arrangement resulted in flow disturbances in the flow stream through the separator and therefore prevented an accurate evaluation of the separator efficiencies. However, the criteria for the testing was obtained. The actual test setup for the Task III tests is shown in Figure 3-55. This test setup was used for all Task III tests. The traps were removed from the separator assembly for Tests No. 1 through 4 and reinstalled for Tests No. 5 through 7.

The preparation of the two test valves for the Task III testing started with some difficulty being encountered with both valve assemblies. The -503 valve was found to have a small crack in the valve-seat bellows and repair was required before testing could be started. The repair was completed, but it was necessary to close two convolutions before a leak tight assembly was obtained. This loss of two active convolutions was the result of difficulty in the EB welding operation and did not indicate that a crack had existed in two separate convolutions. To secure a leak-tight assembly, joining adjacent convolutions was attempted first on the EB welder and 15 welds were tried without sealing the leak. The procedure was then changed, and TIG welding

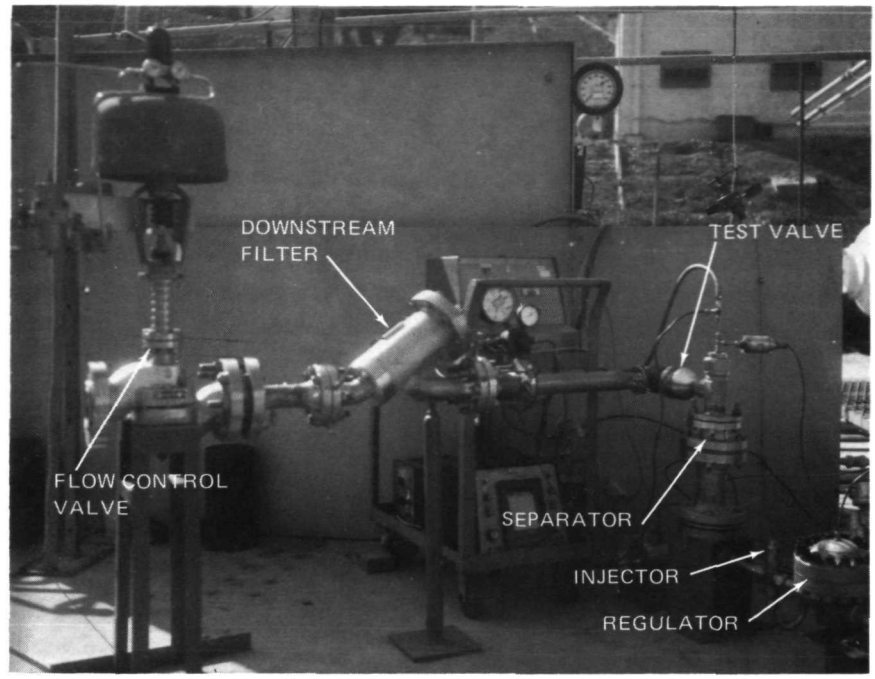

Figure 3-55. Test Setup for Contamination Avoidance Testing

was attempted. The TIG welding did not seal the leak; however, enough filler rod was deposited to make it possible to obtain a leak-tight assembly by EB welding on top of the TIG welded material. After completing the repair of the bellows, the -503 valve was reassembled and a leakage test made to see if the cracked bellows caused the high post test leakage on Test No. 11. The leakage measured after the crack was repaired was 21 SCCM at 7×10^5 N/m^2 (100 psig) GHe. Since the seat assembly had been subjected to a considerable amount of handling (and possible sealing surface damage) it was not possible to make any real conclusions from these data. The valve seat was recoated with Teflon S and the poppet assembly was relapped. The seat assembly was found to have the same type of low spots on the sealing surface face that had occurred on the last two coating operations. It appeared that the light sandblasting operation used to remove the old Teflon S coating and clean the surface for the application of the new coating was still severe enough to destroy the flatness of the seat sealing surface. The sealing surface was smoothed out using the 10^{-4} mm Al_2O_3 blocks at MDAC, however, low spots cause the width of the sealing surface to vary more than was desirable. An investigation was started to determine the probable effects of using the DuPont chemical cleaning method in preparation for applying Teflon S on the A286 seat material.

The rework of the existing -501 valve configuration into the new -505 configuration consisted of cutting the poppet off the poppet shaft and modifying the poppet and shaft to incorporate a threaded attachment arrangement such that replaceable poppets could be installed on the

existing shaft. A new poppet was then fabricated so that the raised portion of the sealing interface was located on the poppet instead of on the seat and the seat assembly was reworked to drop the seat sealing interface at a lower height than the bumper height. The rework seat was plated with a gold plating per MIL-G-45204B. The "B" revision to this specification changed the plating callout from that used on the "A" revision. The new plating is a Type II, Grade C, Class 5 with a Cobalt alloy plating solution.

To put a smooth finish on the submerged gold plated sealing area a special lapping tool was fabricated. This tool was made by flame spraying a coating of Al_2O_3 on to the end surface of a machined cylindrical tool such that the end of the cylinder could make contact with the sealing surface. A 0.67 mm (0.015 in.) coating of 98-percent Al_2O_3 grit in the 17 to 53-μ range was applied over a bond coat of Nickel-Aluminide. The plasma sprayed surface was then lapped until a flat surface was obtained.

After finishing the seat sealing surface (with a new finishing tool) the valve was assembled and leak checked. The internal leakage was excessive. A series of polishing operations on the poppet and seat assembly was completed, however, the internal leakage rate was still excessive. A microscopic examination revealed that the relief radii on the seat sealing surface had been omitted in the machining process. These reliefs were added by MDAC, however, no change in leakage rate occurred. The seat sealing surface was then lapped using the special lapping tool and a 3A grade lapping compound. This compound removed almost all of the gold plating finish, however, a flat surface was obtained. The leakage rate was then measured at 1 SCCM and was within an acceptable range for testing. Since the gold had been removed during the final lapping operation it was decided to replate the gold before starting the first Task III test. The seat was replated and the leakage test repeated. The leakage was found to be excessive again so the finishing operations were repeated. The two poppets were taken to a vendor facility for precision lapping and the seat was lapped at MDAC. This time the gold was slowly removed without obtaining an acceptable leakage rate. The entire valve was then disassembled and a series of special inspections were undertaken. It was found that the poppet would not remain perpendicular with the poppet shaft under normal conditions of poppet assembly. The poppet shaft and both poppets were returned to the rework vendor for correction. After extensive testing it was determined that an interference existed between the threads on the shaft and the poppet and therefore the poppet could not bottom out on the aligning pilot face. This was corrected and the poppets could then be installed such that the total run out did not exceed 0.025 mm (0.001 in.) on any part of the poppet sealing interface.

Since time did not permit extensive development of the removable poppet arrangement of the -505 valve configuration, it was decided to use the thicker Teflon S coating as a seat coating material in place of the originally specified hard gold plating. A coating of Teflon S 958-203 was placed on the seat sealing surfaces. After smoothing out the new Teflon S surface, the valve was found to be acceptable for testing.

The investigation into the possibility of using a chemical cleaning method for the Teflon S coating material indicated some uncertainty as to the effects of the chemical cleaning agent on the highly stressed A286 material.

Since time did not permit a complete material compatibility test program for determining these effects, it was decided to stay with the Sandblast cleaning method. The -503 valve was relapped and recoated two more times before the internal leakage rate was found to be acceptable for testing. The final coating was made with great care using a hand spray method of coating. While this method is acceptable for developmental testing it would not be recommended for production application. Since the results obtained on this program have indicated that the Teflon S material is capable of providing an exceptionally good sealing surface when the coating is properly installed, a more extensive investigation into the methods of coating application is indicated.

The fabrication of the dynamic separator (1T43824-1) was subcontracted to several vendors. The original design of this assembly specifies a rigid weld attachment for the two screens onto the flange assembly. Since this arrangement would be desirable for a production version but not applicable to a development unit (screen removal is required to recover the trapped particles), a change to a detachable screen design was made. A mounting portion was retained on the base end of each screen and a separate detachable mounting ring was installed, as shown in Figure 3-56.

The selection of screen mesh sizes proved to encounter some difficulty during the fabrication process due to the limited availability of certain screen sizes. The optimum 60 to 400 mesh size combination was established as a goal even though the availability of these sizes was limited for the nickel 200 material.

CR184

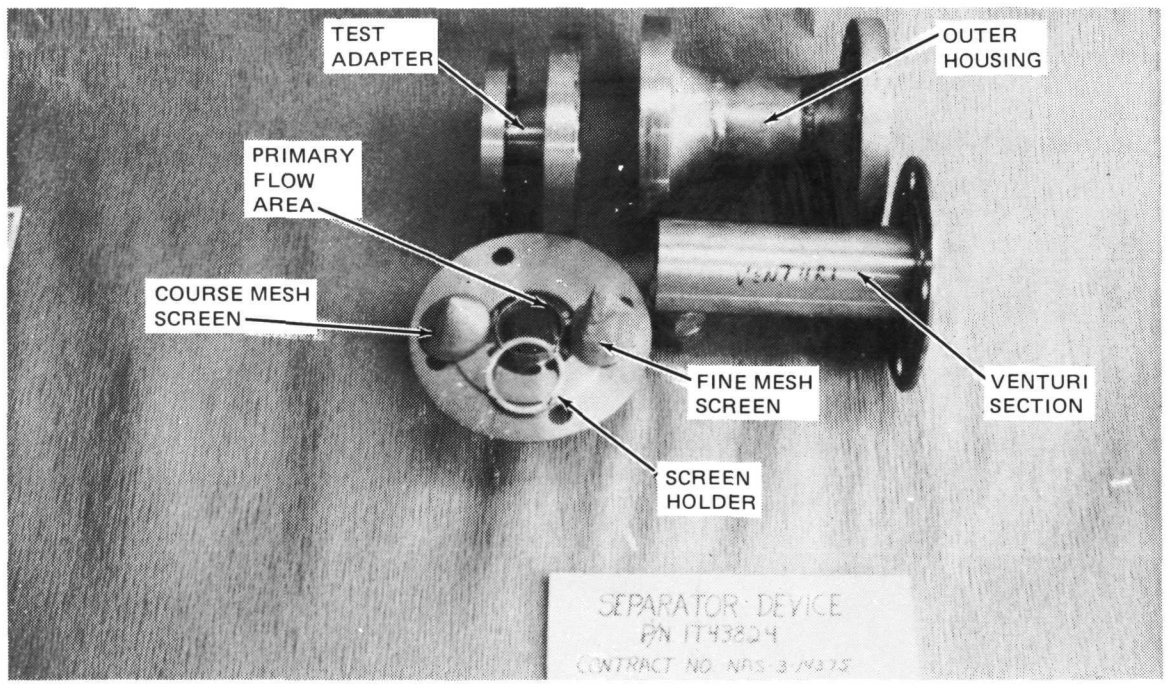

Figure 3-56. Test Model of Dynamic Separator

The best combination available was a 100/250 mesh size combination, and these were the sizes used for testing. The disassembled separator is shown in Figure 3-56.

3.3.3 Contamination Avoidance Device Testing

The redesigned valve (Teflon S coated submerged seat -505 valve) was tested first in the GN_2 flow loop. The results of these tests are shown in Table 3-10. The performance of the redesigned valve was found to be extremely good under the full flow conditions as shown in Tests No. 1 and 2. In addition to the controlled 6 grams of powder injected on test run 2, two pieces of uncontrolled contamination were injected. A piece of shim stock 2.5 cm (1 in.) square and its restraining safety wire were dislodged from the injector holder and entered the flow stream. These two parts are shown in Figure 3-57. The safety wire passed completely through the valve and was found in the downstream filter. The shim stock caught on the valve seat and was trapped between the valve poppet and seat when the valve was closed. After removing the trapped shim stock, the leakage rate was found to be 0.3 SCCM, which was well within the 1.0 SCCM limit arbitrarily assigned to this valve (was 0.15 SCCM pretest). No seat damage was detected as a result of the test No. 2 run even though the deformation to the shim stock was extensive.

The cycle runs (3 and 4) with the redesigned valve were encouraging for the small size contaminant; however, the larger size particles did cause a problem. The Teflon S seat was damaged moderately (by erosion) on the No. 3 run; however, the damage was not in the area where the seat contacts the poppet surface, hence little change in internal leakage was measured. The cyclic run with large size particles (Test No. 4) did show surface damage at the seat sealing interface. The testing accomplished on tests 1 and 2 results in very little damage being done to the Teflon "S" surface and therefore, no recoating was required for the first three tests.

The refurbishment of the sealing surfaces between test 1 and 2 and between 2 and 3 was accomplished by smoothing out the existing Teflon S surface using the Al_2O_3 coated lapping tool. While the damage to the Teflon S surface during test No. 3 was not severe enough to affect the post test internal leakage rate appreciably, it was severe enough on the nonsealing portion of the coating to warrant recoating the seat for the No. 4 test. This recoating procedure was accomplished with the same difficulties experienced on the previous coating operation. The recoated surface required a considerably amount of smoothing before a flat, smooth surface was obtained. This extensive lapping operation resulted in the removal of a considerable amount of the Teflon S coating and the remaining coating was much less than the original 0.025 mm (0.001 in.) coating thickness.

Test No. 4 was conducted with the very thin Teflon S coating which was smooth and flat. A considerable amount of damage was done to the very thin coating during Test No. 4 and the post-test leakage rate was beyond the readability limits of the leakage measuring apparatus. To evaluate the effects of the thinning of the plastic coating, a rerun of Test No. 4 was made with a new coating of Teflon S. This last coating was applied to the existing surface after a very light sand-blast cleanup and the spray was allowed to build up to a maximum one coat thickness. The coating used on

Table 3-10

TEST RESULTS—REDESIGNED (-505) VALVE CONFIGURATION
TEFLON S—COATED, SUBMERGED SEAT

No.	Type	Media	CONTAMINANT			Pretest Leakage (SCCM)	Post-Test Leakage (SCCM)	Leakage Change (SCCM)
			Size (μ)	Inject (Grams)	Recovered at Weight			
1	Full Flow	GN_2	25 to 75	5	1.94	0.15	0.15	0
2	Full Flow	GN_2	75 to 250	6	4.73	0.15	0.30	0.15
3	Cyclic	GN_2	25 to 75	5*	1.94	0.10	0.20	0.10
4	Cyclic	GN_2	75 to 250	1	0.75	1.4**	--	--
4 (Rerun)	Cyclic	GN_2	75 to 250	1	2.50	0.6	21	20

*1 gram was scheduled

**Seat was recoated for Test 4 and seal developed a low spot from precoating processing.

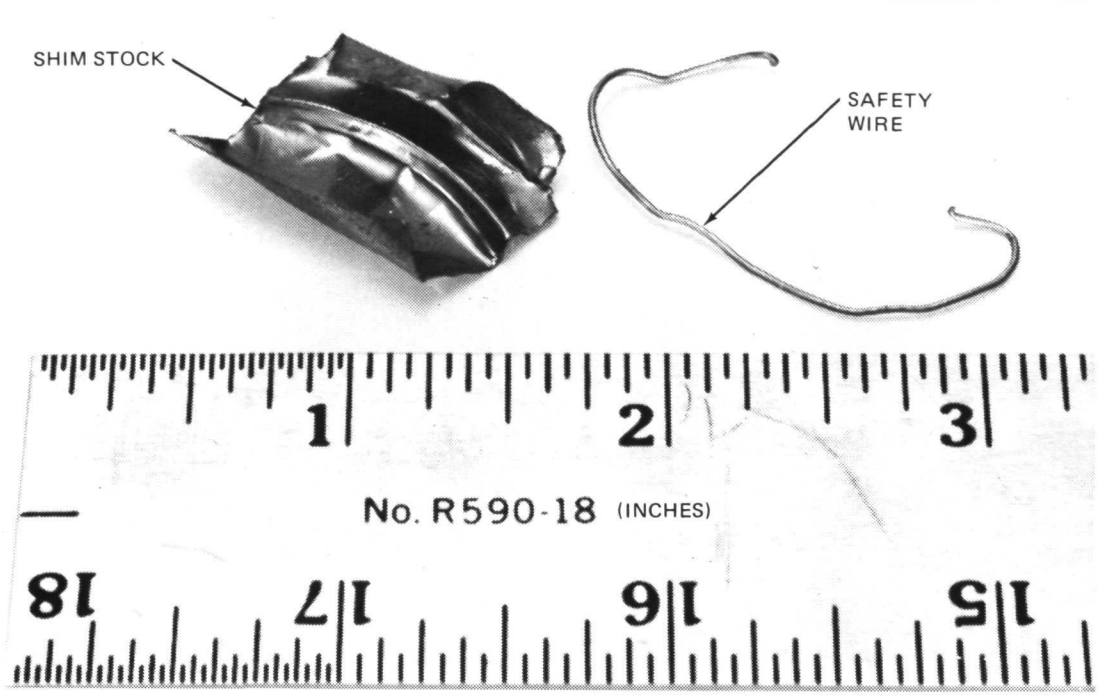

Figure 3-57. Uncontrolled Contamination on Test No . 2

the rerun test was probably within the desired range of 0.025 to 0.037 mm (0.001 to 0.0015 in.) thick, and the results of the rerun test were better than obtained with the very thin coating. The post-test leakage values for the rerun were high but were within the readability range of the measuring apparatus. Four particles were found embedded (particularly) in the seat sealing surface during the post-test inspection. The embedment of these particles was not complete enough for full seat-contact between the poppet and the seat, however, the thicker coating was allowed greater embedment of the particles than had the thin coating.

The preliminary testing of the dynamic separator were completed after the rerun of Test No. 4. Three test runs were made using three different sizes of test powder. The results of these runs are shown in Table 3-11.

The pretest leakage rate for Test No. 5, with the -503 valve was found to be higher than anticipated, and further rework of this valve was required before it was acceptable for testing. Inspection of the valve seat assembly revealed that the seat sealing portion of the assembly was 0.30/0.34 mm (0.012/0.014 in.) out of parallel with the mounting flange. This condition caused the alignment bumper surface to contact the poppet in such a way that the seat could not be loaded around the complete circumference of the sealing surface. To correct this condition the seat assembly was placed on a grinding machine, and the seat sealing surface ground until it was parallel with the mounting flange. The amount of material removed in the grind operation was sufficient to increase the seat sealing surface width from the specified 0.25 mm (0.010 in.) wide to a width of 0.51 mm (0.020 in.) on the narrow side and 1 mm (0.040 in.) on the wide side (average of 0.75 mm). Since the narrow 0.25 mm (0.010 in.) wide surface had been encountering deformation

Table 3-11

TEST RESULTS – DYNAMIC SEPARATOR (IT43824) – TASK III

(-503 Valve, Teflon S-Coated Seat)

No.	Media	Contaminant				Post-Test Leakage (SCCM)	Contaminant		Separator Efficiency (Percent)	Entrapment Efficiency (Percent)
		Powder No.	Size (μ)	Weight Injected (Grams)	Pretest Leakage (SCCM)		Weight in Filter (Grams)	Weight in Separator (Grams)		
5	GN_2	3	25 to 75	6.5	0	0	4.5	1	31	15
6	GN_2	4	75 to 250	6.5	0	0	1.8	2.0	72	31
7	GN_2	5	58 to 150	4.6	0	0.6	1.5	1.0	68	22

Screen Size–Upstream 150μ

Downstream 58μ

of the surface from the precoating sandblasting operation, it was decided to leave the seat sealing surface at the wider dimension and see if this would improve the Teflon S coating operation. It was found that the wider surface was much easier to coat than the narrow surface, and the valve was coated and tested in this condition.

For Test No. 5, the screens were installed into the separator housing (which was already in the test system) and the test conducted for 1 minute with a 45-second injection period. The separator was then disassembled for inspection and it was observed that the screen mounting plate had been installed into the separator backwards. This reverse position of the fine mesh screen resulted in some physical damage to this screen and this invalidated the test run. The system was cleaned and the two spare screen assemblies were installed into the separator. The injection rate had been lower than normal on this first test run, therefore no change in valve internal leakage was detected after this false test. The three tests were then completed with the results shown in Table 3-11.

The weight of test dust injected was selected to greatly exceed the capacity of the particulate trapping section so that the approximate capacity of the trap could be determined. The particle size of the test powder used for the first test was generally smaller than the fine mesh screen, and therefore, most of the powder passed through the separator screens as was expected. The results of runs 2 and 3 indicate that the separator was working as predicted, but that the capacity of the present trap design is a function of the exposed area of the screens and not the trapping volume which exists between the two screens. Once one of the two screens became plugged with trapped particles, the efficiency of the separator in trapping additional particles between the screens decreased due to the loss of the secondary flow.

Since the number of lightweight Al_2O_3 particles trapped on Test No. 2, for example, was approximately 400,000, it is apparent that the dynamic separator did direct many of the particles out of the main flow stream into the entrapment section, and therefore, can be of value in future propulsion fluid systems.

The two efficiencies shown on Table 3-11 reflect two different performance parameters. The separator efficiency shows the ratio of the amount of particulate contaminants removed from the dynamic separator to the total amount injected. The particulate contaminants removed from the separator included both the contaminants trapped between the two conical screens as well as that stopped by the upstream conical screen but which may have fallen back into the venturi diffuser cone when the fluid flow was stopped. The entrapment efficiency shown is the ratio of the particulate contaminants trapped between the two conical screens to the total quantity injected. With either an increase in trapping capacity of the trap assembly or a corresponding reduction in the quantity of contamination injected, the entrapment efficiency should increase to at least the separation efficiency. Since the separator efficiency is influenced by the changes in the secondary flow through the screen assemblies it would appear that the trapping efficiency should increase to a value higher than the indicated separation efficiency if the trap assembly does not plug up completely during the test run. It would

appear that trapping efficiencies of more than 80 percent can be obtained with the dynamic separator design selected when the screen mesh sizes and the injected particulate are in the correct size ranges or if the trap assembly is modified to allow the screen assembly to become self-cleaning (regeneration). The requirements of screen element regeneration were not included in the scope of work covered on the present program, however a preliminary study has indicated that this feature can be incorporated into the present design without extensive modification to the test unit. The determination of the true trapping efficiency of the present design and evaluation of the performance improvements possible with the regenerative versions are recommended for future work.

3.4 SIGNIFICANCE OF PROGRAM RESULTS

Results of the valve cycle-life testing show that the surface coating material selection is very important for long life operation in a reactive propellant environment. While the absolute data obtained applies only to a GH_2 media, the relative life factors would be expected to hold for other propellants. The GH_2 media was selected for this work because this media does not produce a protective surface layer (like the oxide films) and therefore the GH_2 represents a worst-case condition. The data obtained should apply reasonably well for other medias which do not create protective films (GH_2, GHe, etc).

The very poor performance of the Inconel 718-A286 material combination (like-on-like combination) was more severe than anticipated and this combination (or similar combinations) should be avoided in long-life components. The Inconel 718-Gold plating wear rates were found to be approximately the values anticipated while the Inconel 718-Teflon S results were better than anticipated. The Teflon S results indicate that further development of this material could provide a significant improvement in seal life (static and dynamic seals).

The contamination tolerance and avoidance test results indicate that a measurable improvement of the susceptibility to contamination damage of a typical propulsion component can be obtained by applying fundamental principals of avoiding contamination damage in the basic component design. The factors which were found to be significant for damage tolerances and avoidance were:

- Designing to account for the momentum and inertia effects of the particles.
- Provisions to allow use of the self-cleaning characteristics of the valve seat by providing contamination trapping grooves in the area adjacent to the sealing surface.
- Selection of surface coating materials which would provide for the embedment of trapped particles. (This parameter cannot be established satisfactorily for long-life reusable components independent of the effects of the coatings on the component cycle life.)

In general, the last parameter listed (i. e., embedability) can not be optimized for the best damage tolerance characteristics and best cycle life at the same set of conditions. A thick coating would be expected to have greater embedability performance but a lower fatigue life under cyclic loading conditions. Hence, the component designer should select a coating thickness which will meet the cycle-life requirements first, then determine the damage tolerance characteristics of the selected coating and from this information select the filtration requirements of the system. It would appear that most coatings are capable of satisfactory leakage control with exposure to particles in the < 75- size range.

The dynamic separator design evaluated on this program appears to offer a significant improvement in reducing contamination effects when the separator is used as a system prefilter. The separator design selected appears to be capable of reliable operation while the device is still simple, light weight, and can be designed without great difficulty. The basic separator tested represents the simplest version of several possible configuration in a family of separators. This design can be altered for service with variable velocity flow and can be made to exhibit self-cleaning characteristics (regeneration). Since the separator efficiency of the device increases with increasing particle sizes, this device can be used effectively to remove all large particles which cannot be tolerated by the components while being less effective on the particles which are small enough to be tolerated by the components. This is a highly desirable characteristic in propulsion fluid systems and in many other nonspace-oriented fluid systems.

3.5 RECOMMENDATIONS

The following recommendations are based on the results of the work completed on this contract.

A. The cycle-life characteristics of valve seats with surface films should be evaluated for the material combinations of (1) Teflon S on Teflon S, (2) Inconel 718 on High Build Teflon S, and (3) on Inconel 718 on Xylan 1010. While there are a great number of potential coating materials which could offer a performance improvement in propulsive fluid service, the three listed above were selected so that the greatest amount of information can be obtained with the least number of tests. The Teflon S-Teflon S combination should double the particle embedability characteristics of the component, however, the cycle-life characteristics should be obtained first.

   The Teflon S-Teflon S provides a double thickness of film without increasing the absolute thickness of the material on each surface and hence the fatigue life should remain constant (same as Inconel 718-Teflon S). The use of high-build Teflon S is another possibility for improved embedability characteristics. In this case the material combination will be the same as the one tested during the present program (Inconel 718-Teflon S) and hence, the adhesive wear rate would be expected to remain constant however, the thick film of Teflon S would be expected to show a lower fatigue life than was obtained on the present test program. These two tests would evaluate the difference in wear rate from both adhesive wear and fatigue wear on the same Teflon S material.

The third cycle-life test recommended gives another solution to the same problem. The Teflon S plastic coating consists of a polyimide matrix containing a suspended Teflon FEP antistick compound. This material has excellent properties when applied properly, however, it does require some complicated precleaning procedures and a high-temperature curing operation.

The Xylan 1010 material is made up of a similar polyimide matrix and a TFE antistick compound. This combination does not require the same degree of precleaning as the Teflon S and can be cured at a much lower temperature. With the low cure temperature the polyimide is cured while the TFE is left in a suspended uncured state such that a renewable wax type of lubrication is obtained in service. Both of these characteristics would be highly desirable for use on the highly finished surfaces of a low-leakage shutoff valve. However, the Xylan 1010 is a relatively new material and the data available on the physical properties of this coating are limited. Even without sufficient physical property data, this material appears to be close enough to the Teflon S material to warrant a separate cycle-life test; such a test is recommended.

B. The improvements made in the contamination damage tolerance of the 1T32095 valve during the present program were significant. Of the four modes tested, only the cyclic mode with large particles showed unacceptable results after the final testing. The reversal of the raised seat portion of the valve produced improvements in the damage tolerance under all full-flow conditions, however, the design tested was not equipped with the type of contaminant trap grooves used in the original design. Since these grooves should produce improved performance in the cyclic mode, it is recommended that further work be done in this area. The proposed configuration with small double-trap grooves added to the submerged seat design (see Figure 3-46B), should be tested. The proposed redesign offers two separate advantages. Not only does it provide a double-trap groove arrangement which is a primary objective, it also will minimize the radiusing effect (lack of adhesion in the corners) noted on the Teflon -S during the present program and will therefore improve the quality of coatings possible with the Teflon S material. Further work in this area is recommended.

C. The preliminary testing of the dynamic separator indicated that this type of concept operates in a predictable manner, however, the preliminary testing was not directed at the determination of operating efficiencies of the separator. To provide the information necessary to design this device as an integral part of a propulsive fluid system, the efficiency of separation and entrapment must be obtained. It is therefore recommended that the present separator design be tested to determine the true operation efficiencies over the range of conditions of interest to the system designer. These data would be of a fundamental nature and applicable to a number of possible configurations of the dynamic separator/prefilter.

Based on the anticipated requirements for future long-term reusable space systems, some form of regeneration of the prefilter is desirable. It is recommended that a regenerative configuration of the dynamic separator be identified and a test program conducted to verify the self-cleaning capabilities of the selected design. The potential gain in performance of the future propulsive fluid system appears to indicate that a continuation in the recommended program is warranted.

Page Intentionally Left Blank

REFERENCES

1. D. L. Endicott. Development and Demonstration of Criteria for Liquid Fluorine Feed System Components. McDonnell Douglas Astronautics Company, NASA Report No. CR 72543, June 1969.

2. Proposal to Design, Fabricate and Test a Space Storable Oxidizer Valve. McDonnell Douglas Astronautics Company, Report No. DAC 61087P, June 1968.

3. E. Rubinowicz. Friction and Wear of Materials. John Wiley and Sons, New York, 1965.

4. D. L. Endicott. Space Storable Oxidizer Valve. McDonnell Douglas Astronautics Company, NASA Report CR 72690, November 1970.

5. Technical Information Bulletin A61844, Teflon-S. E. I. DuPont de Nemours and Co., Inc., Fabrics and Finishes Dept., August 1968.

6. G. F. Tellier. Poppet and Seat Design Criteria for Contaminant-Particle Resistance. Rocketdyne Division, North American Rockwell Corporation, Report No. AFRPL-TR-70-1, April 1970.

7. Military Specification MIL-F-25475. Hydraulic Systems, Missile, Design, Installation, Tests and Data Requirements, General Requirements.

8. Service Manual, Industrial Airbrasive Unit, Model R. S. S. White Company, Report No. 715-2010, July 1968.

9. A. Brandt and L. L. Perini. Particle Injection into a Uniform Flow. J. Spacecraft, Vol. 7, No. 7, July 1970.

10. Aerospace Fluid Component Designers' Handbook. RPL-TDR-6.4-25, Vol. I, Rev. B, March 1967.

11. James C. Armour and Joseph N. Cannon. Fluid Flow Through Woven Screens. AIChE Journal, Vol. 14, No. 3, May 1968.

12. Roy Kasdorf. S-IVB Stage Orifice Verification by Pressurization/Repressurization System Blowdown. Saturn Analysis Report 4B-405BA, 4/16/70.

13. Propulsion Analysis Handbook. Saturn Propulsion Analytical File Report No. A-383.

14. Ascher H. Shapiro. Dynamics and Thermodynamics of Compressible Fluid Flow. Volume I.

Page intentionally left blank

Appendix A
LABORATORY WORK SHEETS

This appendix contains the results of the laboratory tests made to determine the composition of the wear particles generated on the cycle life tests of the -1 valve (Inconel 718-A286).

Page intentionally left blank

LABORATORY WORK SHEET

FORM 28-603 (8-65)

APPENDIX A

Case No. 98318

Charge: S.O. L77243-01

DWO 66500

Date 10-6-71

Due Date 10-8-71

Submitted by D. L. Endicott Dept. A3 833 Phone 3456/872-551-37

Report to Same Dept. Phone

Assigned to Austin Phillips A3 253 2626

Part No. Part Name Valve poppet shaft

Material Spec. INCO 718 & A286 Size P.O.

History & Purpose: Valve tested in LF_2 and GH_2. Reaction occurred with GH_2. Need chemical analysis of reaction products on valve sealing surface.

DESCRIPTION

Work Plan Electron microscopy examination of particles

Electron diffraction identification

Electron microprobe analysis

SUBMITTED BY

Results The reaction product particles were removed with acetyl cellulose replicating tape. A carbon film was evaporated onto the particles and tape and the tape was dissolved in acetone, leaving the particles embedded in the carbon film. The carbon film and particles were then examined in the electron microscope.

DATE DUE

Disposition The size of the particles and shape are shown on Figure 1. They varied in size from 1/10 micron to 4 or 5 microns. Selected area electron diffraction was accomplished on various particles. The various interplanar spacing measurements are presented on Table 1. Extracted particles on carbon film supported on copper screen and examined in microprobe. No F found. Ni, Fe, Cr found in many particles.

DATE

Case Closed by Date

APPROVED Austin Phillips 10-19-71

No. 98318

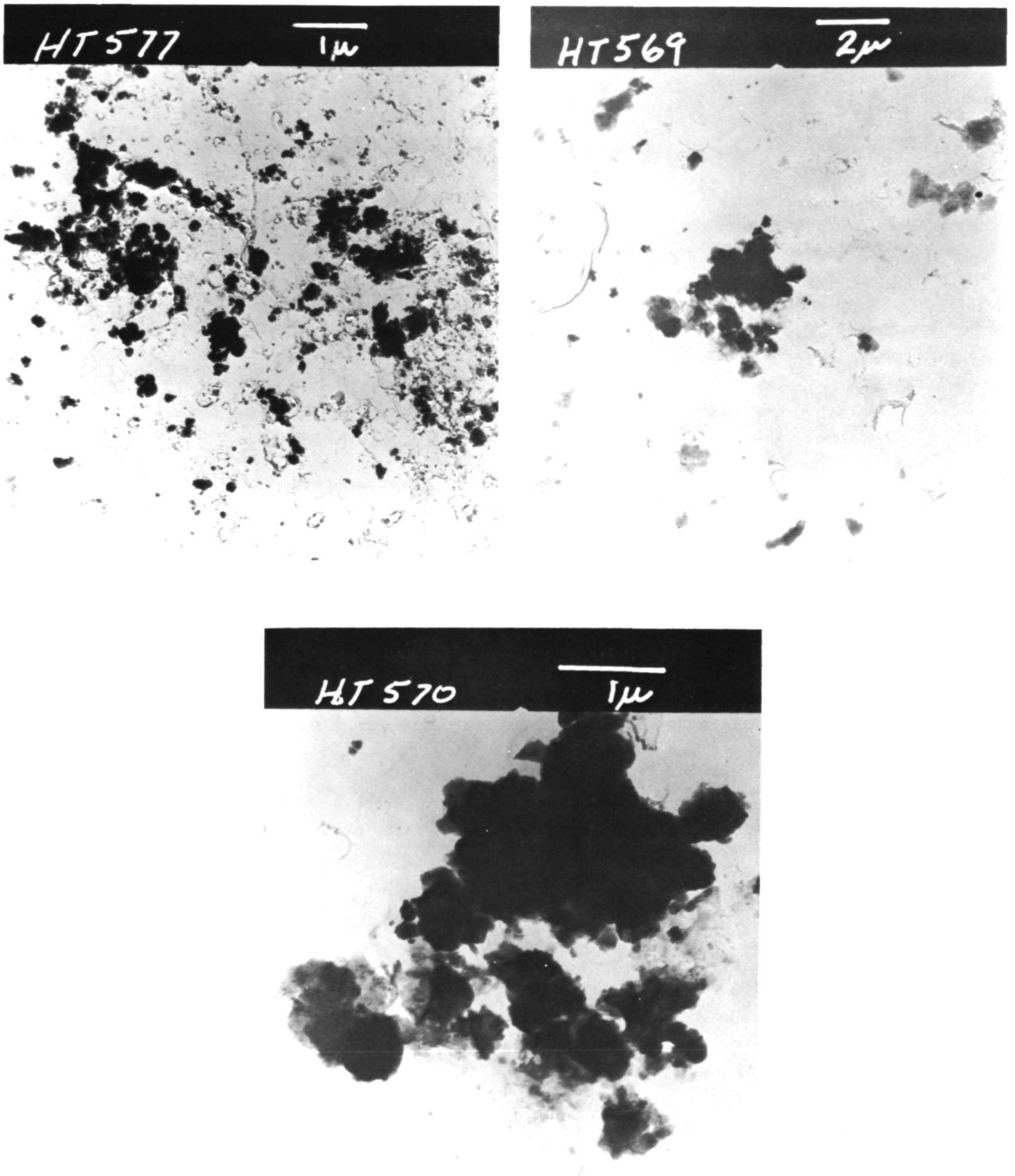

Figure A-1. Electron Micrographs Showing Reaction Product Particles (Page 1 of 2)

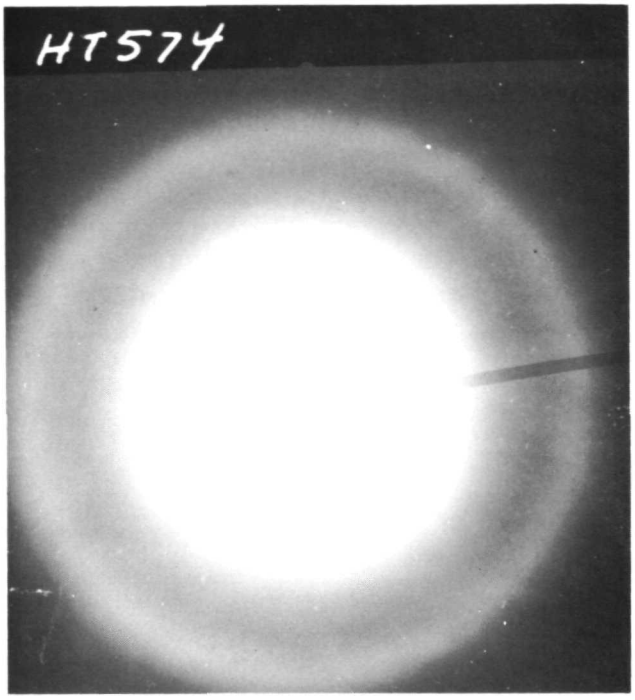

AMORPHOUS PATTERN

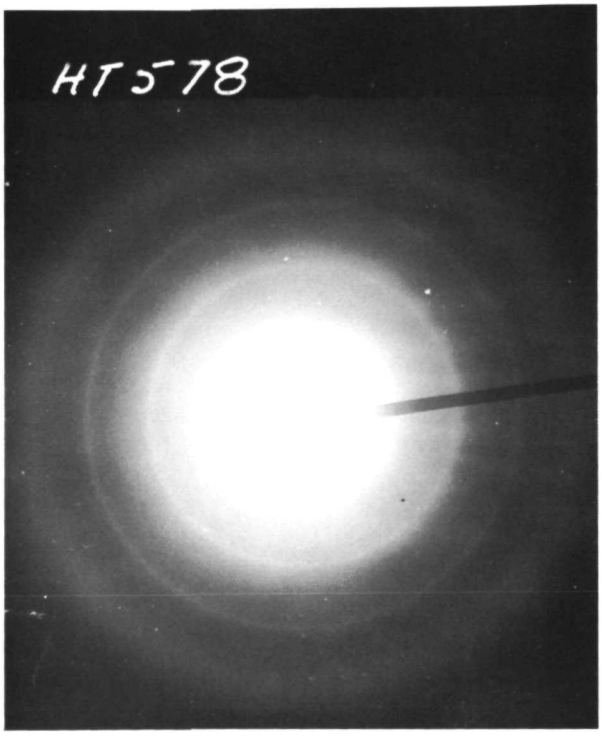

UNKNOWN COMPOUND
INSUFFICIENT RINGS FOR IDENTIFICATION

Figure A-1. Electron Micrographs Showing Reaction Product Particles (Page 2 of 2)

TABLE 1.

D. L. Endicott 10-12-71

ELECTRON DIFFRACTION RESULTS

HT-575 Au Standard		P 2	O 21MM	COND H	KV 100	
	Dcm	dÅ(Au)	K			
1.	3.16	2.35	7.40	3.22	2.35	7.55
2.	3.67	2.04	7.49	3.70	2.04	7.55
3.	5.22	1.44	7.50	5.26	1.44	7.58
4.	6.10	1.23	7.68	6.15	1.23	7.77

K = 7.60

Neg. No. HT-576

Dcm	dÅ
3.63	2.10
5.16	1.47

Neg. No. HT-571

Dcm	dÅ
3.67	2.08

Neg. No. HT-578

	Dcm	dÅ
1)	3.60	2.10
2)	5.14	1.48

Neg. No. HT-572

Dcm	dÅ
3.70	2.06
4.24	1.80
6.06	1.26
7.06	1.08

A 286

C	Mn	Ni	Si	Cr	Mo	Ti	Fe
.05	1.5	25.4	.64	15.8	1.2	2.2	Bal.

X-RAY DIFFRACTION RESULTS ON KNOWN A 286 ALLOY

Cu - tube

dÅ
2.08
1.80
1.27
1.08
1.04

Conclusions: The particles were predominantly metal, consisting of an alloy of nickel, iron and chromium. There was an unknown compound but there was insufficient information to identify it. There was also evidence of amorphous material which was not identified. Microprobe analysis indicated no evidence of fluorine.

Page intentionally left blank

Appendix B
ACOUSTIC SIGNATURE PRINTOUTS

This appendix contains four of the acoustic signature printouts taken on Test No. 5 of the Task I Cycle Life Test program (described in section 3.1.6.4). The -503 valve (Inconel 718/Teflon S) configuration was used for these tests. A complete series of magnetic tape readings were made with both the Endevco accelerometer and the Dunegan transducer. The valve actuation was made with both the normal operating pressure and a higher than normal pressure. The traces shown were taken with the transducer and represent the opening stop and closing stop conditions for both actuation pressure conditions.

Page Intentionally Left Blank

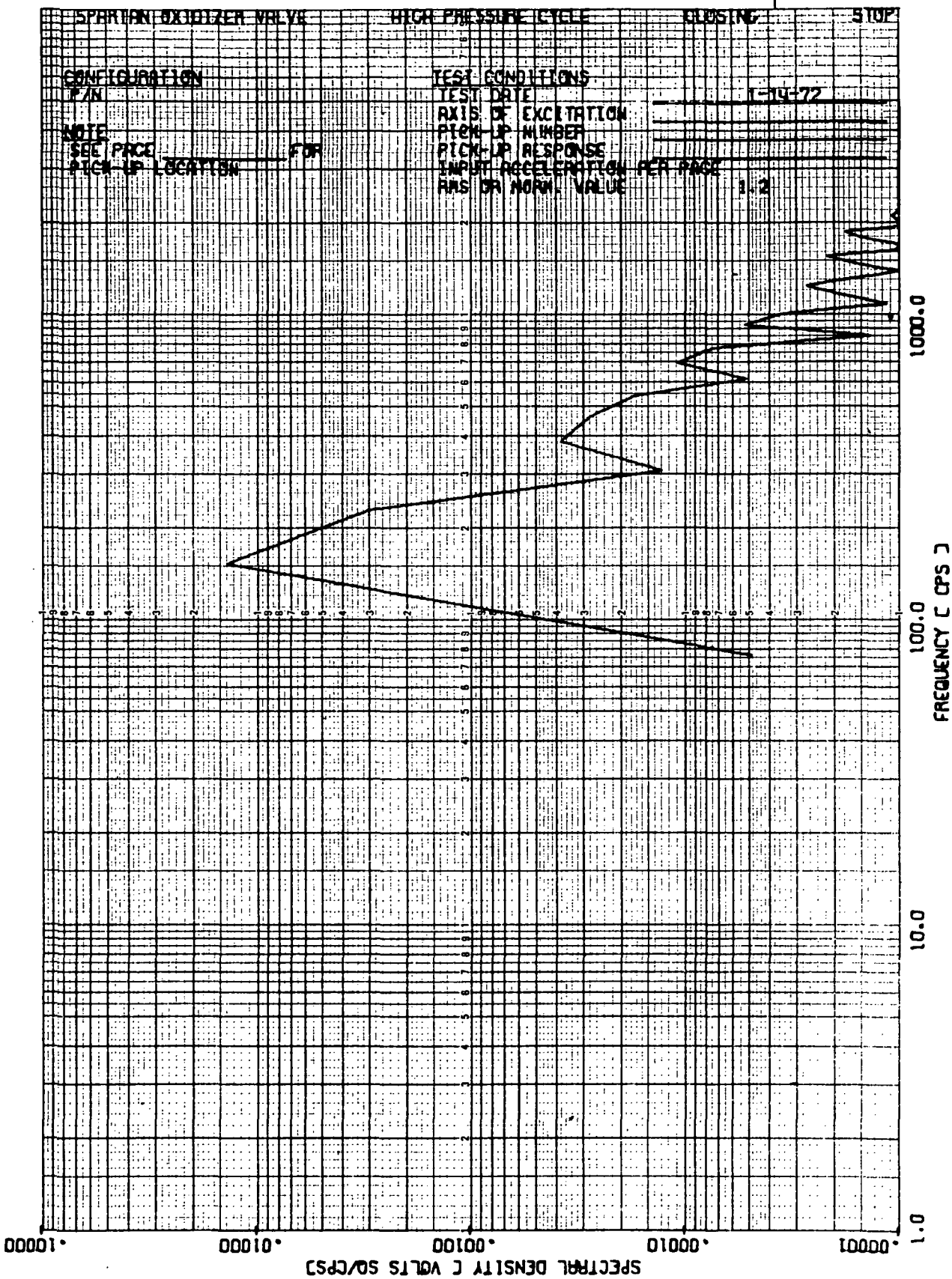
SPARTAN OXIDIZER VALVE
HIGH PRESSURE CYCLE
CLOSING
STOP
CONFIGURATION
P/N
NOTE
SEE PAGE FOR
PICK-UP LOCATION
TEST CONDITIONS
TEST DATE
AXIS OF EXCITATION
PICK-UP NUMBER
PICK-UP RESPONSE
INPUT ACCELERATION PER PAGE
RMS OR NORM. VALUE
1-14-72
1.2
1000.0
100.0
10.0
1.0
FREQUENCY (CPS)
SPECTRAL DENSITY (VOLTS SQ/CPS)
.10000
.01000
.00100
.00010
.00001

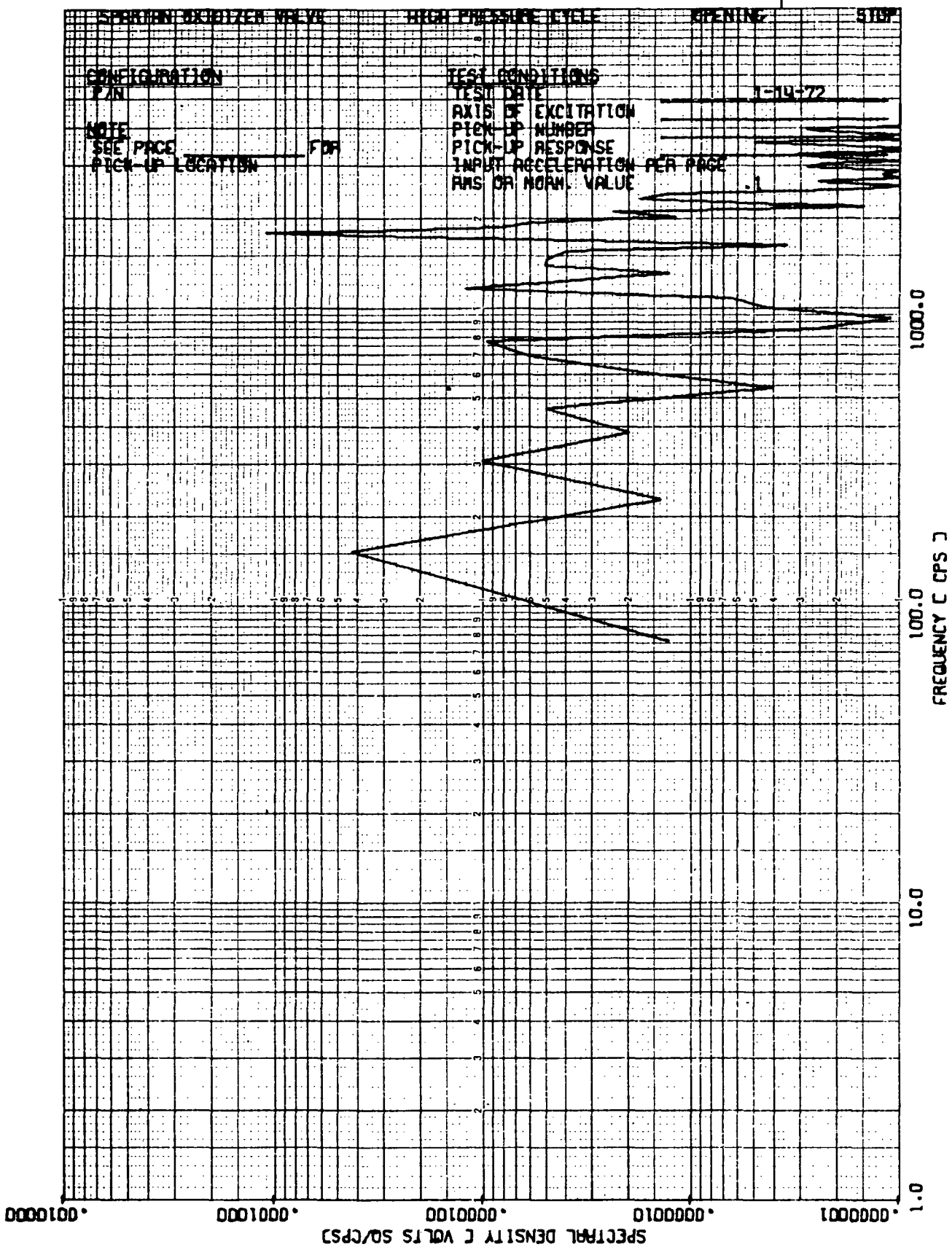
SPARTAN OXIDIZER VALVE
HIGH PRESSURE CYCLE
OPENING
STOP
CONFIGURATION
FAN
NOTE
SEE PAGE FOR
PICK-UP LOCATION
TEST CONDITIONS
TEST DATE
1-14-72
AXIS OF EXCITATION
PICK-UP NUMBER
PICK-UP RESPONSE
INPUT ACCELERATION PER PAGE
RMS OR NORM. VALUE
.1
1000.0
100.0
10.0
1.0
FREQUENCY (CPS)
.0000001
.0000010
.0000100
.0001000
.0010000
SPECTRAL DENSITY (VOLTS SQ/CPS)

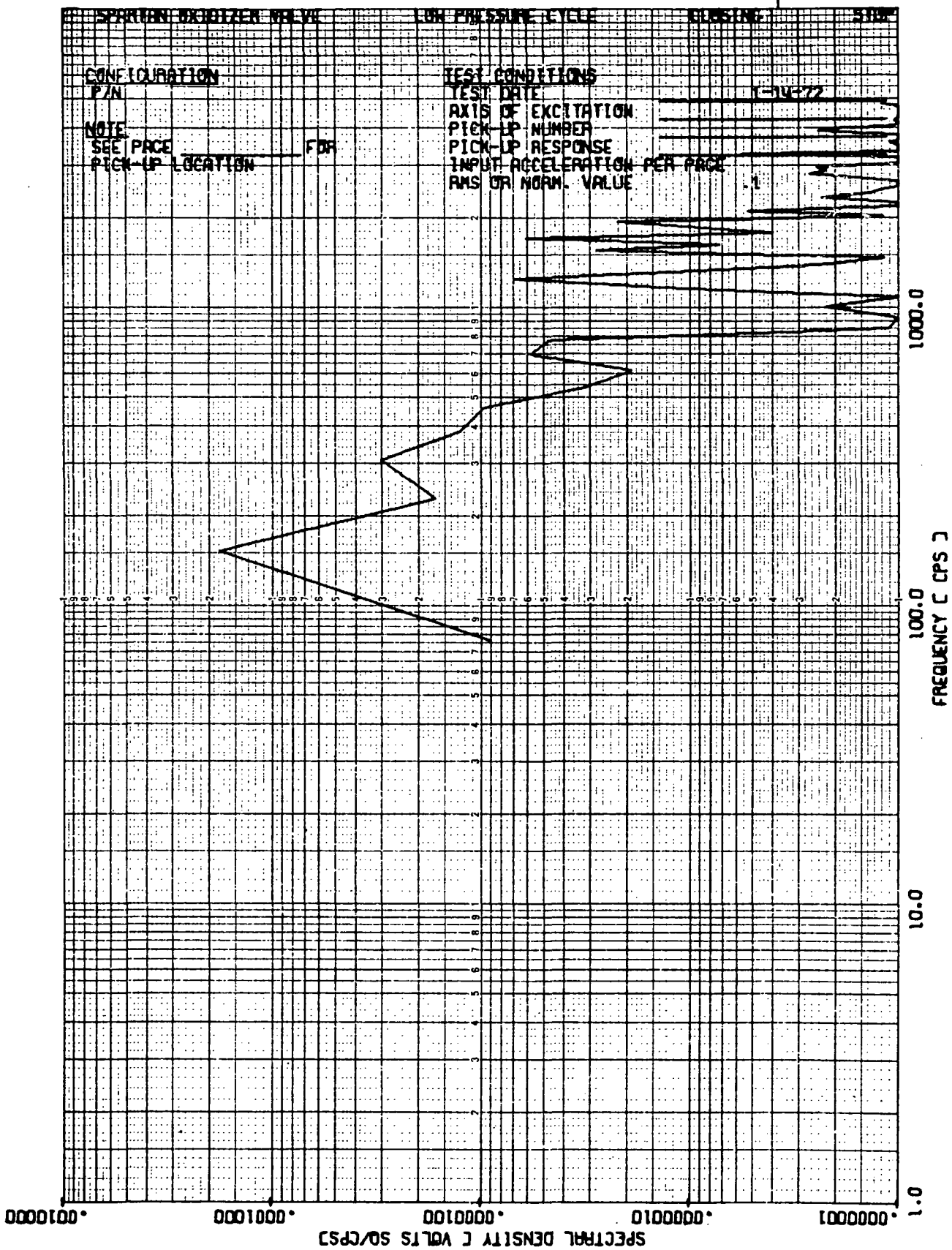
SPARTAN OXIDIZER VALVE
LOW PRESSURE CYCLE
CLOSING
STBY
CONFIGURATION
P/N
NOTE
SEE PAGE FOR
PICK-UP LOCATION
TEST CONDITIONS
TEST DATE
1-14-72
AXIS OF EXCITATION
PICK-UP NUMBER
PICK-UP RESPONSE
INPUT ACCELERATION PER PAGE
RMS OR NORM. VALUE
.1
1000.0
100.0
10.0
1.0
FREQUENCY (CPS)
.0010000
.0001000
.0000100
.0000010
.0000001
SPECTRAL DENSITY (VOLTS SQ/CPS)

MCDONNELL DOUGLAS ASTRONAUTICS COMPANY

PAGE NO._____
REPORT NO._____

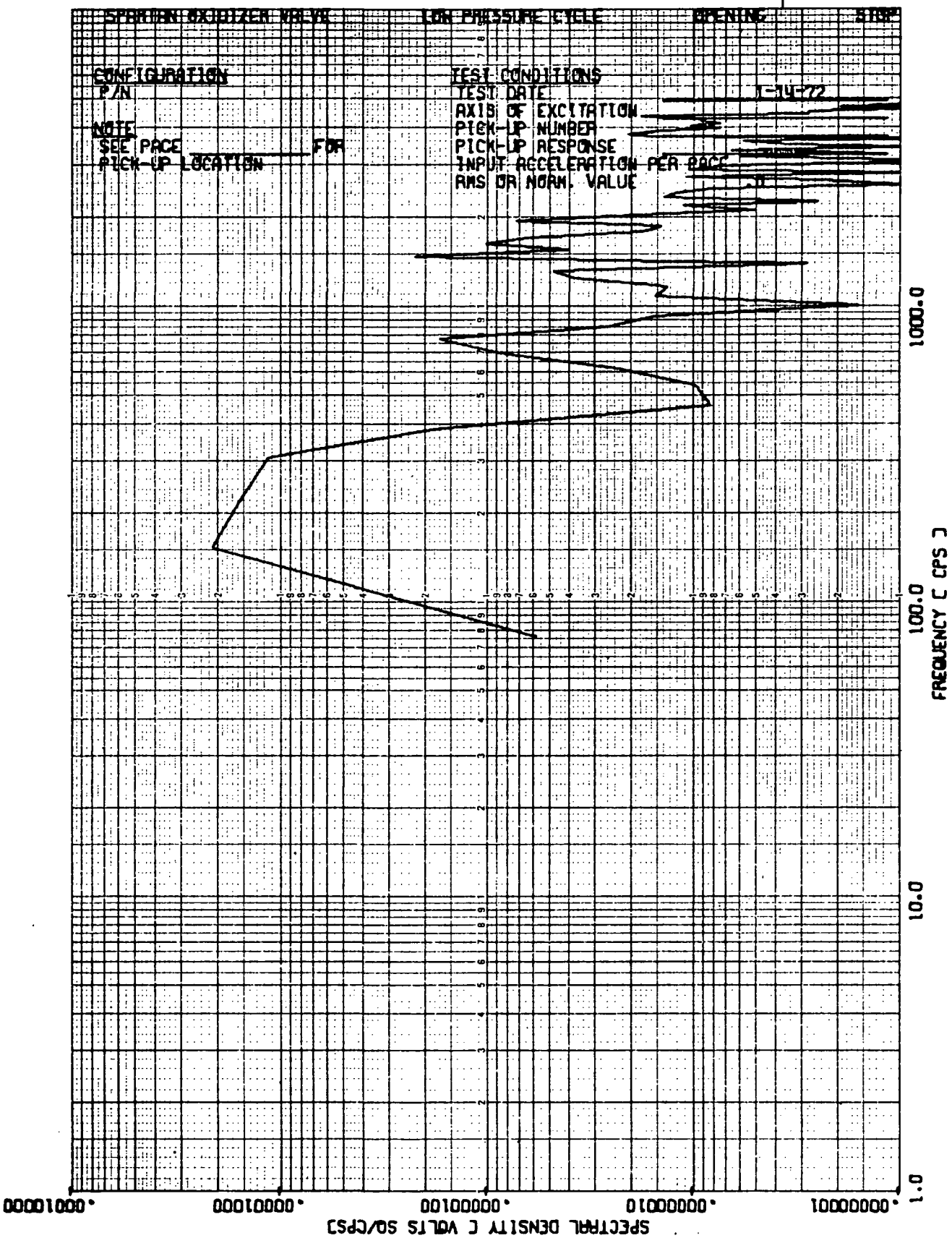

Appendix C
CONTAMINATION AVOIDANCE DEVICE ANALYSIS

This appendix contains the analysis of the basic particulate deflection characteristics of particles moving in a fluid stream and the detail application of the flow model data to various types of dynamic separators.

Page intentionally left blank

Nomenclature

W = Flow rate, lb/sec

A = Area, in^2

ΔP = Pressure drop, psi

K = Resistance coefficient

M = Mach number

R = Gas constant, ft/°R

V_p = Particle velocity, ft/sec

V = Fluid velocity, ft/sec

V_n = Particle initial velocity normal to pipe wall, ft/sec

ϕ = Pipe bend angle, degrees

α = Diffuser section angle, degrees

D = Diameter of pipe, in

D_p = Diameter of particle, ft

a = Diameter of particle, microns

ρ = Fluid density, lb/ft^3

ρ_p = Particle density, lb/ft^3

μ = Fluid viscosity, lb/ft-sec

R_p = Particle Reynolds number

d = Distance particle travels downstream from bend before contacting pipe wall, ft

t = Time, sec

T = Fluid temperature, °R

P = Fluid pressure, psia or psig

γ = Ratio of specific heats

g_c = Gravitational constant, 32.2 ft/sec^2

Subscripts

t = Throat

1 = Point upstream of separator device

2, 3, 4, 5, 6 = Noted points downstream of separator device

0 = Reservoir

A = Filter A

B = Filter B

1.0 PARTICULATE DYNAMICS

1.1 Analytical Model

The analytical model which will be considered during this effort is shown below:

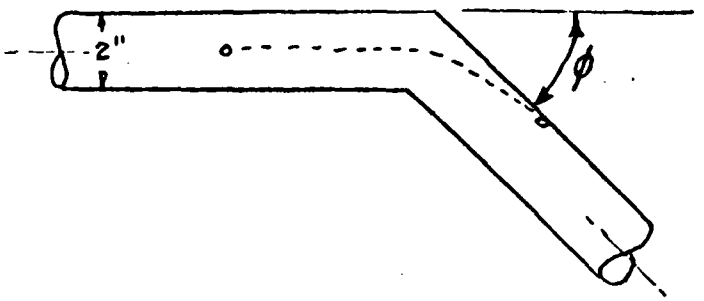

The duct diameter is 2 inches and the bend angle (ϕ) is variable.

1.2 Objective

The objective is to determine particle trajectories for solid particles under the following conditions:

a.	Particle size	25 - 250 microns
b.	Particle density	AL_2O_3, CRES, Ti Carbide
c.	Carrier fluid	GO_2, GH_2, GN_2, LN_2
d.	Fluid velocity	50 to 1200 fps

1.3 Assumptions

a. Particle is spherical

b. Particle and fluid are travelling at same velocity prior to bend

c. Fluid streamlines are parallel to duct wall before and after turn, i.e.,

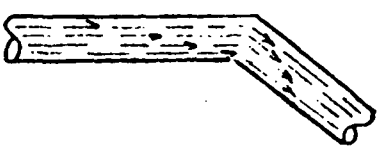

d. The only force acting on the particle is drag force due to the carrier fluid

e. Boundary layer effects are neglected

1.4 Analysis

1.4.1 The particle is travelling in a straight line when the bend is approached and would continue to travel straight if there were no force acting on it. However, the gas will carry the particle downstream before it intercepts the pipe wall:

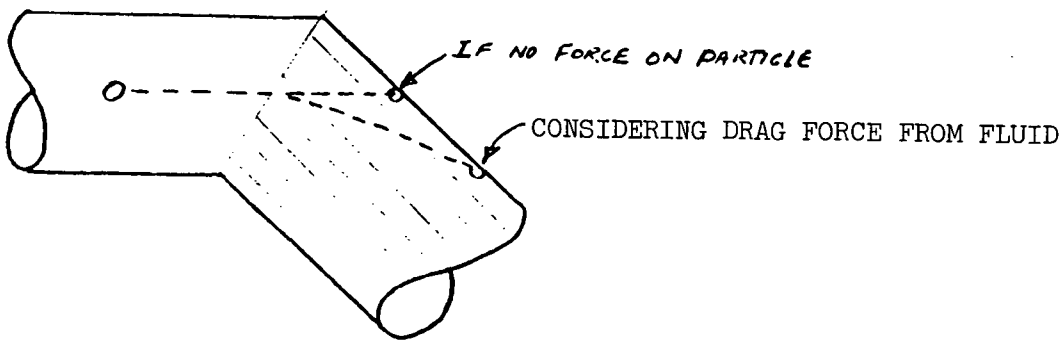

1.4.2 Force and Velocity

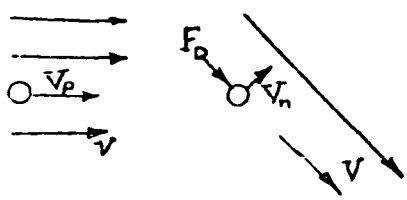

To determine the pipe bend angle required, the analysis will be done assuming the particle is injected into the fluid stream immediately downstream of the bend at a velocity equal to the normal component (V_n) of the particle relative to the fluid stream at the bend:

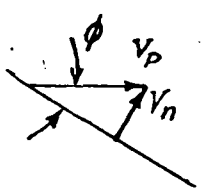

$$\sin\phi = V_n/V_p \qquad (1)$$

$$\phi = \sin^{-1} V_n/V_p \qquad (2)$$

1.4.3 Pipe Bend Angle

Using the analysis presented in Reference (9), the problem becomes one of determining the initial velocity of a particle which causes the particle to travel 2 inches (worst case) normal

1.4.3 Pipe Bend Angle (continued)

to the duct after the turn, i.e.,

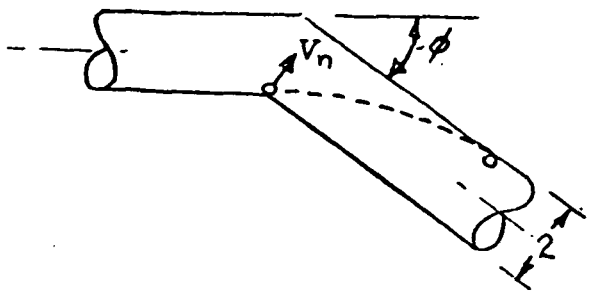

This, in turn, will allow calculation of the minimum angle, ϕ, which will cause all particles to impinge on the opposite wall of the pipe.

Assuming the particle is injected normally and the Stokes Law applies, then equations (15) and (7) from Reference (9) can be applied, and takes the form shown below when the nomenclature associated with this analysis is used:

$$D = (D_p^2 \rho_p / 18 \mu) V_n \qquad (3)$$

The maximum penetration distance is assumed to be the pipe diameter, D.

Solving equation (3) for V_n, substituting 2 inches for pipe diameter, and converting D_p to particle size in microns results in,

1.4.3 Pipe Bend Angle (continued)

$$V_n = \frac{(1/6)(18\mu)}{(a^2 x 10^{-12} x 10.76)\rho_p} = \frac{2.79 x 10^{11}\mu}{a^2 \rho_p} \qquad (4)$$

For a given fluid, particle size, and particle material, a required normal velocity is calculated from equation (4). This velocity is then used to calculate the required pipe bend angle using equation (2) and a candidate fluid velocity.

To present the data in a dimensionless form for all of the candidate fluids, a particle Reynolds number is used:

$$R_p = 3.28 a x 10^{-6} x V_p x \rho_p / \mu \qquad (5)$$

Therefore, for each particle size a curve of pipe bend angle, ϕ, versus Reynolds number can be developed which is applicable to all of the candidate fluids and particle materials. Curves were generated for five particle diameters and are shown in Figure 1. The limiting bend angle was assumed to be 90° since this gives the maximum velocity normal to the pipe. It was noted that there were some cases of low fluid velocity and small particle size where the particle did not have sufficient momentum to penetrate 2 inches of the fluid and therefore even at 90° the particle would not intercept the pipe wall.

Bend angle versus particle velocity was plotted for three particle materials in GN_2 and one particle material in GH_2. These plots are shown in Figures 2 through 5. This same data can be obtained by calculating the particle Reynolds number from equation (5) and entering Figure 1 to the appropriate particle size curve.

1.4.4 Impact Distance

Another area of interest associated with the particle trajectories is the distance from the start of the bend to the point of particle

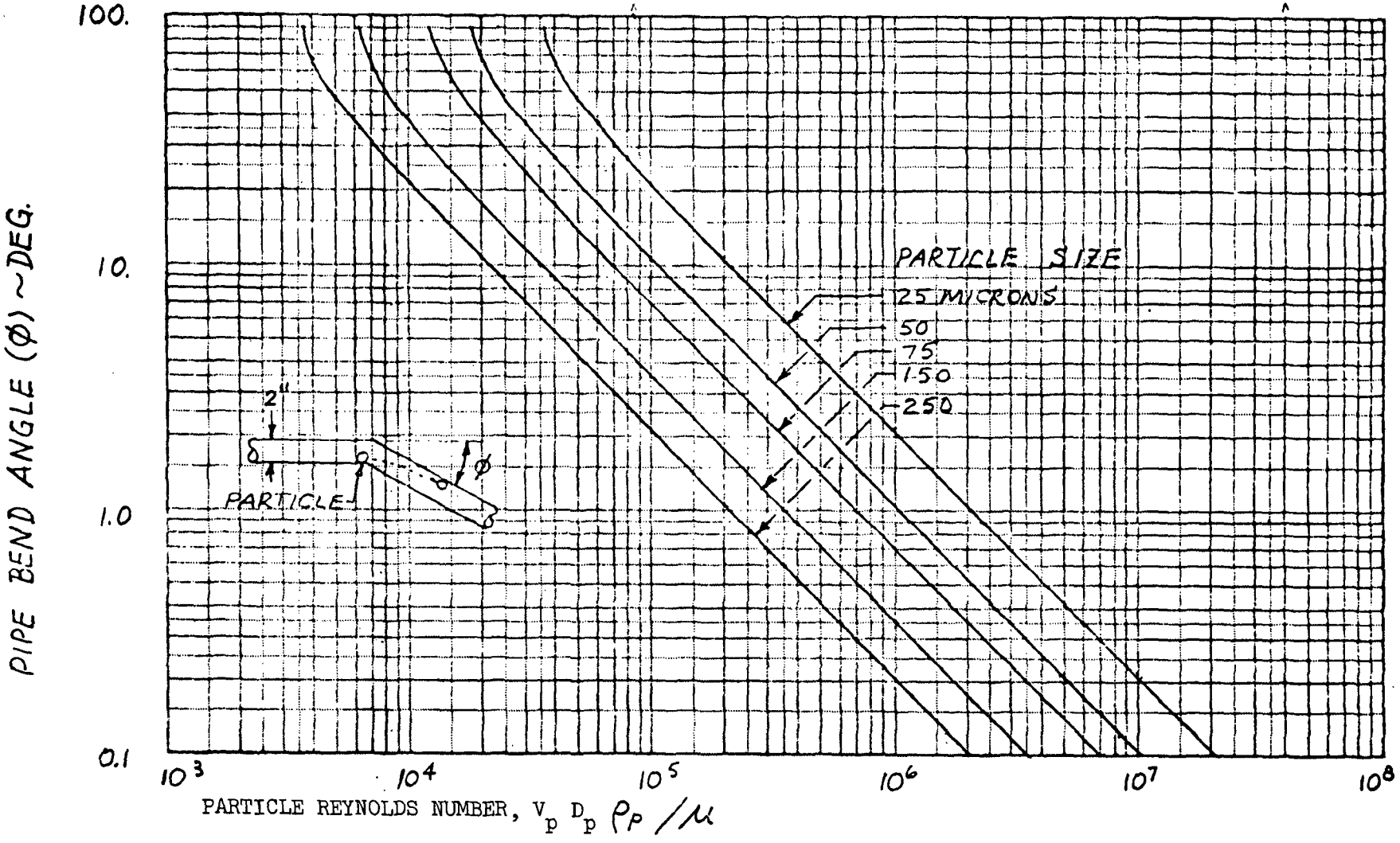

FIG. 1. MINIMUM PIPE BEND ANGLE REQUIRED FOR PARTICLE IMPACT ON PIPE WALL

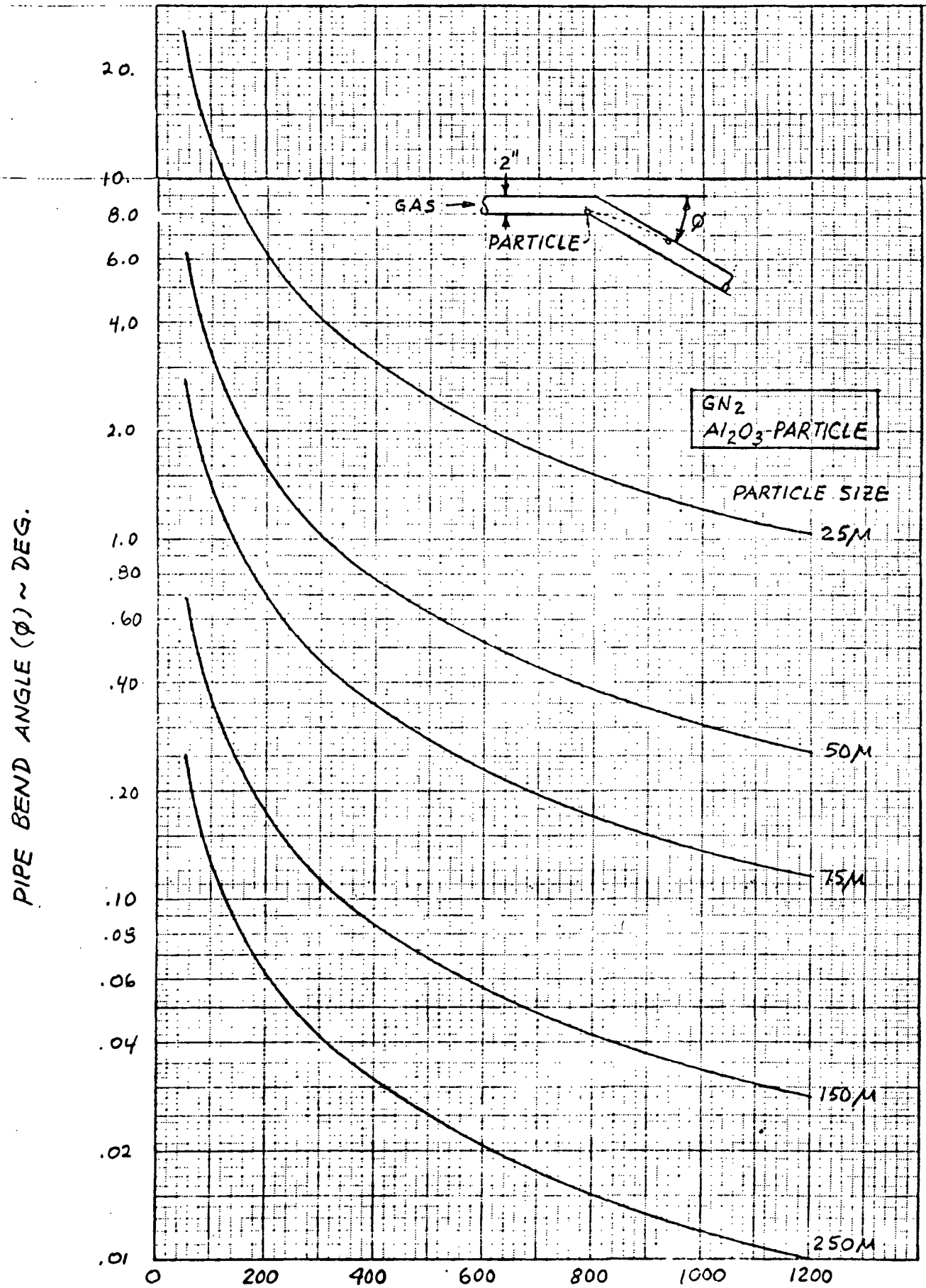
20.
10.
8.0
6.0
4.0
2.0
1.0
.80
.60
.40
.20
.10
.09
.06
.04
.02
.01
0
200
400
600
800
1000
1200
2"
GAS
PARTICLE
Ø
GN2
Al2O3-PARTICLE
PARTICLE SIZE
25M
50M
75M
150M
250M
PIPE BEND ANGLE (Ø) ~ DEG.
PARTICLE VELOCITY PRIOR TO BEND ~ FT/SEC

FIG. 2.

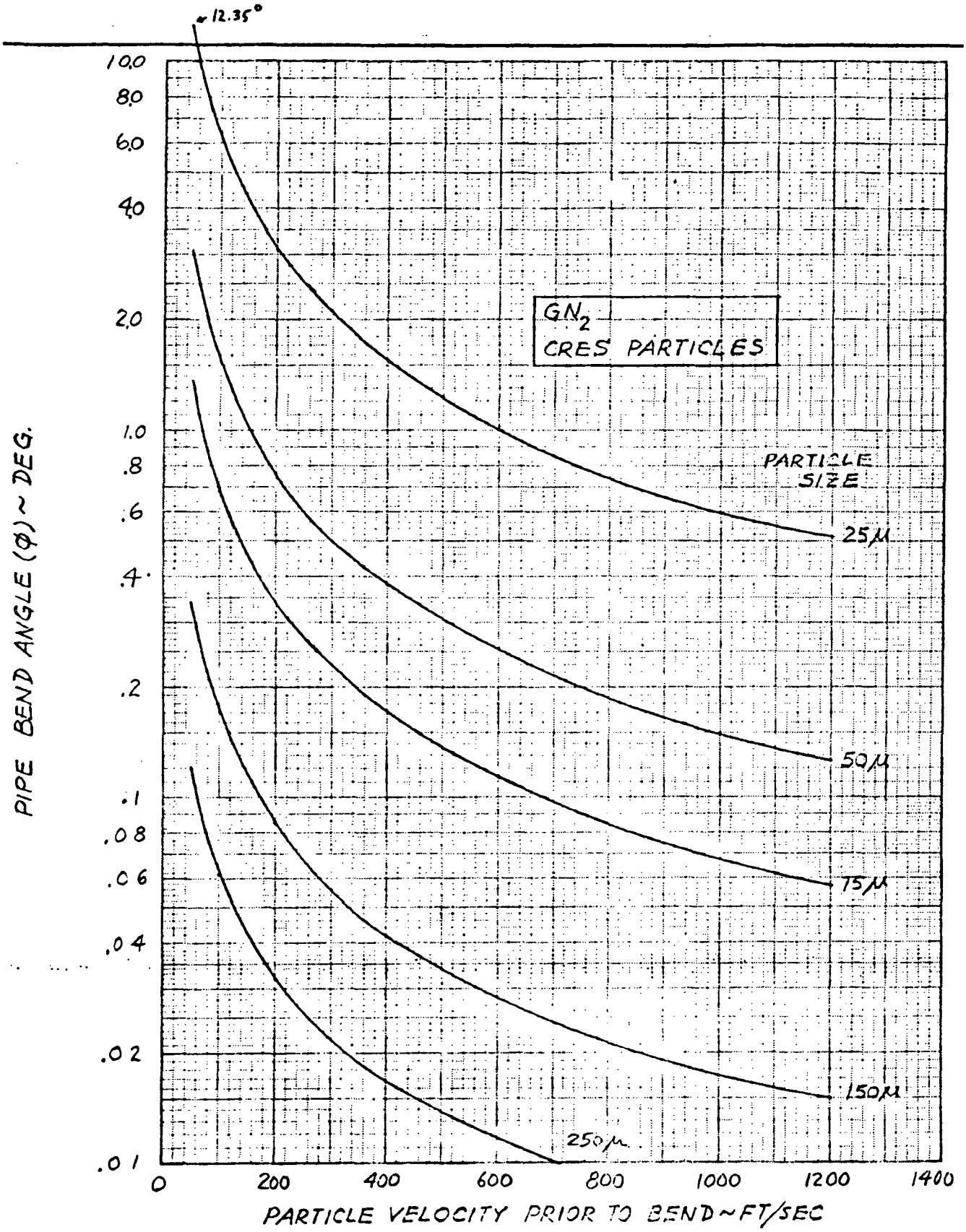

FIG. 3. MINIMUM PIPE BEND ANGLE REQUIRED FOR PARTICLE IMPACT ON PIPE WALL

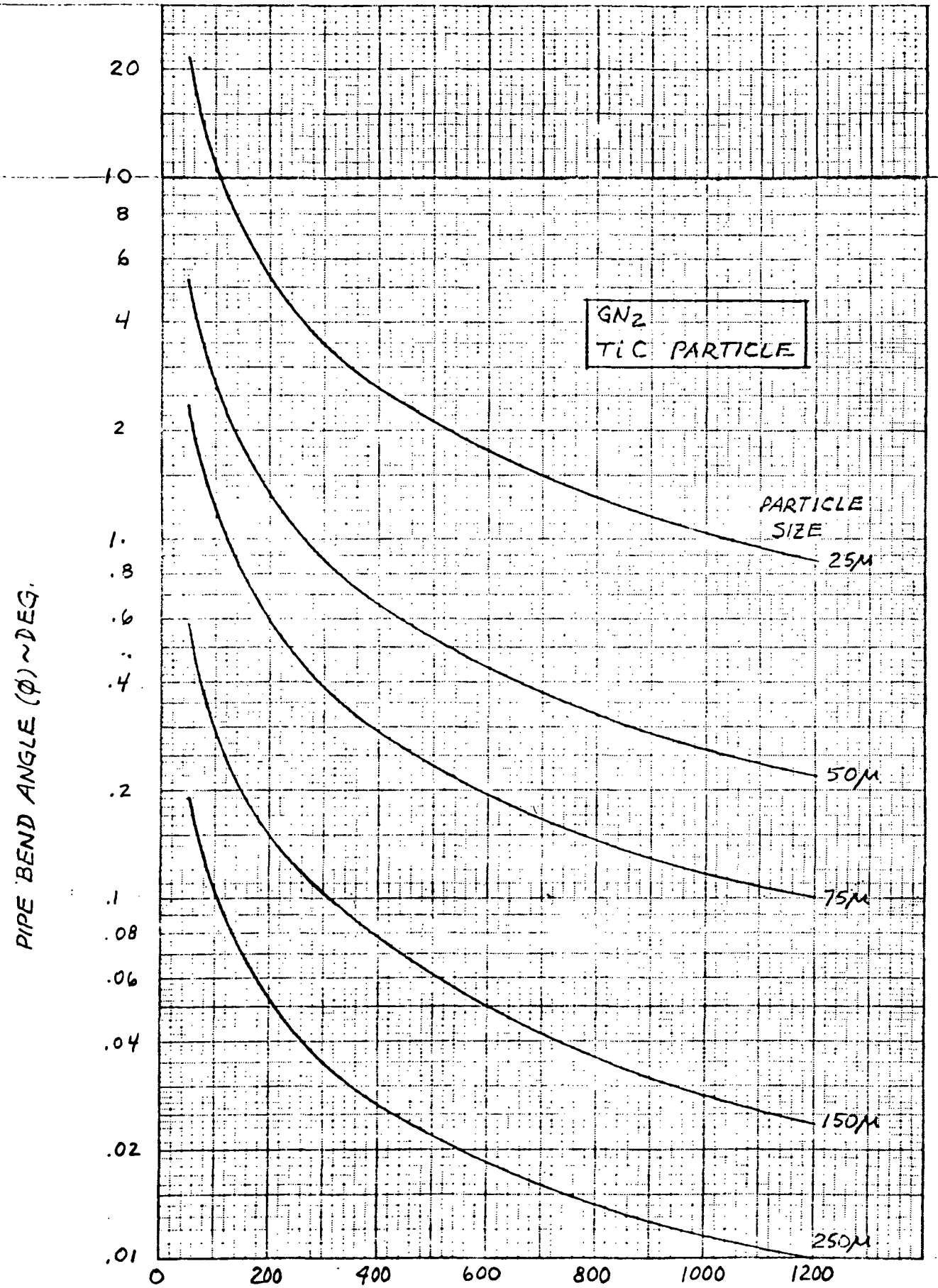

FIG. 4. PARTICLE VELOCITY PRIOR TO BEND ~FT/SEC

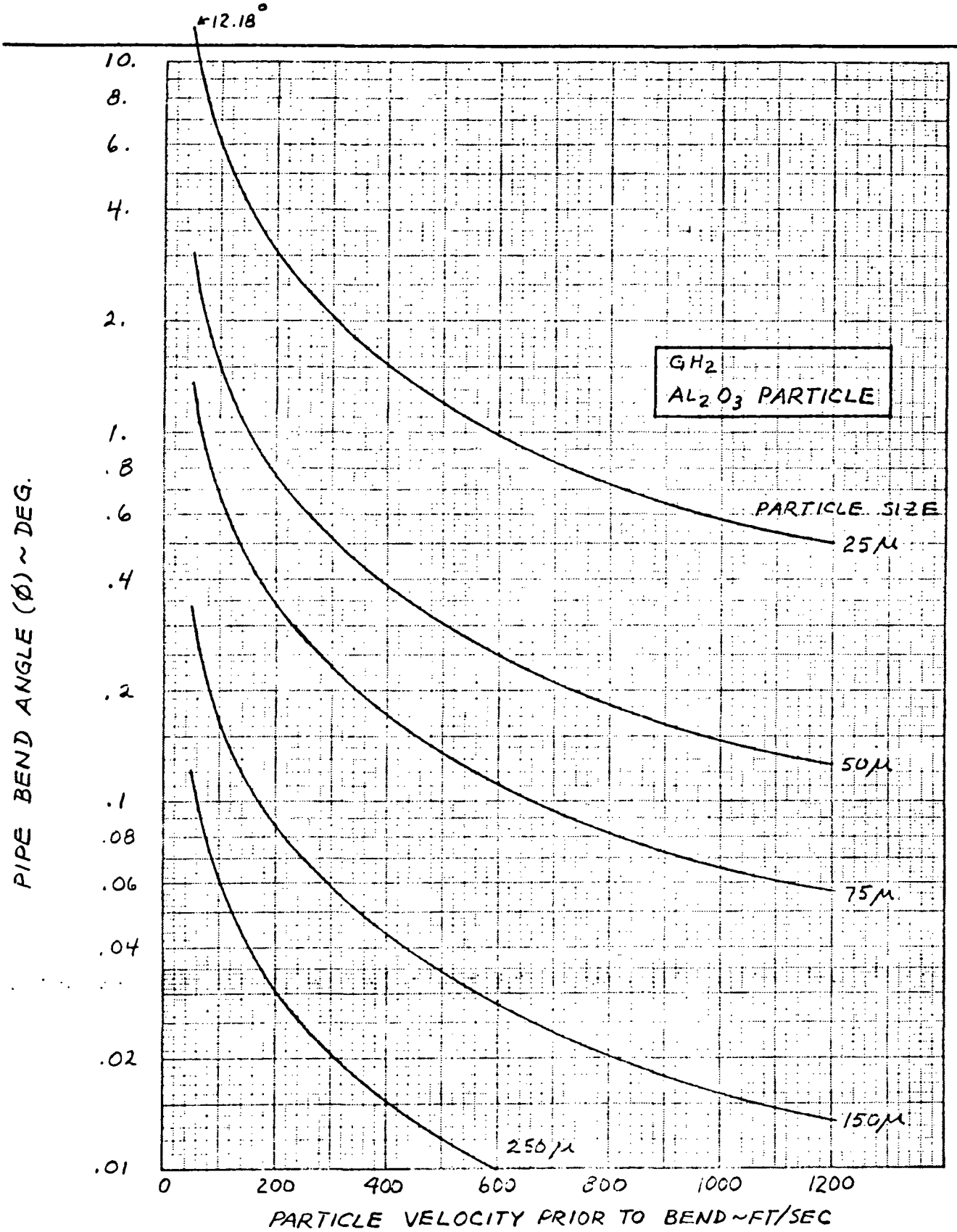

FIG. 5. MINIMUM PIPE BEND ANGLE REQUIRED FOR PARTICLE IMPACT ON PIPE WALL

1.4.4 Impact Distance (continued)

impact with the pipe wall. The maximum distance cases were examined to determine the furtherest downstream travel by the particles. This was done by considering the particle which had the greatest distance to travel across the pipe, and assuming the particle was travelling downstream at the same velocity as the fluid. Therefore,

$$d = V_p\, t \tag{6}$$

where t is the time required for the particle to traverse the 2 inch distance across the pipe. The time is a function of the particle velocity normal to the pipe and since it has been assumed that the particle velocity is essentially zero when it reaches the wall, the average velocity is $V_n/2$. Therefore, equation (6) becomes

$$d = V_p \frac{1/6}{V_n/2} = V_p/3V_n \tag{7}$$

Substituting equation (4) into equation (7)

$$d = V_p a^2 \rho_p / 8.37\times10^{11}\mu = \frac{a^2}{8.37\times10^{11}} \cdot \frac{V_p \rho_p}{\mu} \tag{8}$$

Substituting for $V_p \rho_p/\mu$ from equation (5), equation (8) becomes

$$d = \frac{a^2}{8.37\times10^{11}} \times \frac{R_p}{3.28\times10^{-6}} = 3.64\times10^{-7} a R_p \tag{9}$$

Therefore, using equation (9), curves can be generated for distance versus particle Reynolds number for any particle size. Curves were generated for five particle sizes and are plotted in Figure 6. It can be noted that the distances become very long for particle Reynolds numbers greater than 10^5 to 10^6.

FIG 6. PARTICLE IMPACT DISTANCE FOR MINIMUM BEND ANGLE IN 2-INCH PIPE

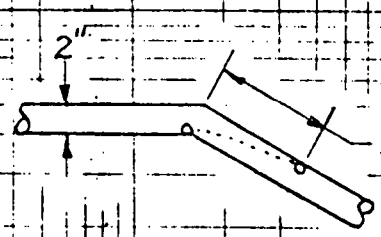

PARTICLE IMPACT DOWNSTREAM OF BEND ~ FT.

1000.
100.
10.
1.0
0.1

PARTICLE SIZE
25 MICRONS
50
75
150
250

10^3 10^4 10^5 10^6 10^7 10^8

PARTICLE REYNOLDS NUMBER, = $V_p D_p \rho_g / \mu$

2.0 PRESSURE DROP

This section contains pressure drop estimates for candidate particle separator devices.

2.1 Nozzle and Plenum

The device considered herein is a nozzle and plenum arrangement where the flow from the nozzle impinges on a filter plate and then makes a 90° bend. The configuration and measurements used are shown below:

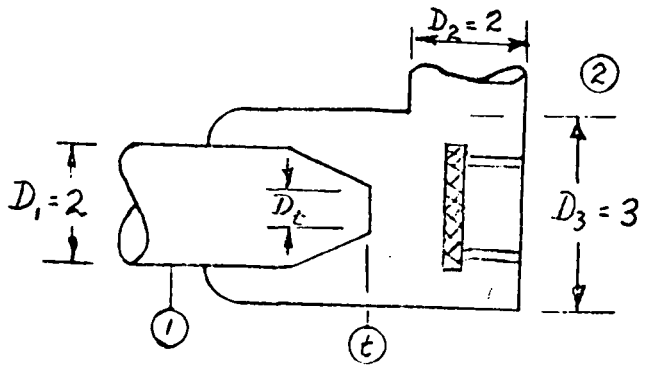

Other data used for the analysis of this configuration is: 2.5 lb/sec GN_2 flowrate, P_1 = 100 psig, and $T_1 = 530^{\circ}R$.

2.1.1 Choked Flow Nozzle

$$P_t = 0.5283P_1 = 0.5283 \times 115 = \underline{58 \text{ psia}} \qquad (10)$$

Therefore as long as downstream pressure is 58 psia or less, the flow will be choked.

$$T_t/T_1 = (P_t/P_i)^{\gamma-1/\gamma} = (0.5283)^{0.2857} = \underline{0.833} \qquad (11)$$

Therefore,

$$T_t = 530 \times 0.833 = \underline{441^{\circ}R} \qquad (12)$$

2.1.1 Choked Flow Nozzle (continued)

Since flow is choked the velocity at the throat is sonic. Therefore,

$$V_t = \sqrt{\gamma g_c RT_t} = \sqrt{(1.4)(32.2)(55.15)(441)} = \tag{13}$$

$$= \sqrt{1.097 \times 10^6} = \underline{1046} \text{ ft/sec}$$

GN_2 density at throat is

$$\rho_t = \frac{P_t}{RT_t} = \frac{58 \times 144}{55.15 \times 441} = \underline{0.343} \text{ lb/ft}^3 \tag{14}$$

From continuity

$$\dot{W} = \rho_t A_t V_t \tag{15}$$

therefore,

$$A_t = \frac{\dot{W}}{\rho_t V_t} = \frac{2.5 \times 144}{0.343 \times 1046} \text{ in}^2 = \underline{1.003} \text{ in}^2 \tag{16}$$

$$D_t = 2\sqrt{A_t/\pi} = 2\sqrt{1.003/\pi} = 2\sqrt{0.32} = \underline{1.132} \text{ in} \tag{17}$$

At 2.5 lb/sec the velocity in the 2 inch pipe is

$$V_i = \dot{w}/\rho_i A_i \tag{18}$$

$$\rho_i = \frac{115 \times 144}{55.15 \times 530} = \underline{.565} \text{ lb/ft}^3 \tag{19}$$

$$A_i = \frac{\pi (2)^2}{4(144)} = \underline{.0218} \text{ ft}^2 \tag{20}$$

$$\therefore \quad V_i = \frac{2.5}{(0.565)(0.0218)} = \underline{203} \text{ ft/sec} \tag{21}$$

From Reference (10) the ΔP from expansion of the nozzle into the plenum is

$$\Delta P_{①-②} = K \rho_t V_t^2 / 2g_c \tag{22}$$

2.1.1 Choked Flow Nozzle (continued)

K is a function of diameter ratio, therefore

$$D_t/D_3 = 1.132/3 = .378$$

$$K = 0.73 \quad \text{(Figure 3.9.4a, Reference (10))}$$

$$\Delta P_{①-④} = \frac{(0.73)(0.343)(1.097\times10^6)}{(64.4)(1.44)} \frac{lb}{in^2} = \underline{29.6} \text{ psi}$$

$$\rho_3 = \frac{P_3}{RT_3} = \frac{(115-29.6)(144)}{(55.15)(530)} = \underline{.419} \frac{lb}{ft^3}$$

$$V_3 = \dot{W} / \rho_3 A_3 = 2.5/(0.419\times0.0218) = \underline{274} \text{ ft/sec}$$

Assuming the plenum bend is a 90° mitered elbow, the K value is 1.4 from Table 3.9.5.2 of Reference (10). Therefore,

$$\Delta P_{④-②} = K \rho_2 V_2^2/2g_c$$

$$\Delta P_{④-②} = \frac{(1.4)(0.419)(274)^2}{(64.4)(144)} = \underline{4.75} \text{ psi}$$

Therefore,

$$\Delta P_{①-②} = 29.6+4.75 = \underline{34.4} \text{ psi}$$

2.1.2 Subsonic Nozzles

In addition to the sonic nozzle system, other nozzle configurations were investigated which had throat diameters larger than sonic. The analysis was accomplished using the Fanno flow tables in Reference (10) and the results are plotted in Figure 7.

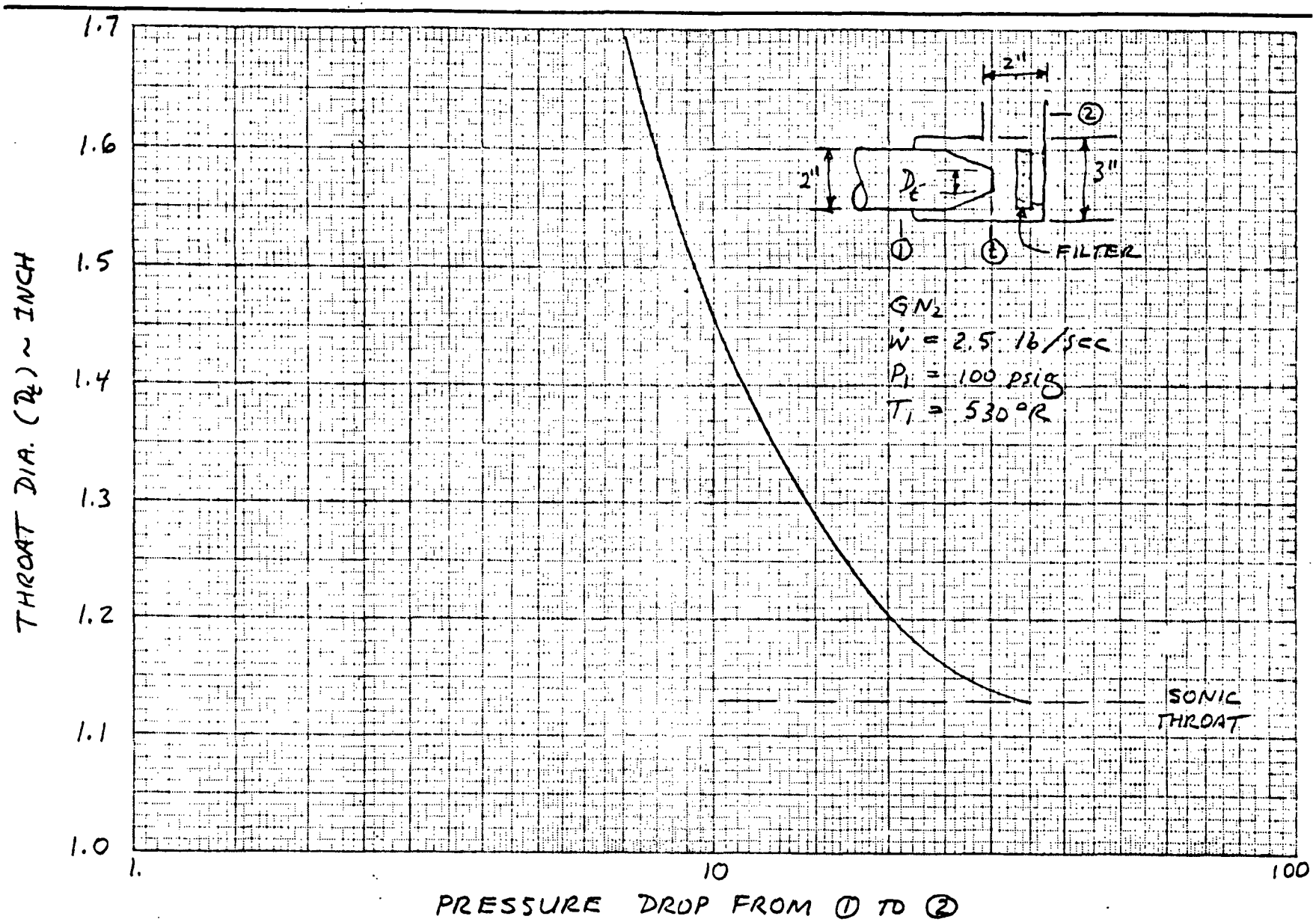

FIG. 7 PRESSURE DROP FOR NOZZLE & PLENUM SYSTEM

2.2 Conical Filters and Plenum

The device considered here is a plenum containing two conical filters where the flow goes through and around the filters. The configuration is shown below.

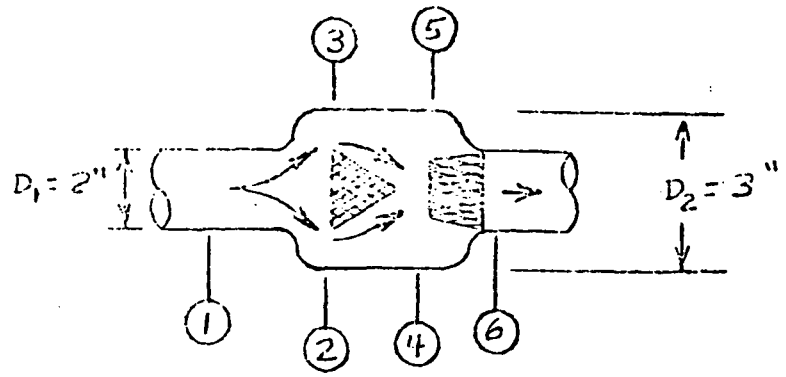

Other data used in the analysis of this configuration are: 2.5 lb/sec GN_2 flowrate, P_1 = 100 psig, and T_1 = 530°R.

2.2.1 Blocked Filters

The maximum pressure drop occurs when no flow goes through the filters. The flow path would then be as indicated by the arrows in the sketch above. K-factors may be found for each station and referenced to the inlet diameter, D_1.

From 2.1.1, V_1 = 203 ft/sec, M_1 = 0.178, P_1 = .565

From Figure 3.9. 4a of Reference (10), K_{1-2} = 0.3

An equivalent geometric diameter for station 3 is $D_3 = \sqrt{D_2^2 - D_1^2} = \sqrt{9-4} = 2.24"$

Again from Figure 3.9.4a of Reference (10), K_{2-3} = .045

Referenced to a 2-inch diameter

$$K_{2-3} = .045 \left(\frac{2}{2.24}\right)^4$$

$$= .045\ (.631)$$

$$K_{2-3} = .028$$

From Figure 3.9.4a of Reference (10)

$$K_{3-4} = .009$$

From Figure 3.8.2.2a of Reference (10)

$$K_{4-5} = .93$$

From Figure 3.9.4a of Reference (10)

$$K_{5-6} = 0$$

Then the total K for the device is

$$K_{1-6} = .3 + .028 + .009 + .93 + 0$$

$$K_{1-6} = 1.267$$

$$\Delta P = \frac{k\rho_1 V_1^2}{2g_c}$$

$$= \frac{1.267\ (.565)(203)^2}{2(32.2)\ (144)}$$

$$\underline{\Delta P = 3.18 \text{ psi}}$$

From the above analysis, it can be seen that the largest resistance occurs at station 4-5. Therefore, changing the inner diameter (I.D.) of the second screen produces more ΔP variation than changing other elements of the device. Following are some calculations showing the effects of changing this diameter. The results are plotted on Figure 8.

Second filter I.D. = $D_5 = 1.5"$

$$K_{4-5} = .93\left(\frac{2}{1.5}\right)^4 = .93\ (3.17) = 2.95$$

$$K_{5-6} = .19$$

$$K_{1-6} = .3 + .028 + .009 + 2.95 + .19$$

$$K_{1-6} = 3.477$$

$$\Delta P = 3.18\ \frac{(3.477)}{(1.267)}$$

$$\underline{\Delta P = 8.73 \text{ psi}}$$

Second filter I.D. = 1.75"

$$K_{4-5} = .93\left(\frac{2}{1.75}\right)^4 = .93\ (1.72) = 1.6$$

$$K_{5-6} = .055$$

$$K_{1-6} = .3 + .028 + .009 + 1.6 + .055$$

$$K_{1-6} = 1.992$$

$$\Delta P = \frac{1.992}{1.267}\ (3.18)$$

$$\underline{\Delta P = 5.00 \text{ psi}}$$

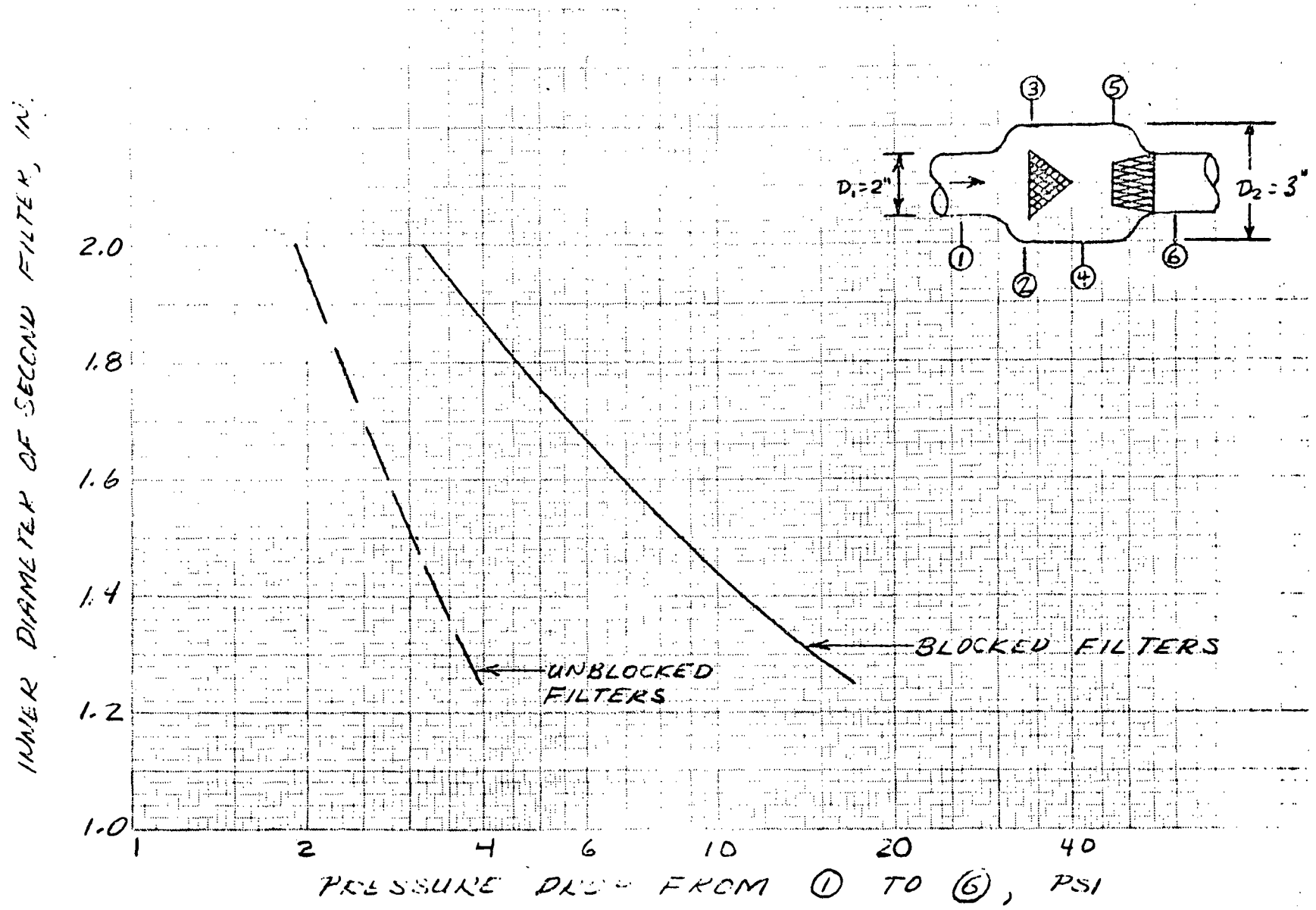

FIGURE 8. PRESSURE-DROP FOR CONICAL FILTERS AND PLENUM

Second filter I.D. = 1.25"

$$K_{4-5} = .93 \left(\frac{2}{1.25}\right)^4 = .93\ (6.56) = 6.10$$

$$K_{5-6} = .36$$

$$K_{1-6} = .3 + .028 + .009 + 6.10 + .36$$

$$K_{1-6} = 6.777$$

$$\Delta P = 3.18 \frac{(6.777)}{(1.267)} = \underline{17.0 \text{ psi}}$$

2.2.2 Unblocked Filters

With unblocked filters, part of the flow will go through the filters, and the pressure drop through the system will be reduced. From Reference (11), a resistance coefficient for a flat screen Dutch filter was obtained, based on the inlet conditions in 2.2.1. The resistance coefficient obtained was 16.1. Since the first filter causes only a small ΔP when blocked, calculations will not be made for an unblocked first filter.

For the second filter, assume the filter cone surface area is twice the area of the 2-inch duct. The equivalent K for the filter, referenced to a 2-inch diameter, is

$$K = 16.1 \left(\frac{4\pi}{8\pi}\right)^2 = 4.025$$

From Reference (12) the equivalent K for parallel flow paths (through the sides and the center of the second cone) is

$$Keq = \frac{K_A K_B}{K_A + 2\sqrt{K_A K_B} + K_B}$$

For a 2-inch inner diameter, $K_A = 4.025$, $K_B = .93 + 0 = .93$ (from 2.2.1)

$$K_{4-6} = \frac{4.025(.93)}{4.955+2\sqrt{4.025(.93)}} = \frac{3.74}{4.955+3.87}$$

$$= \frac{3.74}{8.825} = .424$$

$$K_{1-6} = 1.267 + .424 - .93 = 1.691 - .93 = .761$$

$$\Delta P_{1-6} = \frac{.761}{1.267}(3.18) = \underline{1.91}$$

For a 1.75-inch inner diameter

$$K_B = 1.6 + .055 = 1.655$$

$$K_{4-6} = \frac{4.025(1.655)}{5.68+2\sqrt{6.66}} = \frac{6.66}{5.68+5.16} = \frac{6.66}{10.84} = .614$$

$$K_{1-6} = 1.992 + .614 - 1.655 = 2.606 - 1.655 = .951$$

$$\Delta P_{1-6} = \frac{.951}{1.267}(3.18) = \underline{2.39 \text{ psi}}$$

For a 1.5-inch inner diameter

$$K_B = 2.95 + .19 = 3.14$$

$$K_{4-6} = \frac{4.025(3.14)}{7.165+2\sqrt{12.63}} = \frac{12.63}{14.275} = .885$$

$$K_{1-6} = 3.477 + .885 - 3.14 = 4.362 - 3.14 = 1.222$$

$$\Delta P_{1-6} = \frac{1.222}{1.267}(3.18) = \underline{3.09 \text{ psi}}$$

For a 1.25-inch inner diameter

$$K_B = 6.1 + .36 = 6.46$$

$$K_{4-6} = \frac{4.025(6.46)}{10.485+2\sqrt{26}} = \frac{26}{20.685} = 1.26$$

$$K_{1-6} = 6.777 + 1.26 - 6.46 = 8.037 - 6.46 = 1.577$$

$$\Delta P_{1-6} = \frac{1.577}{1.267}(3.18) = \underline{3.96 \text{ psi}}$$

2.3 Venturi Nozzle and Plenum with 90° Bend

The device considered herein is a nozzle and plenum where the flow from the nozzle impinges on a filter plate and then makes a 90° bend. The configuration and measurements used are shown below:

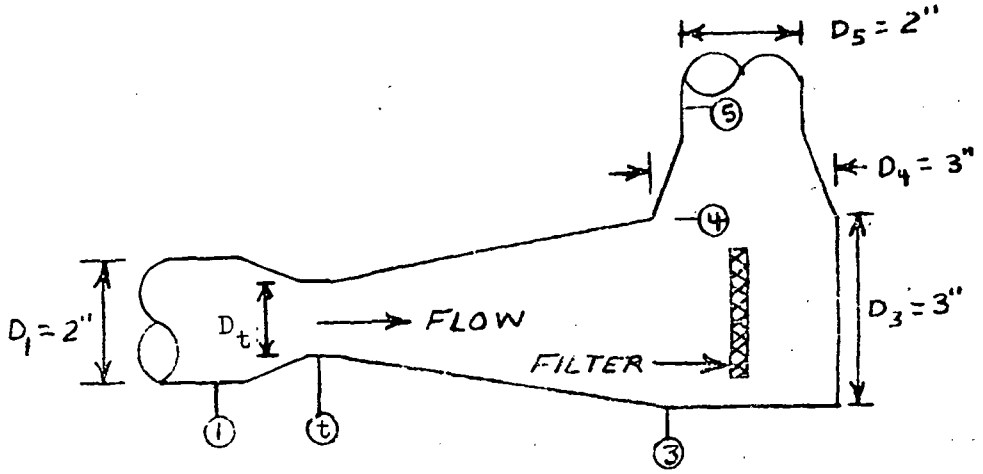

Other data used in the analysis of this configuration are 2.5 lbm/sec GN_2 flowrate, P_1 = 100 psig, and T_1 = 530°R.

From paragraph 2.1, V_1 = 203 ft/sec,, M_1 = 0.178, and ρ_1 = .565 lbm/ft^3. From Reference (10) the resistance coefficient K for the contraction from 1 to 2 is 0.04.

2.3.1 Choked Venturi Nozzle

From 2.1.1, P_t = 58 psia, T_t = 441°R, ρ_t = .343 lb/ft^3, V_t = 1046 ft/sec, D_t = 1.132 in.

$$\Delta P_{1-t} = \frac{\rho_t K_{1-t} V_t^2}{2g_c}$$

$$= \frac{.343(.04)(1046)^2}{144(64.4)}$$

$$\Delta P_{1-t} = 1.62 \text{ psi}$$

From Figure 3.9.4b of Reference (10) the K for the expansion is

$$K_{t-3} = K_{en}\left[1 - \frac{D_t^2}{D_3^2}\right]^2$$

$$= .14\left[1 - \frac{1.132^2}{3^2}\right]^2$$

$$= .12$$

$$\Delta P_{t-3} = (.12/.04)(1.62) = 4.86 \text{ psi}$$

$$P_3 = 115 - (1.62+4.86) = 108.5 \text{ psia}$$

The weight flow parameter,

$$\frac{\dot{w}\ To}{P_3 A_3} = \frac{2.5\sqrt{534}}{108.5\ \left(\frac{\pi}{4}(9)\right)} = .0753$$

From the plot of weight flow parameter vs. mach number for nitrogen in Reference (14)

$$M_3 = .083$$

Since T_o is constant through the system

$$T_3 = T_1\ (T/T_o)_3\ /(T/T_o)_1$$

From Table B-2 of Reference (14)

$$T_3 = 530\ (.9986)/.9937 = 533$$

$$\rho_3 = \frac{P_3}{RT_3} = \frac{108.5(144)}{55.15(533)} = .507$$

$$V_3 = \frac{2.5(144)}{.507\left(\frac{9\pi}{4}\right)} = 100 \text{ ft/sec}$$

For the 90° bend

$$\Delta P_{3-4} = \frac{1.4(.507)(100)^2}{144(64.4)}$$

$$= \underline{.765 \text{ psi}}$$

For the gradual contraction from 4 to 5, K = .04

$$\Delta P_{4-5} = .04\ \rho_5 \frac{V_5^2}{2g}$$

Assuming isentropic flow to get V_5, and using Table B2 (Reference (14))

$$(A/A^*)_5 = \frac{(A_5)}{(A_3)} (A/A^*)_3$$

$$= \frac{(\pi\, 2^2)}{(\frac{\pi}{4}\, 2^2)} \Big/ \frac{(\pi\, 3^2)}{(\frac{\pi}{4}\, 3^2)} (7) = 3.11$$

$M_5 = .19,$

$T_5 = (.9928/.9986)(533)$

$= 530°R$

$$\rho_5 = \frac{(108.5-.765)(144)}{55.15\ (530)}$$

$= .531\ \text{lbm/ft}^3$

$$V_5 = \frac{2.5(144)}{.531\ (\pi)} = 216\ \text{ft/sec}$$

$$\Delta P_{4-5} = \frac{.04(.531)(216)^2}{64.4(144)}$$

$= .107$ psi

$\Delta P_{1-5} = 1.62+4.86+.77+.11$

$= \underline{7.36\ \text{psi}}$

These calculations were also made for subsonic flow. The results are shown in Figure 9.

2.4 Venturi Nozzle and Plenum

The device considered herein is a Venturi nozzle and plenum where flow from the nozzle impinges on a conical filter in the flow path, as shown below.

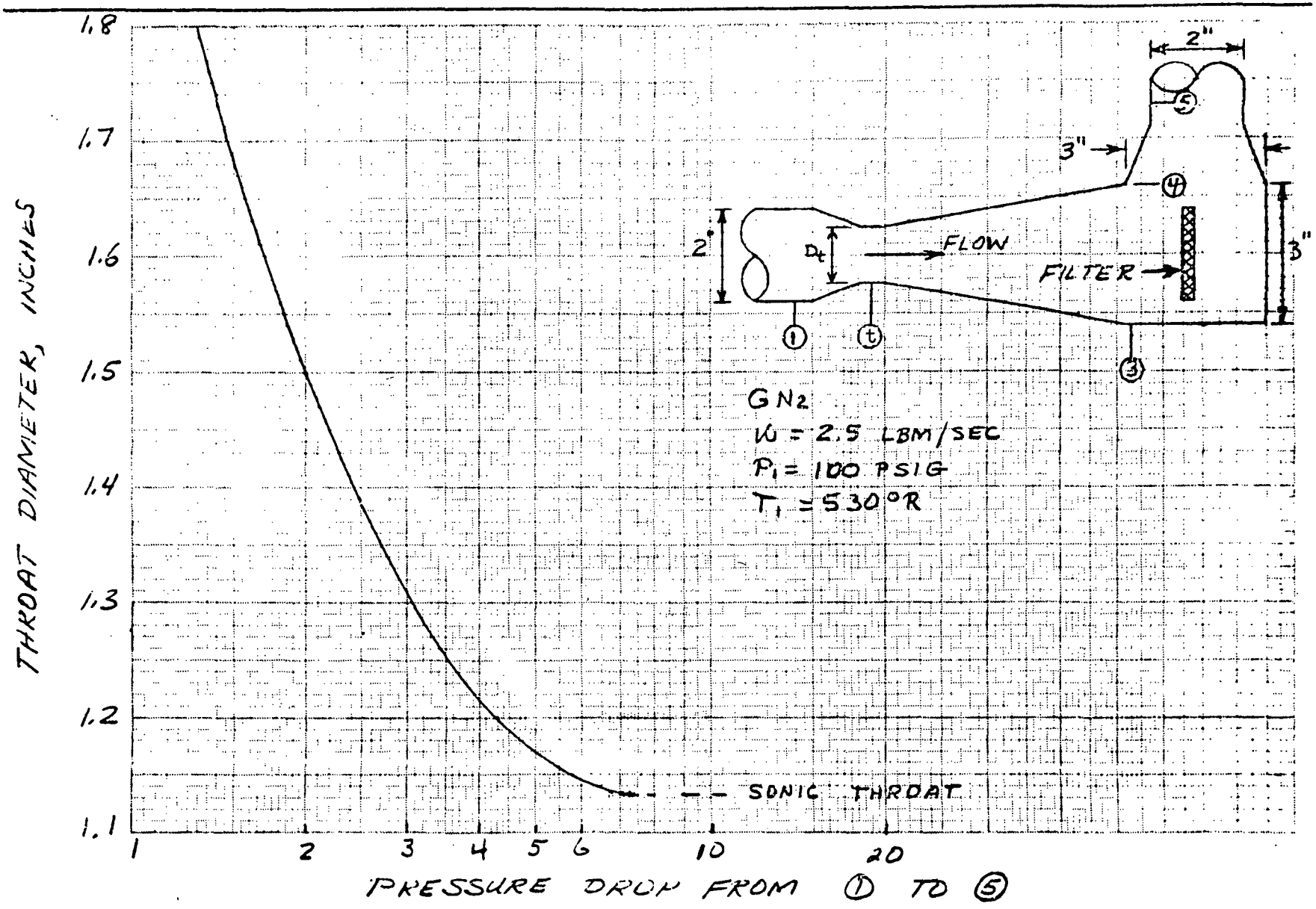

FIGURE 9 PRESSURE DROP FOR VENTURI AND PLENUM SYSTEM

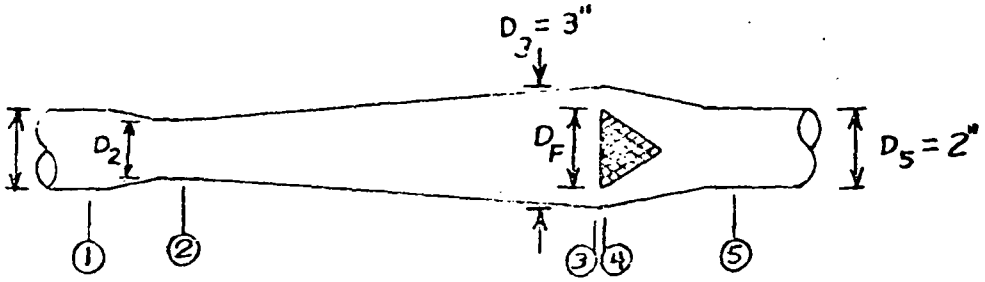

Other data used in the analysis of this configuration are 2.5 lbm/sec GN_2 flowrate, P_1 = 100 psig, and T_1 = 530°R. The included angles for the two contractions are 21°. The included angle for the expansion is 9°. The diameter required for the conical orifice may be obtained using the sketch below and Figures 1 and 6.

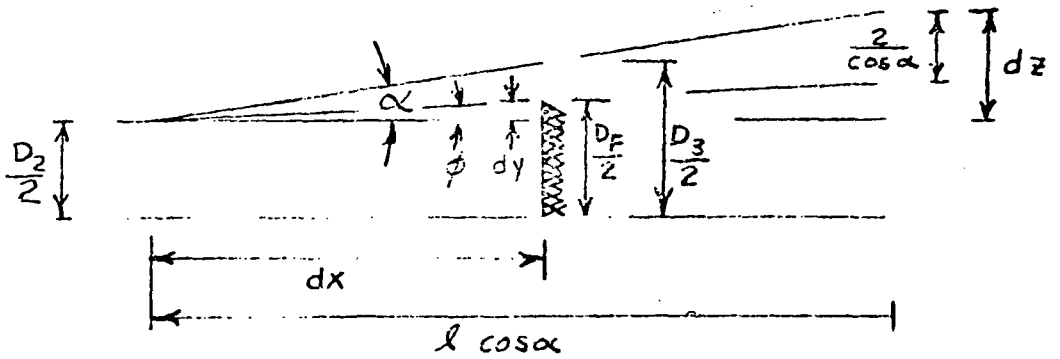

$$\tan\alpha = \frac{(D_3-D_2)/2}{dx}$$

$$dx = \frac{(D_3-D_2)/2}{\tan\alpha} \quad , \; dy = (D_F-D_2)/2$$

$$\alpha = 4.5°, \quad \tan\alpha = .0785$$

$$dx = 6.37\,(D_3-D_2)$$

$$\tan\phi = \frac{dy}{dx} = \frac{dz - 2/\cos\alpha}{\ell \cos\alpha} \qquad \text{(by similar triangles)}$$

where ℓ is the "particle impact distance downstream of bend" from Figure 6.

From Figure 1 for a bend angle of 4.5°, any particle with a Reynolds number greater than 2.3×10^{5} will impact the wall (2" duct). From Figure 6 the impact distance downstream of the bend is 4.3 ft. or 52".

$\cos\alpha = .997, \quad \ell \cos\alpha = 52"$

$d_z = \tan\alpha \, (\ell \cos\alpha)$

$= .0785 \, (52) = 4.1"$

$2/\cos = 2.05"$

$$dy = 11.9 \left(\frac{4.10-2.05}{52}\right) = 11.9 \left(\frac{2.11}{52}\right) = .47$$

$D_F = 1.132 + .948 = 2.080"$

use $\underline{D_F = 2.1"}$

Particle velocities of 200 ft/sec in a 2-in. duct have a sufficient Reynolds number to impact the filter.

The pressure drops for this system are the same as those in paragraph 2.3, except that the 90° bend is not present, and a ΔP is needed for flow past the filter itself.

Considering the filter a solid plate and the resulting area reduction as an orifice, the "orifice" flow area is $\frac{\pi}{4}(3^2-2.1^2) = \frac{\pi}{4}(9-4.4) = \frac{4.6\pi}{4} A_4$

The equivalent geometric orifice diameter is $D_4 = \sqrt{\frac{4}{\pi}\left(\frac{\pi}{4}\right)(4.6)} = \sqrt{4.6} = 2.145$

$$\frac{D_4}{D_3} = \frac{2.145}{3} = \underline{.715}$$

$$Re = \frac{4\dot{w}}{\pi \mu D_3} = \frac{4(2.5)(12)}{(1.2\times10^{-5})(3)} = 1.063 \times 10^{6}$$

From Figure 3.8.2.2d of Reference (11), the flow coefficient $K_F = 0.70$

$$\Delta P_{3-4} = \frac{K_F W^2}{A_4 Y^2 g \rho_3}, \qquad \rho_3 = .507 \text{ from } 2.3$$

$$\Delta P_{3-4} = \frac{(.70)(2.5^2)}{\left(\frac{4.6\pi}{4}\right) Y\ 64.4\ (.507)} = \frac{4.375}{118\,Y}$$

$$= \frac{.0371}{Y}$$

From Fig. 3.8.2.3 of Reference (10)

$$Y \approx 1$$

$$\underline{\Delta P_{3-4} = .037 \text{ psi}}$$

For a sonic Venturi, ($D_2 = 1.132"$)

$$\Delta P_{1-5} = 1.62 + 4.86 + .037 + .11 = \underline{6.63 \text{ psi}}$$

Assuming an unclogged filter will change P_{1-5} by less than .076 psi. Thus, the calculations for ΔP_{1-5} with a blocked filter may also be used for an unblocked filter.

For $D_3 = 3"$, $D_2 = 1.2"$

$dx = 6.37\ (3-1.2) = 11.47$

$$dy = 11.47\ \frac{(2.11)}{(53)} = .457$$

$D_F = 1.20 + .914 = 2.114$; *use* 2.15 in.

For a blocked filter, the flow area is $\frac{\pi}{4}\ (3^2-2.15^2) = \frac{\pi}{4}\ (4.38)$

The equivalent orifice diameter is $D_4 = \sqrt{4.38} = 2.09$

$$\frac{D_4}{D_3} = \frac{2.09}{3} = .697$$

From Figure 3.8.2.2.d of Reference (10)

$K_F = 0.69$

$$\Delta P_{3-4} = \frac{.69}{.70}\ (.037) = .036$$

$$\Delta P_{1-5} = 3.42 + .036 + .10 = \underline{3.6 \text{ psi}}$$

For $D_3 = 3"$, $D_2 = 1.5"$

$$dx = 6.37\ (3-1.5) = 9.55$$

$$dy = 9.55\ \frac{(2.11)}{(53)} = .38$$

$$D_F = 1.5 + .76 = 2.26 \quad \underline{2.3"}$$

For a blocked filter the flow area is

$$\frac{\pi}{4}(3^2-2.3^2) = \frac{\pi}{4}(3.71)$$

The equivalent orifice diameter is

$$D_4 = \sqrt{3.71} = 1.926$$

$$\frac{D_4}{D_3} = \frac{1.926}{3} = .642$$

From Figure 3.8.2.2.d of Reference (10)

$$K_F = .665$$

$$\Delta P_{3-4} = \frac{.665}{.70}\ (.037) = .035$$

$$\Delta P_{1-5} = .33 + .86 + .10 + .035 = \underline{1.33 \text{ psi}}$$

For $D_3 = 3"$, $D_2 = 1.75"$

$$dx = 6.37\ (3-1.75) = 7.96$$

$$dy = 7.96\ (2.11/53) = .317$$

$$D_F = 1.75 + .634 = 2.384; \text{ use } 2.4"$$

By the same method as above,

$$\Delta P_{1-5} = .67 \text{ psi}$$

The filter diameter required for a given throat diameter is shown in Figure 10. Pressure drop results based on these diameters are shown in Figure 11.

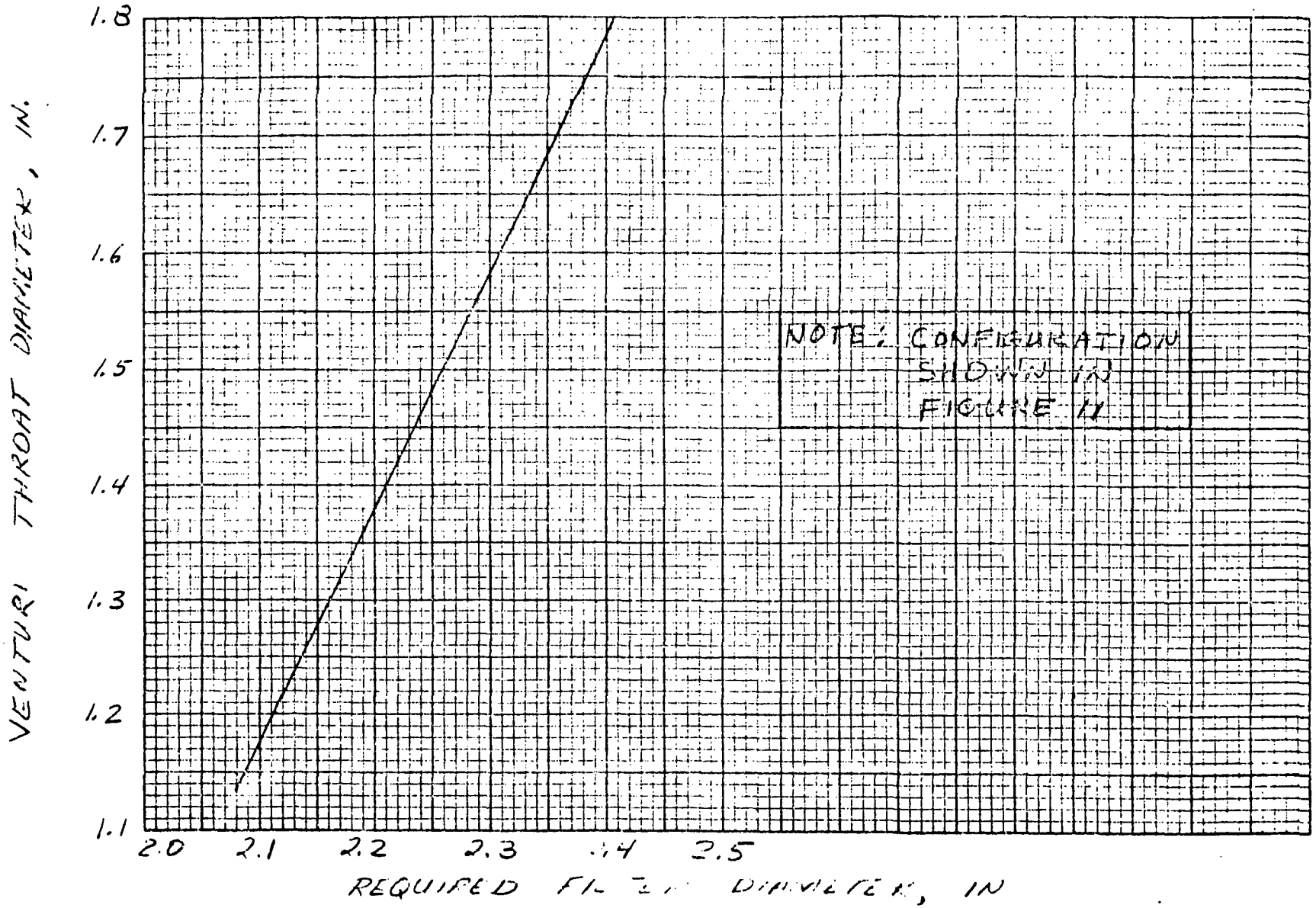

FIGURE 10. REQUIRED FILTER DIAMETER VS. VENTURI THROAT DIAMETER

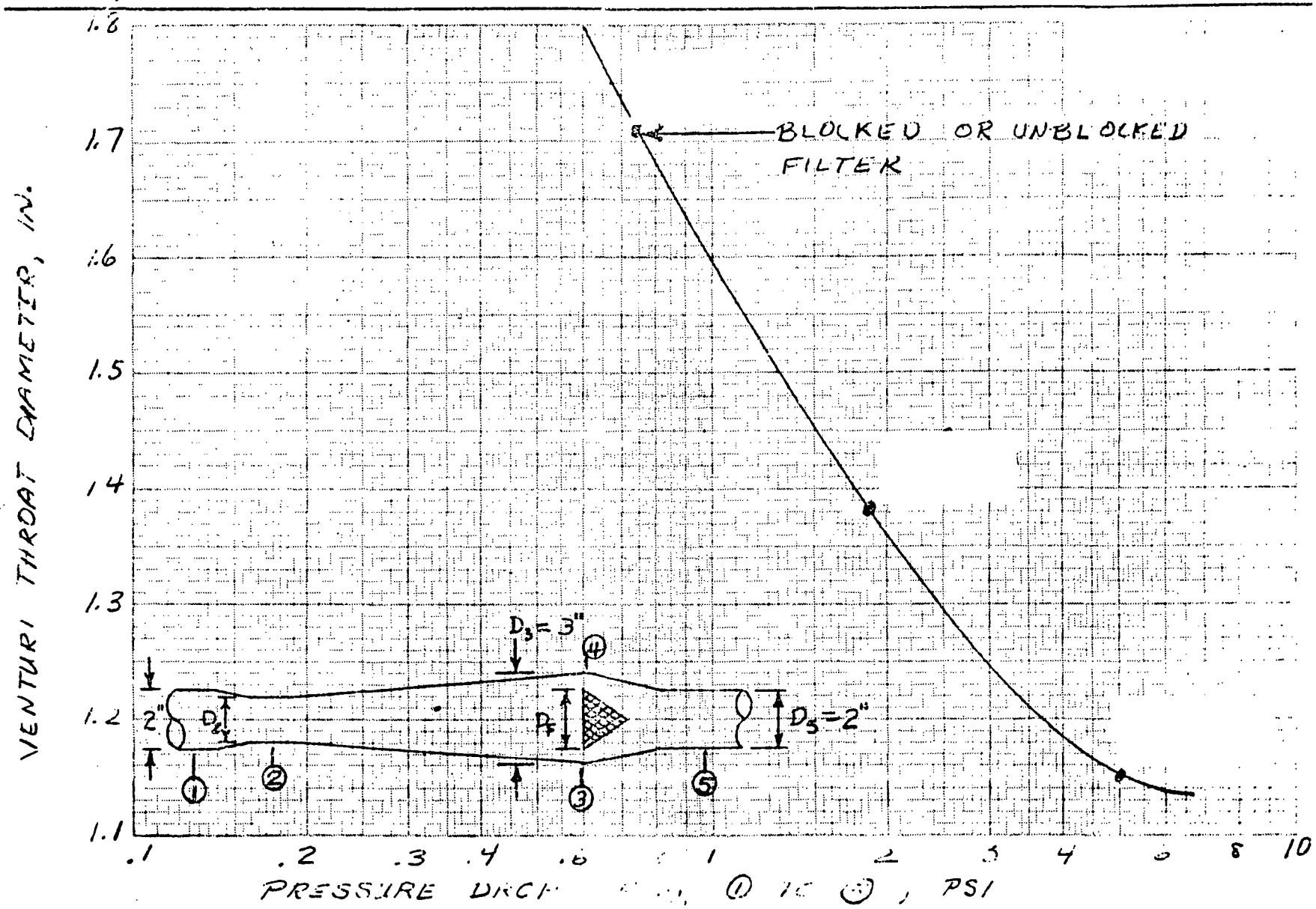

FIGURE 11. PRESSURE DROP FOR VENTURI - TYPE DYNAMIC SEPARATOR

Page Intentionally Left Blank

DISTRIBUTION LIST FOR FINAL REPORT

NAS3-14375 MDAC CR 121125

Instructions:

Final reports are to be sent directly to the "Recipient" and the "Designee" per the quantities specified in the respective columns, R and D. When no copies are specified in column D, a carbon copy of the letter of transmittal should be sent to the person named as the "Designee". The letter of transmittal should contain the contract number and complete title of the final report.

The distribution list, indicating all of the Recipients and Designees, should be included in the final report as an appendix.

REPORT COPIES R	D	RECIPIENT	DESIGNEE
		National Aeronautics & Space Administration Lewis Research Center 21000 Brookpark Road Cleveland, Ohio 44135	
1		Attn: Contracting Officer, MS 500-313	
5		E. A. Bourke, MS 500-203	
1		Technical Report Control Office, MS 5-5	
1		Technology Utilization Office, MS 3-16	
2		AFSC Liaison Office, 501-3	
2		Library	
1		Office of Reliability & Quality Assurance, MS 500-111	
1		J. W. Gregory, Chief, MS 500-203	
5		I. E. Sumner, Project Manager, MS 500-203	
1		R. E. Grey, MS 60-6	
1		W. R. Dunbar, MS 500-103	
1		Director, Manned Space Technology Office, RS Office of Aeronautics & Space Technology NASA Headquarters Washington, D. C. 20546	
1		Director, Physics and Astronomy Programs, S G Office of Space Science NASA, Headquarters Washington, D. C. 20546	
1		Director, Planetary Programs, S L Office of Space Science NASA, Headquarters Washington, D. C. 20546	

REPORT COPIES R	D	RECIPIENT	DESIGNEE
1		Office of Aeronautics & Space Technology, R NASA, Headquarters Washington, D. C. 20546	
1		Minnesota Mining & Manufacturing Company 900 Bush Avenue St. Paul, Minnesota 55106 Attn: Library	
2		Director Space Prop. and Power, RP Office of Aeronatucis & Space Technology NASA Headquarters Washington, D. C. 20546	
1		Director, Launch Vehicles & Propulsion, SV Office of Space Science NASA Headquarters Washington, D. C. 20546	
1		Director, Materials & Structures Div, RW Office of Aeronautics & Space Technology NASA Headquarters Washington, D. C. 20546	
1		Director, Advanced Manned Missions, MT Office of Manned Space Flight NASA Headquarters Washington, D. C. 20546	
5		National Technical Information Service Springfield, Virginia 22151	
1		National Aeronautics & Space Administration Ames Research Center Moffett Field, California 94035 Attn: Library	
1		National Aeronautics & Space Administration Flight Research Center P. O. Box 273 Edwards, California 93523 Attn: Library	
1		Director, Technology Utilization Division Office of Technology Utilization NASA Headquarters Washington, D. C. 20546	
1		Office of the Director of Defense Research & Engineering Washington, D. C. 20301 Attn: Office of Asst. Dir. (Chem Technology)	

REPORT COPIES R	D	RECIPIENT	DESIGNEE
2		NASA Scientific and Technical Information Facility P. O. Box 33 College Park, Maryland 20740 Attn: NASA Representative	
1		National Aeronautics & Space Administration Goddard Space Flight Center Greenbelt, Maryland 20771 Attn: Library	
1		National Aeronautics & Space Administration John F. Kennedy Space Center Cocoa Beach, Florida 32931 Attn: Library	
1		National Aeronautics & Space Administration Langley Research Center Langley Station Hampton, Virginia 23365 Attn: Library	
1	1	National Aeronautics & Space Administration	J. W. Akkerman
	1	Manned Spacecraft Center	J. W. Griffin
	1	Houston, Texas 77001	R. N. Tanner
	1	Attn: Library	Henry Pohl
1		National Aeronautics & Space Administration	Hans G. Paul
		George C. Marshall Space Flight Center	Leon J. Hastings
		Huntsville, Alabama 35912	James Thomas
		Attn: Library	Dale Burrows
	1	Kenneth Anthony	I. G. Yates
			Clyde Nevins
			J. Blumrich
1		Jet Propulsion Laboratory 4800 Oak Grove Drive	
	1	Pasadena, California 91103	Duane Dipprey
		Attn: Library	
1		Defense Documentation Center Cameron Station Building 5 5010 Duke Street Alexandria, Virginia 22314 Attn: TISIA	
1		RTD (RTNP) Bolling Air Force Base Washington, D. C. 20332	

REPORT COPIES R	D	RECIPIENT	DESIGNEE
1		Arnold Engineering Development Center Air Force Systems Command Tullahoma, Tennessee 37389 Attn: Library	
1		Advanced Research Projects Agency Washington, D. C. 20525 Attn: Library	
1		Aeronautical Systems Division Air Force Systems Command Wright-Patterson Air Force Base, Dayton, Ohio Attn: Library	
1		Air Force Missile Test Center Patrick Air Force Base, Florida Attn: Library	
1		Air Force Systems Command Andrews Air Force Base Washington, D. C. 20332 Attn: Library	
1		Air Force Rocket Propulsion Laboratory (RPR) Edwards, California 93523 Attn: Library	
1		Air Force Rocket Propulsion Laboratory (RPM) Edwards, California 93523 Attn: Library	
1		Air Force FTC (FTAT-2) Edwards Air Force Base, California 93523 Attn: Library	
1		Air Force Office of Scientific Research Washington, D. C. 20333 Attn: Library	
1		Space & Missile Systems Organization Air Force Unit Post Office Los Angeles, California 90045 Attn: Technical Data Center	
1		Office of Research Analyses (OAR) Holloman Air Force Base, New Mexico 88330 Attn: Library	
1		U. S. Air Force Washington, D. C. Attn: Library	

REPORT COPIES R	D	RECIPIENT	DESIGNEE
1		Commanding Officer U. S. Army Research Office (Durham) Box CM, Duke Station Durham, North Carolina 27706 Attn: Library	
1		U. S. Army Missile Command Redstone Scientific Information Center Redstone Arsenal, Alabama 35808 Attn: Document Section	
1		Bureau of Naval Weapons Department of the Navy Washington, D. C. Attn: Library	
1		Commander U. S. Naval Missile Center Point Mugu, California 93041 Attn: Technical Library	
1		Commander U. S. Naval Weapons Center China Lake, California 93557 Attn: Library	
1		Commanding Officer Naval Research Branch Office 1030 E. Green Street Pasadena, California 91101 Attn: Library	
1		Director (Code 6180) U. S. Naval Research Laboratory Washington, D. C. 20390 Attn: Library	
1		Picatinny Arsenal Dover, New Jersey 07801 Attn: Library	
1		Air Force Aero Propulsion Laboratory Research & Technology Division Air Force Systems Command United States Air Force Wright-Patterson AFB, Ohio 45433 Attn: APRP (Library)	

REPORT COPIES R	D	RECIPIENT	DESIGNEE
1		Space Division Aerojet-General Corporation 9200 East Flair Drive El Monte, California 91734 Attn: Library	
1		Aerojet Ordnance and Manufacturing Aerojet-General Corporation 11711 South Woodruff Avenue Fullerton, California 90241 Attn: Library	
1	1	Aerojet Liquid Rocket Company P. O. Box 15847 Sacramento, California 95813 Attn: Technical Library 2484-2015A	James Smith
1		Aeronutronic Division of Philco Ford Corp. Ford Road Newport Beach, California 92663 Attn: Technical Information Department	
1		Aerospace Corporation 2400 E. El Segundo Blvd. Los Angeles, California 90045 Attn: Library-Documents	
1		Arthur D. Little, Inc. 20 Acorn Park Cambridge, Massachusetts 02140 Attn: Library	
1		Astropower Laboratory McDonnell-Douglas Aircraft Company 2121 Paularino Newport Beach, California 92163 Attn: Library	
1		ARO, Incorporated Arnold Engineering Development Center Arnold AF Station, Tennessee 37389 Attn: Library	
1		Susquehanna Corporation Atlantic Research Division Shirley Highway & Edsall Road Alexandria, Virginia 22314 Attn: Library	

REPORT COPIES R	D	RECIPIENT	DESIGNEE
1		Beech Aircraft Corporation Boulder Facility Box 631 Boulder, Colorado Attn: Library	
1		Bell Aerosystems, Inc. Box 1 Buffalo, New York 14240 Attn: Library	
1		Instruments & Life Support Division Bendix Corporation P. O. Box 4508 Davenport, Iowa 52808 Attention: Library	
1		Bellcomm 955 L'Enfant Plaza, S. W. Washington, D. C. Attn: Library	
1		Boeing Company Space Division P. O. Box 868 Seattle, Washington 98124 Attn: Library	
1		Boeing Company 1625 K Street, N. W. Washington, D. C. 20006	
1		Boeing Company P. O. Box 1680 Huntsville, Alabama 35801	
1		Chemical Propulsion Information Agency Applied Physics Laboratory 8621 Georgia Avenue Silver Spring, Maryland 20910	
1		Chrysler Corporation Missile Division P. O. Box 2628 Detroit, Michigan Attn: Library	

REPORT COPIES R	D	RECIPIENT	DESIGNEE
1		Chrysler Corporation Space Division P. O. Box 29200 New Orleans, Louisiana 70129 Attn: Librarian	
1		Curtiss-Wright Corporation Wright Aeronautical Division Woodridge, New Jersey Attn: Library	
1		University of Denver Denver Research Institute P. O. Box 10127 Denver, Colorado 80210 Attn: Security Office	
1		Fairchild Stratos Corporation Aircraft Missiles Division Hagerstown, Maryland Attn: Library	
1		Research Center Fairchild Hiller Corporation Germantown, Maryland Attn: Library	
1		Republic Aviation Fairchild Hiller Corporation Farmington, Long Island New York	
1		General Dynamics/Convair P. O. Box 1128 San Diego, California 92112 Attn: Library	
1		Missiles and Space Systems Center General Electric Company Valley Forge Space Technology Center P. O. Box 8555 Philadelphia, Pa. 19101 Attn: Library	
1		General Electric Company Flight Propulsion Lab. Department Cincinnati, Ohio Attn: Library	

REPORT COPIES R	D	RECIPIENT	DESIGNEE
1		Grumman Aircraft Engineering Corporation Bethpage, Long Island, New York Attn: Library	
1		Hercules Powder Company Allegheny Ballistics Laboratory P. O. Box 210 Cumberland, Maryland 21501 Attn: Library	
1		Honeywell, Inc. Aerospace Division 2600 Ridgeway Road Minneapolis, Minnesota Attn: Library	
1		IIT Research Institute Technology Center Chicago, Illinois 60616 Attn: Library	
1		Kidde Aerospace Division Walter Kidde & Company, Inc. 567 Main Street Belleville, New Jersey 07109	
1		Ling-Temco-Vought Corporation P. O. Box 5907 Dallas, Texas 75222 Attn: Library	
1		Lockheed Missiles and Space Company P. O. Box 504 Sunnyvale, California 94087 Attn: Library	
1		Lockheed Propulsion Company P. O. Box 111 Redlands, California 92374 Attn: Library, Thackwell	
1	1	Marquardt Corporation 16555 Saticoy Street Box 2013 - South Annex Van Nuys, California 91409	Horst Wichmann

REPORT COPIES R	REPORT COPIES D	RECIPIENT	DESIGNEE
1		Denver Division *Martin-Marietta Corporation* P. O. Box 179 Denver, Colorado 80201 *Attn: Library*	
1		Orlando Division Martin-Marietta Corporation Box 5827 Orlando, Florida Attn: Library	
1		McDonnell Douglas Aircraft Corporation P. O. Box 516 Lambert Field, Missouri 63166 Attn: Library	
1	1	Rocketdyne Division North American Rockwell Inc. 6633 Canoga Avenue Canoga Park, California 91304 Attn: Library, Department 596-306	Gary Smith
1		*Space & Information Systems Division* North American Rockwell 12214 Lakewood Blvd. Downey, California Attn: Library	
1		Northrop Space Laboratories 3401 West Broadway Hawthorne, California Attn: Library	
1		Purdue University Lafayette, Indiana 47907 Attn: Library (Technical)	
1		Radio Corporation of America Astro-Electronics Products Princeton, New Jersey Attn: Library	
1		Rocket Research Corporation Willow Road at 116th Street Redmond, Washington 98052 Attn: Library	
1		Stanford Research Institute 333 Ravenswood Avenue Menlo Park, California 94025 Attn: Library	

REPORT COPIES R	D	RECIPIENT	DESIGNEE
1		Thiokol Chemical Corporation Redstone Division Huntsville, Alabama Attn: Library	
1		TRW Systems Inc. 1 Space Park Redondo Beach, California 90278 Attn: Tech. Lib. Doc. Acquisitions	
1		TRW TAPCO Division 23555 Euclid Avenue Cleveland, Ohio 44117	
1		United Aircraft Corporation Corporation Library 400 Main Street East Hartford, Connecticut 06108 Attn: Library	
1		United Aircraft Corporation Pratt & Whitney Division Florida Research & Development Center P. O. Box 2691 West Palm Beach, Florida 33402 Attn: Library	
1		United Aircraft Corporation United Technology Center P. O. Box 358 Sunnyvale, California 94038 Attn: Library	Dr. David Altman
1		Vickers Incorporated Box 302 Troy, Michigan	
1		Vought Astronautics Box 5907 Dallas, Texas Attn: Library	
1		Airesearch Mfg. Div. Garrett Corp. 9851 Sepulveda Blvd. Los Angeles, California 90009 Attn: Library	

REPORT COPIES R	D	RECIPIENT	DESIGNEE
1		Airesearch Mfg. Div. Garrett Corp. 402 South 36th Street Phoenix, Arizona 85034 Attn: Library	
1		Marco Research & Development Co. Whittaker Corporation 131 W. Ludlow Street Dayton, Ohio 45402	
1		General Electric Company Apollo Support Dept. P. O. Box 2500 Daytona Beach, Florida 32015	
1		E. I. DuPont DeNemours and Company Eastern Laboratory Gibbstown, New Jersey 08027 Attn: Library	
1		Esso Research & Engineering Company Special Projects Unit P. O. Box 8 Linden, New Jersey 07036 Attn: Library	
1		Commanding Officer U. S. Naval Underwater Ordnance Station Newport, Rhode Island 02844 Attn: Library	
1		National Science Foundation, Engineering Division 1800 G. Street N. W. Washington, D. C. 20540 Attn: Library	
1		G. T. Schjeldahl Company Northfield, Minn. 55057 Attn: Library	
1		General Dynamics P. O. Box 748 Fort Worth, Texas 76101	
1		Cryonetics Corporation Northwest Industrial Park Burlington, Massachusetts	
1		Institute of Aerospace Studies University of Toronto Toronto 5, Ontario Attn: Library	

NO. OF COPIES	RECIPIENT
1	FMC Corporation Chemical Research & Development Center P. O. Box 8 Princeton, New Jersey 08540
1	Westinghouse Research Laboratories Beulah Road, Churchill Boro Pittsburgh, Pennsylvania 15235
1	Cornell University Department of Materials Science & Eng. Ithaca, New York 14850 Attn: Library